8-2011

Examination of 4He droplets and droplets containing impurities at zero Kelvin using a density functional approach

Ellen Brown
ecbrown@utk.edu

To the Graduate Council:

I am submitting herewith a thesis written by Ellen Brown entitled "Examination of 4He droplets and droplets containing impurities at zero Kelvin using a density functional approach." I have examined the final electronic copy of this thesis for form and content and recommend that it be accepted in partial fulfillment of the requirements for the degree of Master of Science, with a major in Chemistry.

Robert J. Hinde, Major Professor

We have read this thesis and recommend its acceptance:

Robert J. Harrison, Jon P. Camden

Accepted for the Council:
Carolyn R. Hodges

Vice Provost and Dean of the Graduate School

(Original signatures are on file with official student records.)

To the Graduate Council:

I am submitting herewith a thesis written by Ellen Cofer Brown entitled "Examination of ^{4}He droplets and droplets containing impurities at zero Kelvin using a density functional approach." I have examined the final electronic copy of this thesis for form and content and recommend that it be accepted in partial fulfillment of the requirements for the degree of Master of Science, with a major in Chemistry.

Robert J. Hinde, Major Professor

We have read this thesis
and recommend its acceptance:

Robert J. Harrison

Jon P. Camden

Accepted for the Council:

Carolyn R. Hodges

Vice Provost and Dean of the Graduate School

(Original signatures are on file with official student records.)

Examination of ^{4}He droplets and droplets containing impurities at zero Kelvin using a density functional approach

A Thesis Presented for
the Master of Science
Degree
The University of Tennessee, Knoxville

Ellen Cofer Brown
August 2011

Dedicated to my Superman, J. R. Strobel.

Acknowledgments

Above all, I would like to express gratitude to RJ Hinde, my major professor, for all of his support and dedication; without which, this manuscript would not exist. I would like to recognize all of the professors whom I have had the privilege of knowing as teachers and mentors—RJ Hinde, George Heard, Stan Guffey, T. F. Williams, Herman Holt, Bert Holmes, Sally Wasileski, Noah Allen, Robert Harrison, Jon Camden, and Charles Feigerle—to name a few. I would be a different person not having known you.

I wish to thank the graduate committee who endeared to see me through the defense of my thesis. I also acknowledge the Hinde group, particularly, Matthew Wilson, Patrick Moehlen, Tim Lillestolen, Britta Johnson, and Hailey Bureau. It was nice to have people around who entertained my insanity.

Thanks to my dear friends and family for the diversions they offered over the past few years; especially Charley, my one blue-eyed friend, and Betty, our little monster who is no longer with us. Thanks to Mike, Eileen, and Jeremiah, so that I may never forget where I came from. Thanks to my sister Anne and her daughter Darby Amalia, both for their scintillating smiles. Thanks to Marshall for bringing originality to a world that could use more. Thanks to Strobel, my greatest distraction and closest friend. Finally, I attribute my mother, Betsy, and my father, Pat, to stimulating my curiosity for the unknown at an early age and encouraging its pursuit.

I would like to express love for those past who taught me that "we make our world significant by the courage of our questions and by the depth of our answers." (Carl Sagan)

Abstract

Detailed in this manuscript is a methodology to model ground state properties of ^{4}He droplets at zero pressure and zero Kelvin using a density functional theory of liquid helium. The density functional approach examined here consists of two noted functionals from the literature and corresponding mean field definitions. A mean field and trial density are defined for each system and optimized to self-consistency using a matrix diagonalization technique. Initial calculations of planar slabs are performed and demonstrate reasonable agreement with experiment and with prior studies using density functional theory. Quantum properties of droplets and droplets containing atomic dopants are calculated. Three different He-dopant potentials are examined to test the limits of the functional methods. For each impurity interaction, an average of 12 atoms were found to reside in the first solvation shell with an atomic dopant placed at the droplet center. Maximum densities in the first solvation shell reached those of solid helium as predicted by DF methods.

Table of Contents

Page

List of Figures

Page

List of Tables

Page

Chapter 1: Summary and motivation for research

1.1 Characteristics of quantum fluids

Quantum fluids have been of great interest to the scientific community for multiple reasons, as they are an illustration of unique quantum properties on a broad scale. Observables on the microscopic level manifest themselves in macroscopic-level behavior, so that individual quantum states, which are represented mathematically, can be visualized with the naked eye. At absolute zero ^{4}He remains a liquid because weak van der Waals interactions are the predominant intermolecular forces within the fluid. Helium exhibits a weakly cohesive internal structure, yet each atom is strongly correlated to every other. Properties of superfluidity arise from zero viscosity, zero entropy, and absolute thermal conductivity. Helium is the one element that does not form a solid at zero Kelvin and atmospheric pressure; it freezes only under the application of external pressure. At the lambda point of 2.17 *K*, the state of liquid ^{4}He sustains a low viscosity and transitions into the superfluid phase due to the expression of Bose-Einstein statistics.

^{4}He has integer spin of a boson, exhibiting Bose-Einstein statistics that predict the non-existence of the Pauli-exclusion principle, so that upon an exchange, the wavefunction remains symmetrical. For bosons this means that ^{4}He particles become indistinguishable upon the condensation to an equivalent ground-state energy. This energetic state occurs as wavefunctions of individual atoms of the Bose condensate

overlap to express a single projection of the wavefunction. Because of respective Bose or Fermi statistics which govern the nature of superfluidity, quantum properties determine whether a system behaves like a quantum fluid.[1] This is visually manifested in quantized spin states. As a beaker of quantum fluid is swirled, it may only spin with allowed velocities as the energy increases by specified increments. Because ^{4}He is a boson with integer spin, quantum characteristics of the atom are expressed on an macroscopic scale as seen in quantum fluids such as the phenomenon of continuous thermal conductivity. The expression of quantum phenomena on a large scale such as in a cluster of atoms has aroused interest in computational work that aims in developing a mean field to accurately discern interactions of ^{4}He. The convention must be defined on the quantum level in order to make predictions and correlation to experimental data.

In order to interpret a density functional for superfluid ^{4}He, dimensionality dependence of the system must be considered—spatially how the density fluctuates within the liquid. Under external constraints of zero temperature and zero pressure, the bulk liquid density for certain system geometries may be approximated to a one dimensional system where the density varies only with alteration of the coordinate direction perpendicular to the planar-liquid interface.[2, 3] This asymptote is defined as the transition from the liquid to vacuum phase as the density fades into vapor and vacuum. Unidimensional dependence may also be adapted from Cartesian coordinates to spherical coordinates when examining a ^{4}He droplet-like system.[3] Similarly, in a spherical conformation the density only deviates with the displacement of one coordinate, defining the radius of the helium sphere. Movement from the Cartesian z axis to a proposed z' axis or r axis to r' axis will track close-range fluctuation throughout the liquid and demonstrate the variation of density in square slabs or spherical shells of the liquid.

Weak van der Waals forces are the cohesive force in superfluid helium, and further motivation for this research comes from inconsistencies in models of dynamic energetic interactions within the liquid. Predictions vary as to whether or not minute oscillations exist at the planar interface as the density decays into the gas phase and then to

vacuum.[2, 3, 4] It has been determined that ^{4}He clusters have less restrictions for bound states, unlike the ^{3}He Fermi condensate, which must form a Cooper pair upon transition to superfluidity.[1] Calculations demonstrate that ^{4}He clusters are bound for all values of N.[5]

Excitations and dynamic properties within the bulk liquid arise from phonon-roton dispersion.[6] Phonons are symmetrical fluctuations of energy which arise from sound wave vibrations and are dependent on the velocity of sound. An accurate description of phonon excitations is likely to incorporate the three-body interaction into the theory as phonons arise from the three-body movement within the condensed helium. Sound waves act as a perturbation, which then resonates as it is periodically absorbed by each atom in the Bose-condensate. Rotons are similar to phonon vibrations except they are motivated by rotational fluctuations. Phonon-roton dispersion is the observed quantum energy fluctuations as a combination of the two[7] and are dependent upon the helium trimer interaction.

The phenomenon of backflow arises from close-range dispersive effects as atoms move within the liquid. While one atom moves, others are pushed into the available empty spaces. Backflow manifests itself as excitations within the bulk liquid, but also influences surface character in quantum evaporation and oscillations of surface density.[8, 9, 10] Backflow and phonon-roton dispersion are dynamic properties within the liquid and echo on the liquid-vacuum interface. The character of these fluctuations can be measured directly from neutron scattering experiment in the dynamic structure factor $S(q,\omega)$[7] and incorporated into parameters of the density functional.[3, 11] The static density response function $\chi(q)$ is inversely proportional to the dynamic structure factor and also defines properties of bulk liquid helium. Van der Waals interactions oversee these internal properties of liquid ^{4}He, which in turn structures the functional. To properly understand quantum interactions at the atomic level, interest lies in the improvement of theoretical methods which define liquid ^{4}He at zero temperature and zero pressure.

1.2 ^{4}He as a cryogenic matrix for spectroscopy

Superfluid ^{4}He is commonly used as an ultra-cold spectral medium to probe an embedded molecule because it creates a unique matrix which can easily be doped upon formation. Helium droplets are best suited for spectroscopy because of their finite size, while samples of bulk fluid are less likely to isolate a single molecule for perturbation. OCS and SF_6 are such molecules of interest. Using helium as the matrix yields increased spectroscopic resolution; one such avenue, by eliminating hot bands since the dopant will most likely be in the ground state upon superfluid transformation at these temperatures.[12] For a more in depth description of experimental design and spectroscopic technique for using ^{4}He as a cryogenic matrix see reference 12 and sources therein.

In order to expand upon the understanding of helium nanodroplets as an experimental matrix, it must be known how the impurity interacts with the helium. The question of whether or not solvation of the dopant occurs and what solvation shells may form is of great importance. The dimensionless value of lambda, dissimilar from the temperature lambda point of superfluid transition, defines the solvation nature of a dopant. Lambda predicts whether or not an impurity will be fully solvated at the center of the droplet, or have little to no solvation and reside in dimples at various depths within the droplet. It has been determined that a lambda value of 1.9 is the threshold of solvation; values below 1.9 are indicative of surface location and above 1.9 predict complete solvation.[13] Lambda is dependent upon the surface tension and particle density of the helium droplet, along with the well depth and equilibrium bond length of the He-dopant interaction potential. With varied He-dopant interactions potentials that include higher order corrections, different behavior of solvation could be calculated for the same impurity near the solvation threshold. Using different levels of computation such as density functional theory (DFT) or quantum Monte Carlo (QMC) may yield different descriptions of He-He interactions within the droplet. The development of more accurate

He-dopant potentials will facilitate the study of borderline impurities, one such example is that of the Mg atom. It is relevant to note here that Mg may reside at varied depths in a spherical system depending upon the size of the droplet and level of theory or experiment used.[14] Correlation of theory can be helpful in the calculation of the chemical potential of superfluid helium systems and binding energies of impurities,[12, 15] which directly leads into the question of solvation. Thus far, density functional theory has found reasonable agreement with diffusion Monte Carlo simulations; however, there are some systems that have yet to find agreement.[16]

As a dopant becomes more and more attractive, the first solvation shell may contain densities approaching solid helium. As the density elevates to densities near the solid-state limit around $0.0287\ \text{Å}^{-3}$, it believed that three-body interactions play a more representative role.[17] The research here aims to analyze the capabilities and weaknesses of density functional methods to examine doped ^{4}He droplets when the impurity is of an attractive nature. We intend to compute energy components calculated with density functional theory which include only two-body potentials.

Superfluids, such as ^{4}He, are of great relevance as ultra-cold matrices suited for high resolution spectroscopy. In the simple ^{4}He quantum fluid, a droplet becomes an ideal environment for cryogenic spectral analysis of embedded molecules;[12] therefore, it is important to understand the interatomic forces within a system of ^{4}He. Further interest of this proposal lies in the description of internal forces within the ^{4}He quantum fluid, with the ultimate goal of examining the importance of two-body interaction potentials of helium droplets and droplets with the presence of alkaline earth metal impurities.

1.3 Outline of current manuscript

The remainder of the manuscript is organized as follows. Chapter two examines the relevant interaction potentials of helium, with division of the chapter considering two-body and three-body with higher order terms. Chapter three is an exploration of recent literature studies, including three noted density functionals used to scrutinize systems of ^{4}He in the form of planar slabs, nanodroplets, and nanodroplets containing atomic dopants placed at the center. Chapter four imparts the methodology and mathematics of the current work, along with details of numerical test cases and fine points to consider in the process. Chapter five presents the results and interpretation of the data. Finally, chapter six concludes with items for future research interests.

Chapter 2: Atomic interactions in condensed phases of helium

2.1 Pairwise additive interactions

In the study of simple quantum fluids, two-body potentials are the primary interactions which influence the character of the liquid.[18] In density functional studies of liquid helium, the most frequent representation of the He-He pair interaction has been the Lennard-Jones 6-12 potential, modified at short-range with a variety of screening effects.[3, 11, 18] The Aziz pair potential is another notable form in the literature with a softer core repulsion than the Lennard-Jones.[19]

The development of the pair interaction relies upon the second virial coefficient, *B(T)* in equation (1), to define properties of weak van der Waals interactions present in ^{4}He. The second virial coefficient is temperature dependent and can be measured from experiment or derived from theory. A form of the virial equation is listed as equation (1), where ρ in this respect is the molar density. The constant R is the molar gas constant, P is the pressure, and T is the absolute temperature. Higher order correction terms are represented by the higher order virial coefficients, *C(T)* and *D(T)*. Deviations from ideal gas behavior in helium can be described by the virial equation, with second order corrections described by the second virial coefficient.[20] From a discrete use of pair potentials, one can determine energy and density values for a system of low-density liquids.[19]

(1)

$$\frac{P}{\rho RT} = 1 + B(T)\rho + C(T)\rho^2 + D(T)\rho^3 + \cdots$$

By deriving properties that arise from pair interactions and that can be defined through the second virial coefficient, we set the groundwork for describing a system of ^{4}He. Such properties can be improved upon with higher order corrections.

2.2 Three-body interactions and higher

The third virial coefficient, *C(T)* from equation (1), has only recently been approximated by theory. *C(T)* grows highly complex because it must include two-body and three-body interactions to the correction term. One such method of derivation is described by Garberoglio and Harvey, using a form of path-integral calculations.[21] Interactions of a higher order become apparent in liquids of higher densities and densities that approach the solid state hexagonal close-packed lattice formation. Exchange nonadditivity is a three-body interaction relevant at short-range and more difficult to quantify than long-range dispersive interactions defined by Axilrod Teller triple dipole interactions.[20] For an explanation of exchange nonadditivity and tripole dipole terms, see references 22 and 23, respectively.

Higher order terms contribute less to atomic interactions within a system of helium. One cannot ignore interactions of a higher order; however, there are certain properties that are dominated by two-body terms used in density functional studies. According to recent progress in the field, QMC simulations have been used as the benchmark to study interactions of liquid helium. Thus far, DFT methods have given reasonable agreement to Monte Carlo studies which can inherently include three-body interactons.[24] At higher densities, the case argues for the inclusion of higher order correlation terms.

Chapter 3: Recent DFT approaches from the literature

3.1 Density functional theory of quantum fluids

The basis of density functional theory for quantum fluids is different from traditional DFT principles which utilizes electron density to write the energy of a system. Here, the energy is dependent upon the one-body density, from this point on, referred to as ρ. In 1990 Dupont-Roc et al.[3] prepared a novel density functional that has been a strong basis for current research studies.[3, 4, 11] In reference 3 the authors make a more concise yet simple model than previous theory. They examine parameters to model nuclear forces as one inclusive mean field interaction, utilizing previous density functional theory considerations and expanding to correct former shortcomings in accordance with experimental data. A many-body problem is averaged to a single mean field expression. Previous to Dupont-Roc et al.,[3] Stringari and Treiner's approach[2] chose a Skyrme interaction to define the density dependent energy functional. Skyrme calculations define ground-state nuclei correlations as a zero-range potential of superfluid ^{4}He. However, this functional is predicted to be unable to govern corrections such as the presence of impurities.[3] Density functional theory has proven a valid resource to examine atomic forces within nanodroplets of ^{4}He. Since the transition between states occurs in a small range of temperature, it is important to incorporate the inhomogeneous equation of state with respect to a small range of temperature.

Density functional theory of superfluid helium defines an approximation of the energy of a model inhomogeneous system of ^{4}He as a function of the fluid's one-body

density. With an appropriate correlation energy, one may readily interpret properties of the density profile, characteristic wavefunction, mean field expression, and calculate energetic properties of the system such as the chemical potential. However, the duplication of theory to experiment does not yet suffice within a reasonable window of error to consistently predict solvation of dopants that have a weak tendency to dissolve in liquid helium. We will refer to the functional developed within the Dupont-Roc paper[3] as the Orsay-Paris collaboration. The authors take a many-body problem and reduce the interacting forces to a one-body problem dependent upon a single variable, where the mean field potential varies with respect to the coordinate axis perpendicular to a liquid-vacuum interface. The simplification is lifted directly from the assumption that the density of bulk fluid or spherical droplets is only dependent upon the direction perpendicular to the interface of the system as the density decays into vacuum; and the energy of the system is a function of the particle density. Density varies with the symmetry of the system, either in planar slabs or spherical shells. The behavior of the system with respect to each atom is characterized by the mean field potential approximation, accounting for long and short-range interaction terms as well as the presence of superfluid, liquid, and solid variations throughout the density of the system.

The Orsay-Paris calculation of the surface tension is agreeable to existing data, quantified within the density profile through the characterization of a value known as surface thickness. The surface thickness is defined $t_{10\text{-}90}$, which represents the interval over which helium undergoes a transition from 10% to 90% of the bulk superfluid density. The surface thickness value from the Orsay-Paris functional was computed to be 5.8 Å, compared to previous calculations of 7 Å.[3] Improvements to calculation of the density profile originate with added parameters extrapolated from experiment, such as the static density response function $\chi(q)$ or consideration of quantum backflow effects. Pricaupenko and Treiner[4] explore excitations within the bulk liquid using the Orsay-Paris functional. However, Dalfovo et al.[11] aggregate the static density response function and backflow effects into an improved density functional theory named the

Orsay-Trento collaboration. The Orsay-Paris functional lacks these corrections. The static response function can be computed from the dynamic structure function $S(q, \omega)$ which is taken directly from neutron scattering data[3] and incorporated into the energy functional. Quantum backflow is responsible for density fluctuations within bulk liquid and distinct excitations at the surface which influence the transition to the vapor phase, arising from phonon-roton excitations.[8, 9] Resultant oscillations from phonon-roton currents occur in density values particularly as defined by the surface profile. Monte Carlo simulations predict these small fluctuations.[16] Calculations of superfluid ^{4}He with the majority of atoms in the ground state must allow for the possibility of excited states, particularly at surface locations which promote movement to and from the vapor phase. The adjustment of existing computational methods to experimental observation and emerging theory, proves the progressive approach to define a sufficient density functional.[4, 11]

The mean field must define bulk ^{4}He interactions at infinite depth throughout the liquid and across the transition to gas phase at a surface. The functional should encompass the consideration of multiple surfaces which project a finite depth formation found in the spherical structure of a nanodroplet and contain an added potential to exploit the possibility of impurities such as nitrogen, neon, alkali and alkaline earth metals. The potential for the presence of impurities takes its value from the energy difference in calculations performed with the impurity and separately without. The energy difference is the potential.[11] Nitrogen and neon add dispersion forces which are stronger than helium-helium attractions because they tolerate an increased mass. Further, it is under debate whether alkali and alkaline earth metals may be absorbed by nanodroplets of liquid helium. Because of the coexistence of He I and He II phases, the classical and quantum nature of the sample must be incorporated into the functional. Inhomogeneous helium includes the equation of state where solid, superfluid, liquid, or gas might coincide. Theory must also take into account the superposition of phase I liquid state and phase II quantum fluid state which may reside in the bulk liquid.[3] As

well as examining depth and surface properties, calculations must also be able to incorporate the presence of impurities that promote van der Waals forces within the liquid. The current literature contains a variety of density functionals which mimic the behavior of inhomogeneous ^{4}He on the quantum level; however, since each functional is an approximation, they each have presuppositions. The proposed research begins with the review of preceding literature papers to determine a density functional which accurately defines a mean field approximation for ^{4}He at zero temperature and zero pressure. The mean field defines an energy potential in units of Kelvin with respect to each atom. Much of the current research begins with the phenomenological functional contained in the Orsay-Paris functional and continues to the Orsay-Trento collaboration. Phenomenological methods incorporate the combination of experimental parameters and theory to improve upon the model system of interest.

Here, we are interested in the ground state properties and static interactions of liquid ^{4}He at zero temperature and zero pressure. The variance of liquid ^{4}He depends upon the surface character of the system and the interface that exists. A few examples could be qualitatively described by a sample of bulk fluid, a thin film which does not approach bulk properties, or a nanodroplet which has spherical shells. The authors of the Orsay-Paris collaboration describe their functional as radical yet simple compared to precedent works, with correlation between the calculated surface tension (σ) and the experimental value, $\sigma = 0.277\,K\,\text{Å}^{-2}$ and $0.274\,K\,\text{Å}^{-2}$, respectively. The functional predicts long-range interactions and represents well the constant-density bulk helium found infinitely far away from an interface, but has less agility when dealing with short-range interactions found in the surface width and vaporization transition.(3) Subsequent work has added a correction to the Orsay-Paris approximation with consideration towards the static response function and phonon-roton dispersion. The Orsay-Trento collaboration developed a functional that predicts minute oscillations in the density profile as it decays at a liquid-gas interface. It is noted however, that these oscillations may be too small to be found in experimental data of the density profile, but have been

congruously predicted in the literature by Monte Carlo simulations.[14]

Imaginary time-step methods, an iterative process outlined by the Orsay-Paris collaboration are used to advance an initial trial wavefunction with the Hamiltonian operator to calculate a self-consistent form of the wavefunction. U is the mean field approximation. Through the process given in equation (2), the system is optimized to self-consistency.

$$|\varphi^{(n+1)}\rangle = e^{-\mathcal{H}\Delta\tau}|\varphi^{(n)}\rangle \approx \left[1 - \Delta\tau\left(\frac{-\hbar^2}{2m}\nabla^2 + U\right)\right]|\varphi^{(n)}\rangle \tag{2}$$

$$\Delta\tau \cong 0.05 \cdot \frac{(\Delta x)^2}{4} \cdot \frac{2m}{\hbar^2}$$

Upon reaching self-consistency of the wavefunction between subsequent time-steps, equation (3) defines the relation to the chemical potential μ with a planar system dependent upon the z direction. A similar iterative process can be performed with a matrix diagonalization technique which calculates the lowest eigenvalue returned as the chemical potential through a Schrödinger-like equation.

Equation (3) defines the relationship between the kinetic energy, mean field, and chemical potential operating on the wavefunction in Cartesian coordinates.

$$-\frac{\hbar^2}{2m}\nabla^2\,\varphi(z) + U(z)\,\varphi(z) = \mu\,\varphi(z) \tag{3}$$

Interactions within liquid ^{4}He are relatively simple as van der Waals forces are the dominant interactions between atoms. Therefore, the predominant forces within the fluid are assumed to be defined mainly by two-body potentials.[18] The relevance of a three-body potential relies upon the strength of theory to describe such terms.[25] It is believed

that the first solvation shell of liquid ^{4}He approaches densities of the solid phase where three-body interactions then become important. Properties of interest of quantum fluids are the structure, phase transitions, binding energies, excitation spectra, and properties where bulk character is apparent.

Szybisz[24] looks at DFT compared to Monte Carlo (MC) techniques for energetic calculations of free films of liquid helium. DFT lacks an inherent test for accuracy, and so it is imperative to examine the results from a secondary method. QMC simulations are accepted as a highly accurate computational analysis of a quantum system of bosons. Three-body interactions of importance in liquid argon and krypton suggest that they play a role in liquid helium as well. At the critical density, triple dipole (DDD) interactions exhibit the largest contribution to the potential for liquid krypton. The triple dipole or Axilrod Teller terms define weak, long-range, three-body interactions that must be damped at close-range. Calculations of krypton indicate that three-body corrections play a larger role in the energy per particle calculations.[26]

Pairwise additive interaction potentials can currently be calculated with a high degree of accuracy using *ab initio* methods. Much improvement in correlation with experimental data has been made in calculations of ^{4}He ground state properties with terms added to account for phenomenological data. As mentioned previously, an interesting question of current literature is whether a Mg or Ca atom will be solvated or remain in dimples closer to the surface of the helium droplet. Both Mg and Ca are close to the cutoff point of potential solvation, noted by the dimensionless lambda. According to Hinde,[15] a Mg atom is indeed solvated, while Ca is proposed to reside in deep pockets below the surface, but not entirely solvated by the ^{4}He droplet. This is also dependent upon the size of the ^{4}He droplet. Further, it is determined that for $N < 30$ atoms Mg resides on the surface.[14] DFT has been used to examine solvation properties of atomic dopants.

3.2 Earliest functional for ^{4}He: Stringari and Treiner

Density functional theory of simple fluids begins with the definition of the energy as a function of the one-body density, where the overall energy is the quantum kinetic energy plus the potential energy interaction. A thorough discussion of the choice of terms can be found in references 2 and 3. For initial forms of the energy functional shown in equation (4), the potential interaction is defined by the simplistic Skyrme interaction with mathematical expressions to represent long and short-range effects.[2, 3]

(4)

$$E_{kinetic}\,[\rho] + E_{Skyrme}\,[\rho] = \int d^3r \frac{\hbar^2}{2m}|\nabla\varphi|^2 + \int d^3r \left\{\frac{b}{2}\rho^2 + \frac{c}{2}\rho^{(2+\gamma)} + d(\nabla\rho)^2\right\}$$

Where the one-body density is equal to the square of the wavefunction.

(5)

$$\rho = \varphi^2$$

Parameters are chosen to reproduce experimental values of surface tension, equation of state, and bulk liquid properties with the following definitions for ^{4}He.[2, 3]

$$b = -8.88810\ x\ 10^2 K\ \text{Å}^3$$
$$c = 1.04554\ x\ 10^7 K\ \text{Å}^{3(1+\gamma)}$$
$$d = 2.383\ x\ 10^3 K\ \text{Å}^5$$
$$\gamma = 2.8$$

To discuss the terms which contribute to the Skyrme potential, each will be referenced in relation to their corresponding coefficients of *b*, *c*, and *d*. The *b* term is a negative

contribution to the energy, defining the attractive forces with a favorable interaction potential dependent upon the square of the density. The *c* term is positive, indicative of a repulsive term that contains the density held to a power greater than two. As the atoms become closer and closer together, this term becomes more significant than a squared term. The gradient term with the *d* coefficient favors bulk density over surface positions, since the term is zero where the density remains constant and non-zero at places of fluctuation in the density such as at surface interactions.

With an expression for the kinetic and potential energies, one can extrapolate directly the mean field potential, represented by $U[\rho]$, by taking the first functional derivative of the potential with respect to the one-body density represented by equation (6). The total energy is a definition of the entire system, while the mean field potential delineates an effective interaction with respect to one atom.

$$\frac{\delta E[\rho]}{\delta \rho} = U[\rho] \tag{6}$$

The mean field expression for the Stringari and Treiner functional is given by equation (7), where *r* is the generic variable of change along the coordinate system.

$$U(r) = b\rho(r) + \frac{2+\gamma}{2} c\, \rho(r)^{(1+\gamma)} - 2d\nabla^2\rho(r) \tag{7}$$

The initial density profile guess from Stringari and Treiner is given in equation (8). The use of this equation is dependent upon the location of the interface. A fair trial density, along with the mean field expression, is produced to intiate the matrix diagonalization process.

(8)

$$\rho(r) = \frac{\rho_0}{\left[1 + \exp\left(\frac{r}{a_{in}}\right)\right]^{\upsilon}}$$

The trial density has the following parameters.

$$\rho_0 = 0.021836\ \text{Å}^{-3}$$

$$a_{in} = 1.96\ \text{Å}$$

$$\upsilon = 2.5$$

With the mean field of equation (7), there is now a practical application of the density functional theory to produce a self-consistent density profile, along with the corresponding chemical potential from the implementation of a matrix diagonalization subroutine.

3.3 First improvements: Orsay-Paris collaboration

Improvements to the Stringari and Treiner functional are seen in adjustments to the Skyrme potential,[3] replacing the attractive b term with a Lennard-Jones 6-12 potential seen as the first term of the $E_{potential}$ of equation (9). This creates an effective screening at short distances and an attractive interaction at long-range distances. The positive c term from the Skyrme interaction is replaced by the second term of the potential energy that increases in response to hard core repulsion at short distances. Equation (9) is the overall energy interaction, corresponding to the Stringari and Treiner expression in equation (4). The vector $\boldsymbol{r}$ describes the point at which the function exists on the grid coordinate system, while the vector $\boldsymbol{r'}$ represents movement along a second axis throughout the fluid.

(9)

$$E_{kinetic}\ [\rho] + E_{potential}\ [\rho] = \int d^3r \frac{\hbar^2}{2m} |\nabla\varphi|^2 + \frac{1}{2}\int\int d^3r\ d^3r'\ \rho(\boldsymbol{r})\rho(\boldsymbol{r}')V_l(|\boldsymbol{r}-\boldsymbol{r}'|) + \int d^3r\ \frac{c}{2}\rho(\boldsymbol{r})\bar{\rho}_{\boldsymbol{r}}{}^{(1+\gamma)}$$

With the Lennard-Jones potential defined by $V_l(|\boldsymbol{r}-\boldsymbol{r}'|)$, with appropriate screening at short distances.

| **r- r'** | > h $\qquad$ $V_l(|\boldsymbol{r}-\boldsymbol{r}'|) = 4\varepsilon\left[\left(\frac{\alpha}{|\boldsymbol{r}-\boldsymbol{r}'|}\right)^{12} - \left(\frac{\alpha}{|\boldsymbol{r}-\boldsymbol{r}'|}\right)^{6}\right]$

| **r - r'** | ≤ h $\qquad$ $V_l(|\boldsymbol{r}-\boldsymbol{r}'|) = V_l(h)\left(\frac{|\boldsymbol{r}-\boldsymbol{r}'|}{h}\right)^4$

The parameters for the ^{4}He Lennard-Jones potential are listed below.

$$\varepsilon = 10.22\ K$$
$$\alpha = 2.556\ \text{Å}$$
$$\gamma = 2.8$$
$$h = 2.377\text{Å}$$
$$c = 1.04554\ x\ 10^7 K\ \text{Å}^{3(1+\gamma)}$$

The coarse-grained density represented by $\bar{\rho}_{\boldsymbol{r}}$ is given in equation (10) and is used in lieu of the Skyrme interaction term *c*. This sets up an averaging sphere over which the density is calculated.

(10)

$$\bar{\rho}_{\boldsymbol{r}} = \int d^3r\, \rho(\boldsymbol{r})\, \Pi_h(\boldsymbol{r} - \boldsymbol{r}')$$

The following are limitations for $\Pi_h(\boldsymbol{r} - \boldsymbol{r}')$.

$$|\ \mathbf{r} - \mathbf{r'}\ | > \mathrm{h} \qquad \Pi_h(\boldsymbol{r} - \boldsymbol{r}') = 0$$

$$|\ \mathbf{r} - \mathbf{r'}\ | \leq \mathrm{h} \qquad \Pi_h(\boldsymbol{r} - \boldsymbol{r}') = \frac{3}{4\pi h^3}$$

The limit h is parameterized to the coefficient b, which comes from experimental data. The mean field is taken as the first functional derivative to the potential energy with respect to the density. This yields the Orsay-Paris mean field expression seen in equation (11).

(11)

$$U(\boldsymbol{r}) = \int d^3r'\, \rho(\boldsymbol{r}')\, V_l(|\boldsymbol{r} - \boldsymbol{r}'|) + \frac{c}{2}\,(\bar{\rho}_{\boldsymbol{r}})^{(\gamma+1)} + \frac{c}{2}(1+\gamma)\int d^3r'\, \Pi_h(|\boldsymbol{r} - \boldsymbol{r}'|)\rho(\boldsymbol{r}')(\bar{\rho}_{\boldsymbol{r}'})^{\gamma}$$

Here, $\boldsymbol{r}$ and $\boldsymbol{r'}$ are vector quantities, which must be integrated out over two variables, following the assumption that the density is dependent upon the movement perpendicular to the phase transition interface. Further details of the exploitation of this functional form can be found in a later section.

Calculation of the quantum kinetic energy density given by equation (12) and free energy density given by equation (13) is useful in the analysis of the final self-consistent mean field along the fluid-vacuum interface. Appropriate units are $K\text{Å}^{-3}$.

The quantum kinetic energy density,

$$\hbar^2|\nabla\phi|^2/_{2m} \tag{12}$$

and free energy density,

$$\mathcal{H}[\rho] - \mu\,\rho \tag{13}$$

are shifted to the sharpest part of the density profile along the coordinate system. The location of these curves in relation to the density profile is an appropriate recreation of the character of van der Waals fluids.[3]

3.4 Further improvements: Orsay-Trento collaboration

The Orsay-Trento functional[11] is an advancement to the Orsay-Paris collaboration, with the total energy given by equation (14). Here, the Lennard-Jones potential is entirely screened at short-distances and replaced by a gradient-gradient term, which more effectively assimilates short-range interactions into the energy expression. The *c* term from the original Skyrme potential is replaced with two terms dependent upon varying powers of a coarse-grained density averaged over sphere with radius *h*. For the Orsay-Trento functional, *h* takes on a different value from the preceding Orsay-Paris functional.

(14)

$$E_{kinetic}\,[\rho] + E_{potential}\,[\rho] = \int d^3r\,\frac{\hbar^2}{2m}|\nabla\varphi|^2 + \frac{1}{2}\int\int d^3r\,d^3r'\,\rho(\boldsymbol{r})\rho(\boldsymbol{r}')V_l^e(|\boldsymbol{r}-\boldsymbol{r}'|)$$

$$+\frac{c_2}{2}\int d^3r\,\rho(\boldsymbol{r})(\bar{\rho}_{\boldsymbol{r}})^2 + \frac{c_3}{3}\int d^3r\,\rho(\boldsymbol{r})(\bar{\rho}_{\boldsymbol{r}})^3 - \frac{\hbar^2}{4m}\alpha_s\int\int d^3r\,d^3r'\,F(|\boldsymbol{r}-\boldsymbol{r}'|)$$

$$\times\left(1-\frac{\rho(\boldsymbol{r})}{\rho_{0s}}\right)\nabla\rho(\boldsymbol{r})\cdot\nabla\rho(\boldsymbol{r}')\left(1-\frac{\rho(\boldsymbol{r}')}{\rho_{0s}}\right)$$

The additional terms allow for enhanced sensitivity of energetic calculations across the transition interface of the density profile. The coarse-grained density is similarly defined as before by equation (15).

(15)

$$\bar{\rho}_{\boldsymbol{r}} = \int d^3r\,\rho(\boldsymbol{r})\,\Pi_h(\boldsymbol{r}-\boldsymbol{r}')$$

for $|\,\mathbf{r}-\mathbf{r'}\,| > \mathrm{h}$ $\qquad\qquad$ $\Pi_h(\boldsymbol{r}) = 0$

for $|\,\mathbf{r}-\mathbf{r'}\,| \leq \mathrm{h}$ $\qquad\qquad$ $\Pi_h(\boldsymbol{r}) = \frac{3}{4\pi h^3}$

The three dimensional Gaussian weighting function is given by equation (16),

$$F(|\boldsymbol{r}-\boldsymbol{r}'|)=\frac{1}{\pi^{3/2}\ l^3}\ e^{-|\boldsymbol{r}-\boldsymbol{r}'|^2/l^2} \tag{16}$$

where $l = 1$ Å.

The Lennard-Jones pair potential is given below and entirely screened at short-distances.

$|\ \mathbf{r}-\mathbf{r'}\ |\ > \mathrm{h}$ $\qquad V_l^e(|\boldsymbol{r}-\boldsymbol{r}'|)=4\varepsilon\left[\left(\frac{\sigma}{|\boldsymbol{r}-\boldsymbol{r}'|}\right)^{12}-\left(\frac{\sigma}{|\boldsymbol{r}-\boldsymbol{r}'|}\right)^{6}\right]$

$|\ \mathbf{r}-\mathbf{r'}\ |\ \leq \mathrm{h}$ $\qquad V_l^e(|\boldsymbol{r}-\boldsymbol{r}'|)=0$

The screening effect is replaced by the gradient-gradient term. Parameter constants for the mean field expression are defined below.

$$h = 2.1903\ \text{Å}$$
$$\rho_{0s} = 0.04\ \text{Å}^{-3}$$
$$c_2 = -2.411857x10^4\ K\ \text{Å}^6$$
$$c_3 = 1.858496x10^6\ K\ \text{Å}^9$$
$$\alpha_s = 54.31\ \text{Å}^3$$

Here σ and ε correspond to the Lennard-Jones parameters of the He-He pair interaction.

$$\sigma = 2.556\ \text{Å}$$
$$\mathcal{E} = 10.22\ K$$

Finally, through similar measures, the form of the mean field is given by equation (17) and can be found as equation 14 in reference 29. Authors Eloranta et al. note that the weighted average term $\tilde{\rho}(\boldsymbol{r})$ in the division with ρ_{0s} is reduced to $\rho(\boldsymbol{r})$ in order to simplify computational time. This is a fair approximation in most cases.

(17)

$$U(\boldsymbol{r}) = \int d^3r'\,\rho(\boldsymbol{r}')V_l^e(\boldsymbol{r},\boldsymbol{r}') + \frac{c_2}{2}(\bar{\rho}_{\boldsymbol{r}})^2 + c_2\int d^3r'\,\rho(\boldsymbol{r}')\bar{\rho}_{\boldsymbol{r}'}\,\Pi_{\mathrm{h}}(\boldsymbol{r},\boldsymbol{r}') + \frac{c_3}{3}(\bar{\rho}_{\boldsymbol{r}})^3$$

$$+c_3\int d^3r'\,\rho(\boldsymbol{r}')(\bar{\rho}_{\boldsymbol{r}'})^2\Pi_{\mathrm{h}}(\boldsymbol{r},\boldsymbol{r}')$$

$$+\frac{\hbar^2}{2m}\alpha_s\left(1-\frac{\rho(\boldsymbol{r})}{\rho_{0s}}\right)\int d^3r'\,\nabla_{\boldsymbol{r}}F(|\boldsymbol{r}-\boldsymbol{r}'|)\cdot\nabla\rho(\boldsymbol{r}')\left(1-\frac{\rho(\boldsymbol{r}')}{\rho_{0s}}\right)$$

Due to the vector quantities ***r*** and ***r'***, the mean field must also be integrated to a form dependent upon one-dimension for the application of the Schrödinger-like formulation of equation (3). The manipulation of the three mean field functionals is discussed in the following chapter.

Chapter 4: Methodology of current research

4.1 Definitions of the mean field

Much of the following mean field definitions can be pieced together from various papers throughout the literature in one version or another. See references 2, 3, 11, 24, and 27. The current treatment of the mean field potentials and surface density profiles are included in the following sections.

4.1.1 Stringari and Treiner

The Stringari and Treiner functional is the least demanding of the three examined in this work because integration is not required to obtain the mean field potential.

4.1.1.1 Planar symmetry

Planar slabs are designed with a system of Cartesian coordinates, so that the pertinent form of the mean field is given by equation (18), where the z coordinate is perpendicular to the fluid-vacuum interface.

(18)

$$U(z) = b\rho(z) + \frac{2+\gamma}{2} c\,\rho(z)^{(1+\gamma)} - 2d\nabla^2\rho(z)$$

The mean field will then employ an approximation that will be discussed in the technical details section of the present research to write the Laplacian in terms that are accessible to computer languages.

$$U(z) = b\rho(z) + \frac{2+\gamma}{2} c\,\rho(z)^{(1+\gamma)} - \frac{2d}{(\Delta z)^2}[\rho(z+\Delta z) - 2\rho(z) + \rho(z-\Delta z)] \tag{19}$$

Here, Δz is the z grid-coordinate system spacing between each point on the z-axis. This value can be arbitrarily chosen to allow for sufficient spacing resolution of the system. With the mean field approximation in equation (19) and the kinetic energy operator, the Hamiltonian and corresponding wavefunction calculated from the density profile can be input to the eigenvalue subroutine. The subroutine calculates all of the eigenvalues using the iterative process of matrix diagonalization, returning the lowest eigenvalue in the form of the chemical potential. This process is looped until self-consistency is achieved when the difference between the density values in subsequent time-steps becomes inconsequential.

4.1.1.2 Droplet with spherical symmetry

For the Stringari and Treiner mean field applied to helium droplets, the Laplacian is merely evolved into spherical polar coordinates, where the density is dependent only upon r, the direction perpendicular to the phase transition interface. The spherical mean field is defined by Equation (20).

(20)

$$U(r) = b\rho(r) + \frac{2+\gamma}{2} c\, \rho(r)^{(1+\gamma)} - 2d\nabla^2\rho(r)$$

Equation (21) utilizes central difference approximations for the first and second derivatives to appeal to a viable form of the Laplacian in the mean field expression.

(21)

$$U(r) = b\rho(r) + \frac{2+\gamma}{2} c\, \rho(r)^{(1+\gamma)}$$

$$-2d\left\{\left(\frac{1}{(\Delta r)^2}\left(\rho(r+\Delta r) - 2\rho(r) + \rho(r-\Delta r)\right)\right) + \left(\frac{1}{r\Delta r}\left(\rho(r+\Delta r) - \rho(r-\Delta r)\right)\right)\right\}$$

With the mean field forms given in equations (19) and (21), an iterative process can propagate the wavefunction in time with a matrix diagonalization of the eigenfunctions of the Hamiltonian to return the lowest eigenvalue. Upon self-consistency of this cycle, the optimized wavefunction can be used to model energetic properties of ^{4}He systems of planar slabs and droplets.

4.1.2 Orsay-Paris collaboration

The total energy or correlation energy of the Orsay-Paris collaboration contains double integration, which influences the integro-form of the mean field expression dissimilar to the Stringari and Treiner mean field.

4.1.2.1 Planar symmetry

For a planar system in Cartesian coordinates, the vector quantity $|\boldsymbol{r} - \boldsymbol{r'}|$ is defined by the following the relation $|\boldsymbol{r} - \boldsymbol{r}'| = \sqrt{(x - x')^2 + (y - y')^2 + (z - z')^2}$. With z chosen as the direction perpendicular to the fluid-vacuum, the first step is to reorder the limits of integration, so that the function can be integrated out over dx' and dy' with the use of trigonometric identities. The prime variables track the movement throughout the liquid in relation to the non-prime variables. Upon the integration of x' and y' directions, the mean field becomes dependent upon the z' direction for each value of z, following previously established theory of superfluid helium systems. The z coordinate defines the location along the coordinate system, while z' is the variable of integration. Two integrals, one of the coarse-grained density expression and one for the mean field functional, must be established to set the precedence for utilization of the time-step method. The coarse-grained density is given in equation (22) for a planar system. Limits of integration for close range exchanges are defined for values of z' between $z - h$ and $z + h$.

(22)

$$\bar{\rho}_z = \frac{3}{4h} \int_{z-h}^{z+h} dz' \rho(z') \left(1 - \left(\frac{z - z'}{h}\right)^2\right)$$

Equation (23) is the mean field equation dependent upon the z direction. Equation (23) is given in references 3 and 24 while equation (22) can also be found in reference 24.

(23)

$$U(z) = 4\pi\varepsilon\alpha^2 \int_{z+h}^{\infty} dz' \, \rho(z') \left\{ \frac{1}{5} \left(\frac{\alpha}{z - z'} \right)^6 - \frac{1}{2} \right\} \left(\frac{\alpha}{z - z'} \right)^4$$

$$+ 4\pi\varepsilon\alpha^2 \int_{z-h}^{z+h} dz' \rho(r') \left\{ \left(\frac{8}{15} \left(\frac{\alpha}{h} \right)^6 - \frac{5}{6} \right) - \frac{1}{3} \left(\left(\frac{\alpha}{h} \right)^6 - 1 \right) \left(\frac{z - z'}{h} \right)^6 \right\} \left(\frac{\alpha}{h} \right)^4$$

$$+ 4\pi\varepsilon\alpha^2 \int_{-\infty}^{z-h} dz' \, \rho(z') \left\{ \frac{1}{5} \left(\frac{\alpha}{z - z'} \right)^6 - \frac{1}{2} \right\} \left(\frac{\alpha}{z - z'} \right)^4$$

$$+ \frac{3c}{8h} (1 + \gamma) \int_{z-h}^{z+h} dz' \left(1 - \left(\frac{z - z'}{h} \right)^2 \right) \rho(z') (\bar{\rho}_{z'})^{\gamma} + \frac{c}{2} (\bar{\rho}_z)^{\gamma+1}$$

Parameters are defined in the previous chapter within the original definition of the mean field. The first three terms include the Lennard-Jones potential at long range and a screening effect at short distances according to the limits of integration, while the fourth and fifth terms represent the short-range exchanges of hard core repulsion.

4.1.2.2 Droplet with spherical symmetry

The previous technique is applied to a spherical droplet system in the form of spherical polar coordinates (r, θ, ϕ) and (r', θ', ϕ'). The r coordinate is perpendicular to the interface, and θ' and ϕ' variable forms are integrated out of the functional leaving a dependence upon r'. Here, to define the vector quantity $|\boldsymbol{r} - \boldsymbol{r'}|$, we use the Law of

Cosines, relating *cos θ'* in terms of *r* and *r'*. The integral containing *dθ'* undergoes a change of variable to *dcos θ'* for the ease of integration, according to the implementation of equation (24).

$$(|\boldsymbol{r} - \boldsymbol{r}'|)^2 = u^2 = r^2 + (r')^2 - 2\, r\, r' \cos\theta' = h^2 \tag{24}$$

Solving for *cos θ'*, one arrives at equation (25), which will be used to define limits of integration for *cos θ'* with respect to the constant *h*.

$$\cos\theta' = \frac{r^2 + (r')^2 - h^2}{2\, r\, r'} \tag{25}$$

Due to constraints upon the limits of integration in varied regions of the coordinate grid, the system must be divided into three unambiguous regions in space, $r = 0$, $r \leq h$, and $r > h$. The limits for ϕ' are from *0* to 2π in all cases.

For the point at which $r = 0$, the center of the averaging sphere between $r - h$ and $r + h$ lies exactly at the origin of the coordinate grid system, where the limiting regions for *r'* are divided between *0* to *h* and *h* to ∞, with corresponding limits $1 \leq \cos\theta' \leq -1$ for both areas in space. Limits are dependent upon the location of the *r'* value of integration.

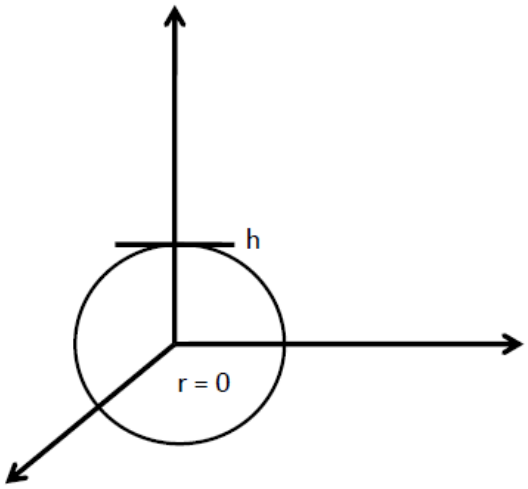

Figure 1. Short-range averaging sphere for $r = 0$.

For $r = 0$,

(26)

$$\bar{\rho}_r = \frac{3}{h^3}\int_0^h dr'(r')^2\rho(r')$$

To avoid the singularity of dividing by 0, *U(r)* must be defined for the special case of $r = 0$.

(27)

$$U(r) = \frac{16\pi\varepsilon}{h^4}\left[\left(\frac{\alpha}{h}\right)^{12} - \left(\frac{\alpha}{h}\right)^{6}\right]\int_0^h dr'\,(r')^6\,\rho(r') + 16\pi\varepsilon\int_h^\infty dr'\,\rho(r')\left\{\left[\frac{\alpha^{12}}{(r')^{10}}\right] - \left[\frac{\alpha^6}{(r')^4}\right]\right\}$$

$$+ \frac{3c}{h^3}(1+\gamma)\int_0^h dr'(r')^2\rho(r')\,(\bar{\rho}_{r'})^{\gamma} + \frac{c}{2}(\bar{\rho}_r)^{\gamma+1}$$

For r values less than or equal to h, the averaging sphere must be divided into two spheres with limits on r' of 0 to $h - r$ and $h - r$ to $r + h$. This depiction allows for the separation of an inner and an outer sphere with unique limits on $\cos\theta'$. For the inner sphere, limits have the following values $0 < r' \leq h - r$ and $1 \leq \cos\theta' \leq -1$. For the outer sphere, the limits become $h - r \leq r' \leq r + h$ and $1 \leq \cos\theta' \leq \frac{r^2+(r')^2-h^2}{2\,r\,r'}$. Refer to Figure 2 for a schematic drawing of the regions in space.

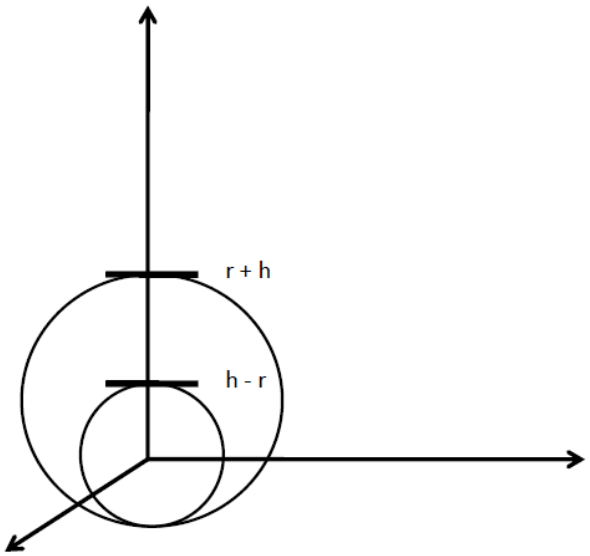

Figure 2. Depiction of the inner and outer averaging spheres.

In this the region where $r \leq h$, the coarse-grained density takes the form of equation (28).

(28)

$$\bar{\rho}_r = \frac{3}{h^3}\int_0^{h-r} dr'\,(r')^2\rho(r') + \frac{3}{2h^3}\int_{h-r}^{r+h} dr'\,(r')^2\rho(r')\left(1 - \frac{-h^2 + r^2 + (r')^2}{2\,r\,r'}\right)$$

The spherical mean field expression for r values less than or equal to h is described by equation (29).

(29)

$$U(r) = \frac{4\pi\varepsilon}{3h^4}\left[\left(\frac{\alpha}{h}\right)^{12} - \left(\frac{\alpha}{h}\right)^{6}\right]\int_0^{h-r} dr'\,\frac{r'\rho(r')}{r}\{(r^2 + (r')^2 + 2\,r\,r')^3 - (r^2 + (r')^2 - 2\,r\,r')^3\}$$

$$+ \frac{4\pi\varepsilon}{3h^4}\left[\left(\frac{\alpha}{h}\right)^{12} - \left(\frac{\alpha}{h}\right)^{6}\right]\int_{h-r}^{r+h} dr'\,\frac{r'\rho(r')}{r}\,[h^6 - (r^2 + (r')^2 - 2\,r\,r')^3]$$

$$+ 8\pi\varepsilon\int_{r+h}^{\infty} dr'\,\frac{r'\rho(r')}{r}\left\{\frac{\alpha^{12}}{10}\left(\frac{1}{(r^2 + (r')^2 - 2\,r\,r')^5} - \frac{1}{(r^2 + (r')^2 + 2\,r\,r')^5}\right)\right.$$
$$\left. - \frac{\alpha^6}{4}\left(\frac{1}{(r^2 + (r')^2 - 2\,r\,r')^2} - \frac{1}{(r^2 + (r')^2 + 2\,r\,r')^2}\right)\right\}$$

$$+ 8\pi\varepsilon\int_{h-r}^{r+h} dr'\,\frac{r'\rho(r')}{r}\left\{\frac{\alpha^{12}}{10}\left(\frac{1}{h^{10}} - \frac{1}{(r^2 + (r')^2 + 2\,r\,r')^5}\right) - \frac{\alpha^6}{4}\left(\frac{1}{h^4} - \frac{1}{(r^2 + (r')^2 + 2\,r\,r')^2}\right)\right\}$$

$$+\frac{3c}{h^3}(1+\gamma)\int_0^{h-r} dr'(r')^2\rho(r')\,(\bar{\rho}_{r'})^{\gamma}+\frac{c}{2}(\bar{\rho}_r)^{\gamma+1}$$

$$+\frac{3c}{2h^3}(1+\gamma)\int_{h-r}^{r+h} dr'(r')^2\rho(r')(\bar{\rho}_{r'})^{\gamma}\left(1-\frac{-h^2+r^2+(r')^2}{2\,r\,r'}\right)$$

The third form of the functional comes from values of r greater than h. Figure 3 is an arbitrary set-up of r' located outside of the averaging sphere with r values greater than h. Notice the definitions of h, r, r', θ', ϕ' and $|r-r'|$.

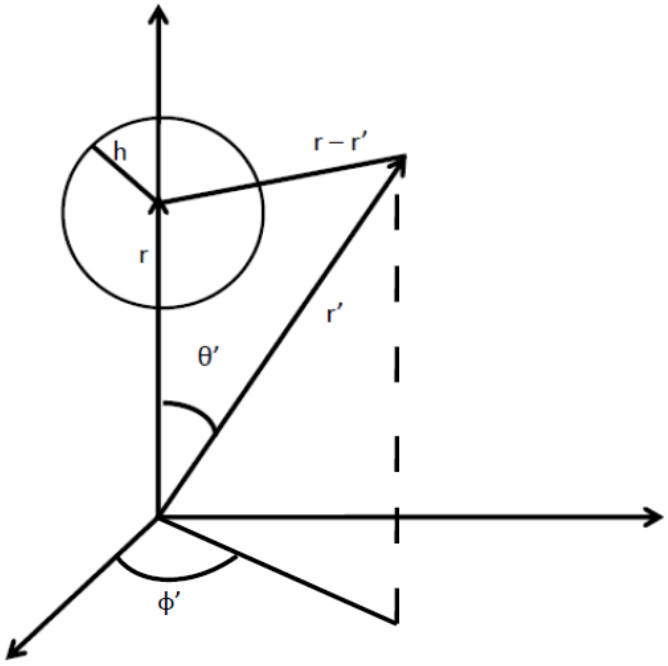

Figure 3. Generalized depiction of the averaging sphere.

For values of r greater than h, the coarse-grained density in spherical coordinates is given by equation (30).

(30)

$$\overline{\rho}_r = \frac{3}{2h^3}\int_{r-h}^{r+h} dr'\,(r')^2\rho(r')\left(1-\frac{-h^2+r^2+(r')^2}{2\,r\,r'}\right)$$

The form of equation (30) comes from integration over the variables $cos\ \theta'$ and φ'. The corresponding mean field is expressed by equation (31).

(31)

$$U(r) = 8\pi\varepsilon\int_0^{r-h} dr'\,\frac{r'\rho(r')}{r}\left\{\frac{\alpha^{12}}{10}\left(\frac{1}{(r^2+(r')^2-2\,r\,r')^5}-\frac{1}{(r^2+(r')^2+2\,r\,r')^5}\right)\right.$$
$$\left.-\frac{\alpha^6}{4}\left(\frac{1}{(r^2+(r')^2-2\,r\,r')^2}-\frac{1}{(r^2+(r')^2+2\,r\,r')^2}\right)\right\}$$

$$+\,8\pi\varepsilon\int_{r+h}^{\infty} dr'\,\frac{r'\rho(r')}{r}\left\{\frac{\alpha^{12}}{10}\left(\frac{1}{(r^2+(r')^2-2\,r\,r')^5}-\frac{1}{(r^2+(r')^2+2\,r\,r')^5}\right)\right.$$
$$\left.-\frac{\alpha^6}{4}\left(\frac{1}{(r^2+(r')^2-2\,r\,r')^2}-\frac{1}{(r^2+(r')^2+2\,r\,r')^2}\right)\right\}$$

$$+\,\frac{4\pi\varepsilon}{3h^4}\left[\left(\frac{\alpha}{h}\right)^{12}-\left(\frac{\alpha}{h}\right)^{6}\right]\int_{r-h}^{r+h} dr'\,\frac{r'\rho(r')}{r}\left[h^6-(r^2+(r')^2-2\,r\,r')^3\right]$$

$$+ 8\pi\varepsilon \int_{r-h}^{r+h} dr' \frac{r' \rho(r')}{r} \left\{ \frac{\alpha^{12}}{10} \left(\frac{1}{h^{10}} - \frac{1}{(r^2 + (r')^2 + 2\, r\, r')^5} \right) - \frac{\alpha^6}{4} \left(\frac{1}{h^4} - \frac{1}{(r^2 + (r')^2 + 2\, r\, r')^2} \right) \right\}$$

$$+ \frac{c}{2} (\bar{\rho}_r)^{(\gamma+1)} + \frac{3c}{2h^3} (1 + \gamma) \int_{r-h}^{r+h} dr' \, (r')^2 \, \rho(r') (\bar{\rho}_{r'})^{\gamma} \left(1 - \frac{-h^2 + r^2 + (r')^2}{2\, r\, r'} \right)$$

Parameters are previously noted within the definition of the mean field. *U(z)* of the Orsay-Paris collaboration is now in an appropriate form to compute energetic calculations, such as the chemical potential, and optimized density profiles for ground state systems of ^{4}He at *0 K* and zero pressure.

4.1.3 Orsay-Trento collaboration

With the repetition of the approach previously undertaken for both Cartesian and spherical polar coordinates, a similar derivation can be obtained for the Orsay-Trento mean field and corresponding equations.

4.1.3.1 Planar symmetry

For a planar system, the vector quantity $|\mathbf{r} - \mathbf{r'}|$ is again defined by the following, $|\boldsymbol{r} - \boldsymbol{r}'| = \sqrt{(x - x')^2 + (y - y')^2 + (z - z')^2}$. The variable vector $\boldsymbol{r}$ indicates location in the fluid, while $\boldsymbol{r'}$ examines movement within the fluid. Similar to the Orsay-Paris collaboration for a planar slab, the definition of the coarse-grained density is given by equation (32).

(32)

$$\bar{\rho}_z = \frac{3}{4h}\int_{z-h}^{z+h} dz'\rho(z')\left(1-\left(\frac{z-z'}{h}\right)^2\right)$$

The corresponding mean field is given in equation (33) with the consideration of novel terms due to improvements upon the Orsay-Paris functional. A version of equation (33) can be found in reference 24 as equation A.11.

(33)

$$U(z) = 4\pi\varepsilon\sigma^2\int_{-\infty}^{z-h} dz'\,\rho(z')\left\{\frac{1}{5}\left(\frac{\sigma}{z-z'}\right)^6-\frac{1}{2}\right\}\left(\frac{\sigma}{z-z'}\right)^4$$

$$+4\pi\varepsilon\sigma^2\int_{z+h}^{\infty} dz'\,\rho(z')\left\{\frac{1}{5}\left(\frac{\sigma}{z-z'}\right)^6-\frac{1}{2}\right\}\left(\frac{\sigma}{z-z'}\right)^4$$

$$+4\pi\varepsilon\sigma^2\int_{z-h}^{z+h} dz'\rho(z')\left\{\frac{1}{5}\left(\frac{\sigma}{h}\right)^6-\frac{1}{2}\right\}\left(\frac{\sigma}{h}\right)^4+\frac{c_2}{2}(\bar{\rho}_z)^2+\frac{3c_2}{4h}\int_{z-h}^{z+h} dz'\rho(z')\,\bar{\rho}_{z'}\left\{1-\left(\frac{z-z'}{h}\right)^2\right\}+$$

$$+\frac{c_3}{3}(\bar{\rho}_z)^3+\frac{3c_3}{4h}\int_{z-h}^{z+h} dz'\rho(z')(\bar{\rho}_{z'})^2\left\{1-\left(\frac{z-z'}{h}\right)^2\right\}$$

$$+\frac{\hbar^2}{2m}\frac{\alpha_s}{\rho_{0s}}\int_{-\infty}^{\infty} dz'F(|z-z'|)\left(\frac{d\rho(z')}{dz'}\right)I(z')+\frac{\hbar^2}{2m}\alpha_s\frac{d}{dz}\left\{\left(1-\frac{\tilde{\rho}(z)}{\rho_{0s}}\right)I(z)\right\}$$

The intermediate function *I(z)* is represented by the following equation.

(34)

$$I(z) = \int_{-\infty}^{\infty} dz' \left(1 - \frac{\tilde{\rho}(z')}{\rho_{0s}}\right) F(|z - z'|) \frac{d\rho(z')}{dz'}$$

A new function, the average weighted density in three dimensions is introduced in equation (35).

(35)

$$\tilde{\rho}(z) = \int d^3\boldsymbol{r}' \rho(z') F(|\boldsymbol{r} - \boldsymbol{r}'|)$$

Since the density variation lies in one direction, equation (35) is simplified to equation (36) as an adequate approximation.

(36)

$$\tilde{\rho}(z) = \int_{-\infty}^{\infty} dz' \rho(z') F(|z - z'|)$$

With $F(|\boldsymbol{r} - \boldsymbol{r}'|)$ simplified to a one-dimensional Gaussian; however, this approximation does not work as well in circumstances of strong binding.[27]

(37)

$$F(|z - z'|) = \frac{1}{\pi^{1/2}\, l} e^{-(z-z')^2/l^2}$$

$$l = 1\ \text{Å}$$

Now, the Orsay-Trento functional has been evolved into a complete set of equations and constants that allow manipulations of planar slabs of superfluid helium. The process continues with the optimization of the wavefunction to produce the chemical potential and density profile. Further emphasis will be examined in the technical details of the current report.

4.1.3.2 Droplet with spherical symmetry

The spherical droplet system of the Orsay-Trento collaboration follows the previously established methodology for droplets with the exception of variance in certain terms between the Orsay-Paris and Orsay-Trento. Variables of θ' and ϕ' are integrated out of the functions to yield dependence only upon r'. The expressions are divided into three unambiguous regions in space and the Law of Cosines is used to encapsulate the variables of integration. Since the methodology has not yet been tested, the representative equations for this section are included in Appendix B.

At the current point, the mean fields have undergone viable formatting to reach coding capacity. Representative programs for the mean fields may be found in the appendices.

4.2 Iterative approach

Initially, a simple program is written to define a trial density profile that mimics both bulk and surface properties with movement along a grid coordinate system. The general form of equation (8) has been used as the density guess for all systems.[2] A simple linear decay is not efficient as an initial guess for the density profile. The

coordinate grid system is defined by the distinctive symmetry of the system of interest, either planar or spherical symmetries with resolution or either Δz or Δr. The density is input into the main program to calculate the mean field, and the wavefunction is defined as the square root of the density. The kinetic energy operator is also delineated here. The mean field plus the kinetic energy becomes the Hamiltonian operating on the wavefunction from which eigenvalues are calculated in a matrix diagonalization subroutine which returns the lowest eigenvalue. From the enhanced wavefunction, a new density is established and a new mean field calculated and returned as the Hamiltonian into the subroutine. The propagation cycle continues until the divergence between each step of the subroutine becomes minimal. Figure 4 depicts the cycling of the wavefunction in Cartesian coordinates towards optimization. The cycle continues until the wavefunction reaches self-consistency.

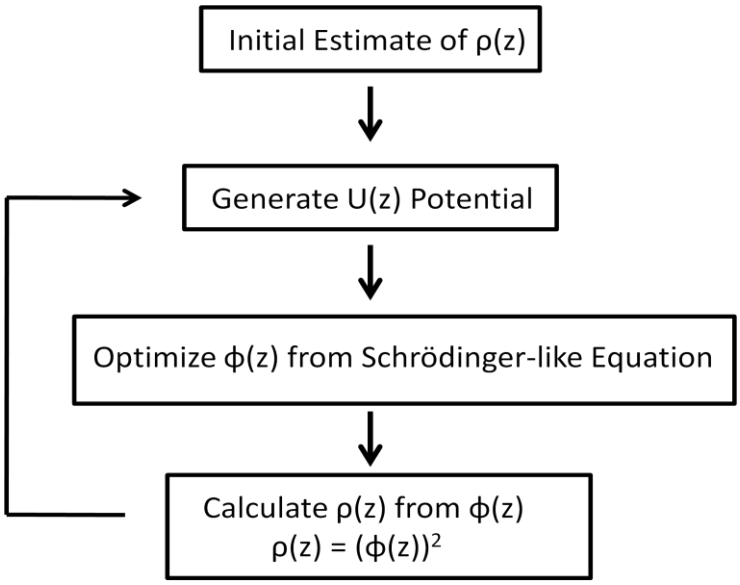

Figure 4. Schematic representation of the optimization cycle.

To incite a proper progression of the wavefuntion between subsequent cycles of the subroutine, a dampening of the density values must occur from old to new. This ensures a small change of the wavefunction from one iteration to the next.[27] The ratio in most calculations of our work is 99.85 % of old density to 0.15 % new density returned as the squared wavefunction from the subroutine. This cycle continues until the difference between each iteration of the subroutine becomes obsolete. The difference at this point is recorded on the order of 1×10^{-5} between iterations.

Planar slabs and droplets are normalized to the integration of the original density function, which in effect normalizes each step in the iterative process to a set number of atoms. This accounts for a systematic approach and maintains a unified system throughout the optimization cycle. In a different manner, altering the initial trial density and subsequent integration value allows us to examine droplets with varied number of atoms in separate simulations.

The presence of an impurity is modeled according to a supplemental He-dopant potential interaction added on to the mean field potential. As an intial characterization of the atomic dopant, the Lennard-Jones pair potential is used to define the helium-impurity interaction. Factors of 2 x LJ potential, 1.5 x LJ potential, and 0.703898 x LJ potential are utilized to test the limits of the helium system. The factor of 0.703898 x LJ potential is chosen to imitate the Mg-He pair interaction extrapolated from a calculation by Hinde.[15] A doped density profile is also created to exhibit zero density at the center of the droplet for the location of the atomic impurity. The matrix diagonalization calculations and iterative process for pure droplets are followed in a similar manner to simulate the doping of droplets.

4.3 Technical details

Section 4.3 deals with particularities applied to the mean field functions. The first consideration is the resolution of Δz or Δr for each of the defined systems. The Stringari and Treiner functional in planar symmetry has a resolution of $\Delta z = 0.1$ Å. For spherical symmetry, the functional is correlated to the Orsay-Paris functional value of h, so that $\Delta r = 0.02377$ Å. All systems of the Orsay-Paris functional use a resolution value of 0.02377 Å for simplicity. Systems that correspond to the Orsay-Trento collaboration have a spacing resolution of 0.021903 Å related to the value of h for the Orsay-Trento functional.

When examining the input of derivatives for the special case of the -∞ endpoint, the derivative is assumed to be constant, so that $\rho(z - \Delta z) = \rho(z)$. The previous also applies to the kinetic energy operator on spherical systems at the $r = 0$ endpoint, which requires a second derivative at a phantom point previous to $r = 0$. The eigenvalue subroutine used for matrix diagonalization of spherical coordinates must be set for real general matrices to account for an asymmetrical Hamiltonian matrix produced in the mean field program. Planar slabs are defined with two interfaces, which produce a symmetrical Hamiltonian operator and utilize a real symmetric matrix for diagonalization. For the +∞ endpoint, the density has decayed to zero, so that the mean field function is itself zero and directly defined as such.

For spherical droplets, the form of certain equations must be multiplied by $2rr'$ to remove the possibility of zero in the denominator for points at which r or $r' = 0$. Although the representative equations from the previous chapters are not explicitly shown in this format, this multiplication is performed when programming the expressions into computer code in order to avoid a singularity in the denominator. Equation (38) is an example of such.

(38)

$$\bar{\rho}_r = \frac{3}{4h^3} \int_{r-h}^{r+h} \frac{dr'(r')\rho(r')}{r} (2\, r\, r' - (-h^2 + r^2 + (r')^2))$$

Evolving the density functionals into a form that could be mathematically represented by the **Fortran** coding, requires the application of certain techniques. Further formatting for the approximations are encompassed in the following sub-sections. Sample code for most of the systems can be found in Appendix A for some of the relevant systems. Upon removal of the dopant potential, the code is the same for pure droplets.

4.3.1 Trapezoid approximation for integration

In circumstances where analytical integration methods are not feasible, the trapezoidal rule of integration can arrive at a finite value for a continous integral. Refer to equation (39) for the definition of the trapezoid rule. The result of the trapezoidal rule is an equitable approximation to exact integration; however, it is highly dependent upon the value of the spacing dz used. For the intents of the research here, the trapezoid rule is used to simplify the integral terms of the density functional to a viable form in the computer code. The calculation is highly limited by the resolution of the slices by which the function is divided. The smaller the spacing, the greater the accuracy and the greater the expenditure. Simulations must find a balance between computational costs and limitations with accuracy of the technique. Even though minimal, the greatest source of error of this work comes from the employment of this technique.

(39)

$$\int_a^b f(z)dz \cong \frac{b-a}{2n}\left[f(z_0) + 2f(z_1) + 2f(z_2) + \cdots 2f(z_{n-1}) + f(z_n)\right]$$

Where, a is the lower limit of integration and b is the upper limit. The function is defined by $f(z)$ at each separation point *0, 1, 2, 3,….* The number of slices is represented by n, while dz is the distance between each segment of the function.

4.3.2 Central difference approximations

The central difference approximations begin with Taylor series expansions of $f(z+h)$ and $f(z-h)$, represented by equations (40) and (41), respectively. Approximations of the first and second derivatives, $f'(z)$ and $f''(z)$, are extracted from these expressions. The h is equivalent to a quantity of Δz or dz, which define the resolution and movement of the ordinate variable of the function.

(40)

$$f(z+h) = f(z) + h\,f'(z) + \frac{1}{2}h^2 f''(z) + \frac{1}{6}h^3 f'''(z) + \frac{1}{24}h^4 f''''(z) + \cdots$$

(41)

$$f(z-h) = f(z) - h\,f'(z) + \frac{1}{2}h^2 f''(z) - \frac{1}{6}h^3 f'''(z) + \frac{1}{24}h^4 f''''(z) \pm \cdots$$

The first-order central difference approximation is truncated at the first-order derivative term and given by the subtraction of the backward step of the function from the forward step, seen in equation (42).

$$f(z+h) - f(z-h) = 2\,h\,f'(z) \pm \cdots \tag{42}$$

Solving for the first derivative gives the expression represented by the following equation.

$$f'(z) \approx \frac{1}{2h}\,[\,f(z+h) - f(z-h)\,] \tag{43}$$

The second-order central difference approximation is pared at the second-order derivative term by the addition of equations (40) and (41) and term cancellation.

$$f(z+h) + f(z-h) = 2\,f(z) + \frac{2}{2}h^2 f''(z) + \cdots \tag{44}$$

Solving for the $f''(z)$ represents the second derivative in a suitable form for the programming language.

$$f''(z) \approx \frac{1}{h^2}[\,f(z+h) - 2\,f(z) + f(z-h)] \tag{45}$$

The reduction of higher order terms lowers the accuracy of the Taylor series expansion; however, this method allows for a direct determination of the first and second derivatives of a function. The central difference formulas are utilized in the next section to format the mathematical operators for ∇ and ∇^2. Error arises from this approximation in the value of h, which could be addressed with increased resolution in the z and r coordinate step size at the cost of greater computational time.

4.3.3 Application of central difference approximations applied to ∇ and ∇^2

Based upon the original definition of liquid helium systems, the uniformity of the density varies only in the coordinate direction that is perpendicular to the liquid to vacuum interface. Therefore, this promotes the simplification of the ∇ and ∇^2 operators to the dependence on one dimension of the system.

4.3.3.1 Cartesian coordinates

The density variation of a planar system of superfluid helium is throughout planar slabs of the fluid and delimited by a system of Cartesian coordinates. With the previous statement of a single dimensionality dependence, comes the simplification of ∇ in equation (46) to $\frac{d}{dz}$ because the z direction is defined as the direction perpendicular to the interace and contains the only nonzero derivative.

$$\nabla f = \frac{\partial}{\partial x} + \frac{\partial}{\partial y} + \frac{\partial}{\partial z} \tag{46}$$

Therefore in Cartesian coordinates, the gradient simplifies to equation (47),

(47)

$$\nabla f(z) = \frac{d}{dz}$$

which then creates an opportunity for a substitution with the first-order central difference approximation.

Equation (48) is now easily formulated for computer code.

(48)

$$\nabla f(z) = \frac{1}{2h}\,[f(z+h) - f(z-h)]$$

The Laplacian may be formulated in a similar manner. The Laplacian in Cartesian coordinates is defined by equation (49), three partial second derivatives with respect to x, y, and z.

(49)

$$\nabla^2 f = \frac{\partial^2}{\partial x^2} + \frac{\partial^2}{\partial y^2} + \frac{\partial^2}{\partial z^2}$$

With the established density dependence upon the z coordinate direction, equation (49) simplifies to the second derivative of the function with respect to movement along the z axis. Therefore, the function no longer has partial derivatives as seen in equation (50).

(50)

$$\nabla^2 f(z) = \frac{d^2}{dz^2}$$

With the incorporation of the second-order central difference approximation, $\nabla^2 f(z)$ can be written in the form of equation (51).

(51)

$$\nabla^2 f(z) = \frac{1}{h^2}[\, f(z+h) - 2\, f(z) + \, f(z-h)]$$

The ultimate manipulation of approximations creates a version of the operators in terms that are easily accessible for computation of the density functionals in **Fortran 77**.

4.33.2 Spherical polar coordinates

For the spherical polar coordinate system of helium nanodroplets, the *r* coordinate direction contains the only non-zero derivative. The gradient expression of spherical polar coordinates is defined by equation (52) with the additional interaction terms of θ and φ.

(52)

$$\nabla f = \frac{\partial}{\partial r} + \frac{1}{r}\frac{\partial}{\partial \theta} + \frac{1}{r \sin\theta}\frac{\partial}{\partial \varphi}$$

The gradient term becomes equation (53), dependent only upon the r-axis while the θ and φ terms drop out of the expression.

(53)

$$\nabla f(r) = \frac{d}{dr}$$

Equation (54) expresses the gradient of the spherical polar coordinates in terms of the central difference approximation.

(54)

$$\nabla f(r) = \frac{1}{2h}[f(r+h) - f(r-h)]$$

The Laplacian operator for spherical polar coordinates is seen in equation (55) and used here to define droplet systems.

(55)

$$\nabla^2 f = \frac{1}{r^2 sin\theta}\left[\sin\theta \frac{\partial}{\partial r}\left(r^2 \frac{\partial}{\partial r}\right) + \frac{\partial}{\partial \theta}\left(\sin\theta \frac{\partial}{\partial \theta}\right) + \frac{1}{\sin\theta}\frac{\partial^2}{\partial \varphi^2}\right]$$

Upon abridgement of the Laplacian with the assumption that the density is dependent upon variation of the r coordinate only, the Laplacian for the helium nanodroplets becomes equation (56) with the supplemental first derivative term. Interaction terms from θ and φ now influence change with respect to the second derivative of the r coordinate.

(56)

$$\nabla^2 f(r) = \frac{d^2}{dr^2} + \frac{2}{r}\frac{d}{dr}$$

Equation (56) contains both a first and second derivative, which will then incorporate the first and second-order central difference approximations in the form of equation (57).

(57)

$$\nabla^2 f(r) = \frac{1}{h^2}[f(r+h) - 2f(r) + f(r-h)] + \frac{1}{h\,r}[f(r+h) - f(r-h)]$$

Section 4.3 composes the central tools for articulating the mean field from a general form into a characteristic expressions that are easily maneuvered with computer programming.

4.4 Numerical tests

Numerical testing of the mean field programming was originally examined with the imaginary time-step method instead of the matrix diagonalization approach.

4.4.1 Trial with harmonic oscillator

Numerical testing of the methodology was carried out with the harmonic oscillator as an exemplar for the imaginary time-step method. The intent was to begin with a sample wavefunction of the known harmonic oscillator that deviated from the accurate

form. The starting wavefunction was purposely faulted to investigate if the time-step methods would optimize a mean field potential, given in equation (58), to a fixed value for helium parameters. Where z is the grid coordinate of the system, $U(z)$ is the mean field, and k is the spring constant calculated to a system of ^{4}He.

$$U(z) = \frac{1}{2} k\, z^2 \tag{58}$$

Application of the mean field into the time-step method is given in equation (59).

$$|\varphi^{(n+1)}\rangle = e^{-\mathcal{H}\Delta\tau}|\varphi^{(n)}\rangle \approx \left[1 - \Delta\tau \left(\frac{-\hbar^2}{2m} + \frac{1}{2} k z^2\right)\right]|\varphi^{(n)}\rangle \tag{59}$$

Due to the simplicity of the system and the ease at which to define an initial guess of the wavefuntion, blending of the wavefunction between each step was not necessary for optimization to the correct form. Two intial guesses of the wavefunction were set; one that was twice the height of the harmonic oscillator and the second that was half the height with a greater width. Each of the false guesses propagated in time, yielding the accurate helium wavefunction from the harmonic oscillator approximation.

Chapter 5: Results and discussion

Chapter 5 is a discussion of the relevant results and conclusions from this work. We begin with an overall summary and comparison of the functionals on various systems, given in Table 1. In the case of planar slabs, the chemical potentials are not extrapolated to bulk density. The recorded chemical potentials from Table 1, come from a direct calculation of a planar slab that nears bulk density at the interior.

Table 1. Comparison of chemical potentials and maximum densities. (Read values across for each functional). The number of atoms in each system is given by n, where μ is the chemical potential in units of Kelvin, and ρ_{max} is the maximum density in units of $atoms/\text{Å}^3$.

Comparison of chemical potentials and maximum densities

dopant	n_{ST} (atoms)	μ_{ST} (K)	$\rho_{max\ ST}$	n_{OP} (atoms)	μ_{OP} (K)	$\rho_{max\ OP}$	n_{OT} (atoms)	μ_{OT} (K)	$\rho_{max\ OT}$
-----	planar slab	-7.150	0.021832	planar slab	-7.175	0.021832	planar slab	-7.155	0.021788
-----	----	----	----	232	-5.237	0.022662	----	----	----
-----	795	-6.786	0.022120	795	-5.903	0.022657	----	----	----
-----	----	----	----	2252	-6.319	0.022472	----	----	----
Mg-He	----	----	----	12,165	-6.671	0.033267	----	----	----
1.5 x L J	----	----	----	12,165	-6.671	0.042117	----	----	----
2 x L J	----	----	----	12,165	-6.671	0.047794	----	----	----

Bulk density of liquid ^{4}He is established at the value $\rho_{liquid} = 0.021836\, atoms/\text{Å}^3$, while solid ^{4}He densities near $\rho_{solid} = 0.04\, atoms/\text{Å}^3$.[27] Freezing is experimentally calculated to occur at $\rho_{freezing} = 0.029\, atoms/\text{Å}^3$.[17] As a benchmark comparison, the chemical potential of bulk superfluid ^{4}He is $-7.15\ K$ from experiment.[2] All three of the functionals produce values near the bulk chemical potential for planar slabs; however, a standard deviation for these values is not calculated. Orsay-Trento data for the droplet systems and systems containing impurities is not yet finalized and will be discussed in a future publication.

Droplets of assorted sizes report a divergence between chemical potentials, due to the contribuation from a greater or fewer number of atoms in the system. Variance in surface area positions also contribute to the chemical potential. An increase in droplet size is favored due to a decrease in the chemical potential as the number of interior positions grows. Also, droplet calculations with the previously discussed dopant potentials are given here. Since the impurities were applied to large droplets, the added He-dopant interaction did not change the overall chemical potential between varied dopant interactions with the same density functional.

The following sub-sections are further divided according to the symmetry of the systems of ^{4}He that are analyzed.

5.1 Planar systems

Figure 5 plots the density profiles for fluid-vacuum interface of the three density functionals, shifted along the z axis to align 50 % density values at $z = 0$. The Stringari and Treiner functional is characteristic of a less steep transition, while the Orsay-Paris and Orsay-Trento functionals are more similar. The Orsay-Trento functional exhibits greater oscillation, as expected, as it decays along the interface to zero density.

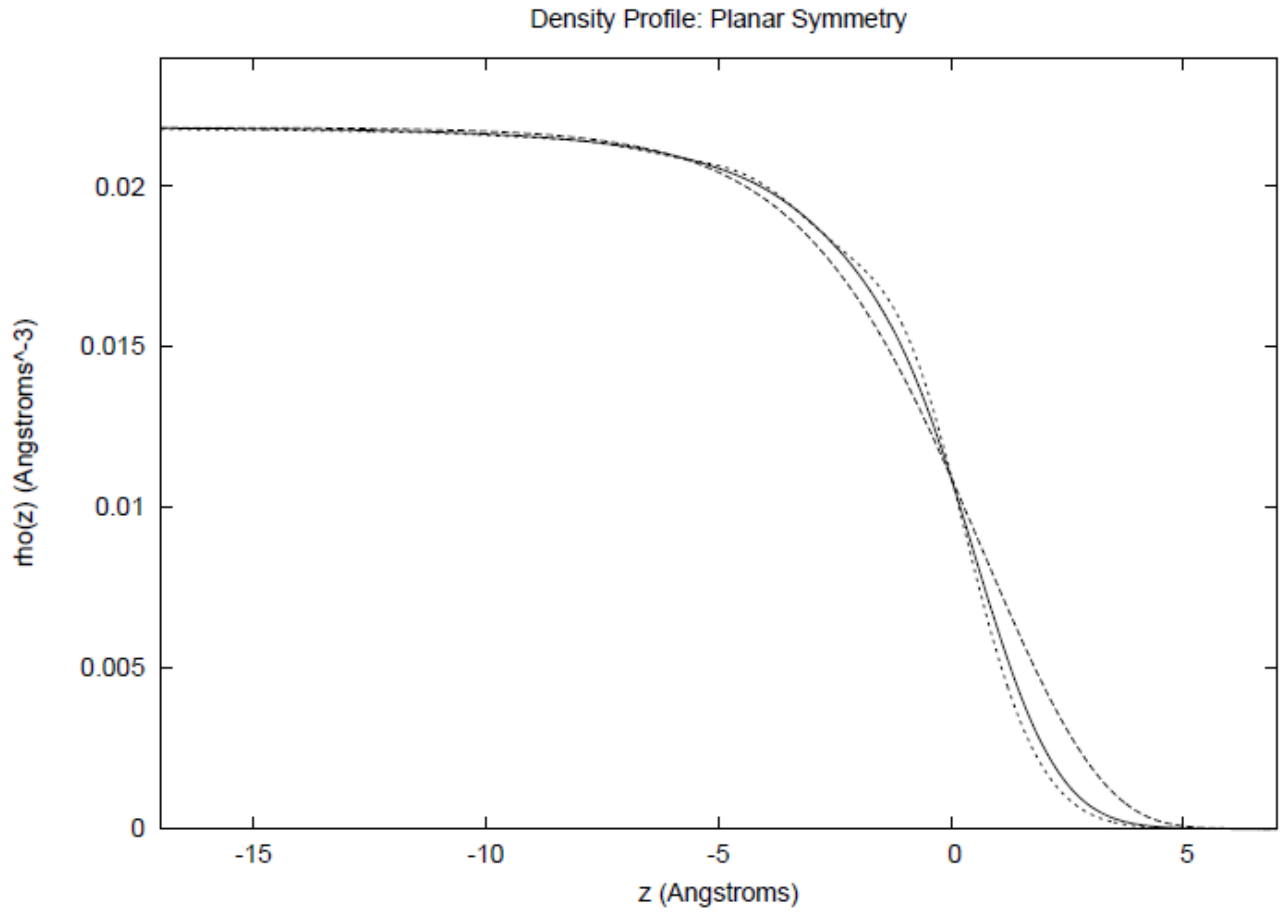

Figure 5. Density Profile: Planar Symmetry. Comparison of density functional methods with planar symmetry. Long dash: Stringari and Treiner (+2.15 *z*-shift). Solid line: Orsay-Paris (-22.308 *z*-shift). Short dash: Orsay-Trento (-20.4909 *z*-shift). Note: Density profiles are shifted to align 50% density at $z = 0$.

Figure 6 plots the corresponding Stringari and Treiner, Orsay-Paris, and Orsay-Trento mean field expressions along the interface with 50 % density shifted to $z = 0$. The relevant *z* shifts are given in the caption of Figure 5. Notice that the Stringari and Treiner mean field does not produce the well evident in the other two mean field calculations.

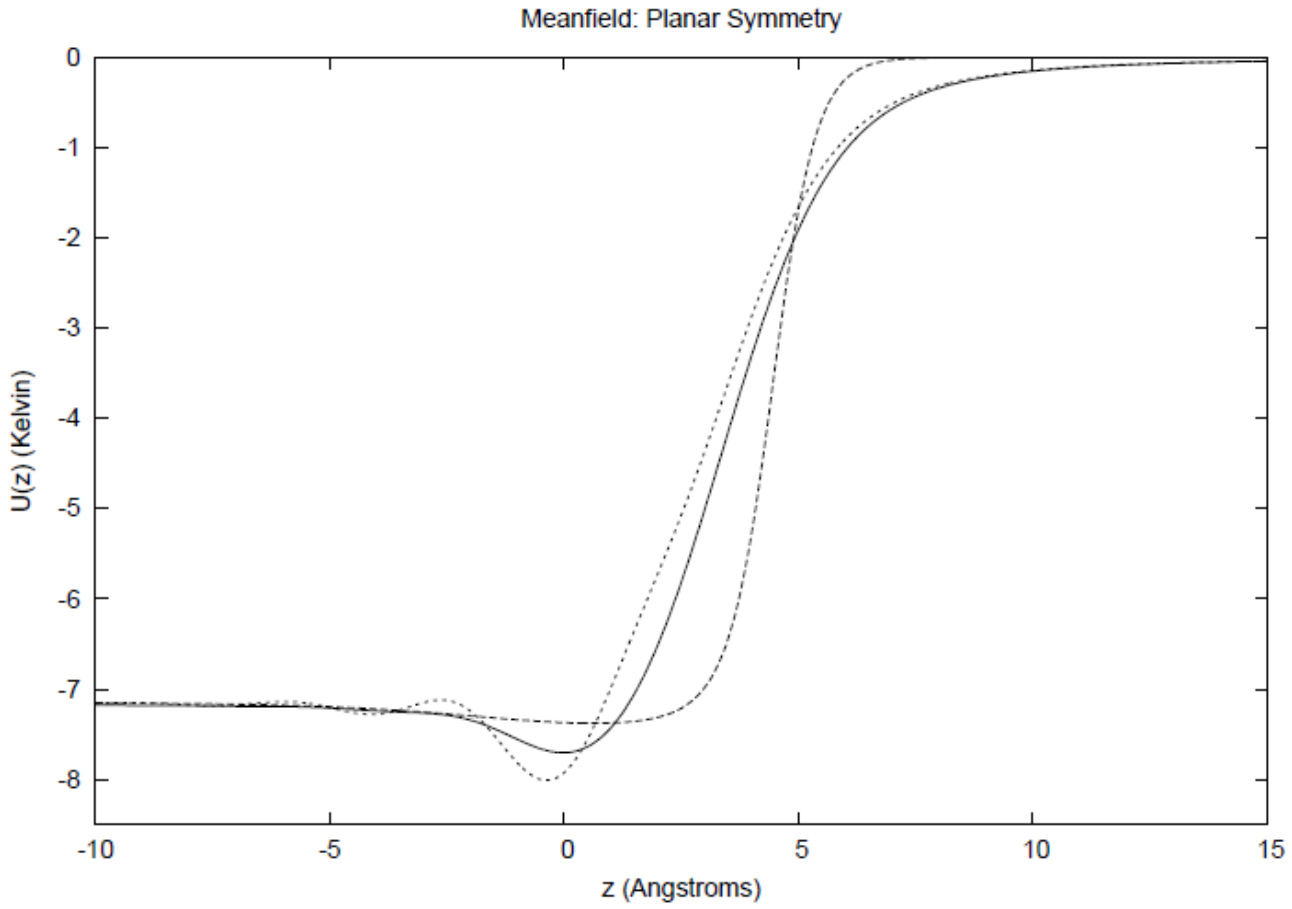

Figure 6. Mean Field: Planar Symmetry. Comparison between density functional methods with planar symmetry. Long dash: Stringari and Treiner. Solid line: Orsay-Paris. Short dash: Orsay-Trento. Note: mean fields correspond to the shifts in Figure 5, aligning 50 % density with $z = 0$.

Tables 2 – 4 give numerical data for values of the mean field, density profile, and z coordinate over the transition interface. These values are shifted to align 50 % density at $z = 0$.

Table 2. Stringari and Treiner Functional: Planar Slab. Mean field, density, and z coordinate values for the Stringari and Treiner density functional, corresponding to Figures 1 and 2. The z coordinate has a z-shift of +2.15 Å to align 50 % density to $z = 0$.

Stringari and Treiner Functional: Planar Slab		
U (z) (Kelvin)	ρ (z) (Å^{-3})	z (Å)
-7.15254867	0.021773	-11.25
-7.15604479	0.021673	-9.35
-7.16637517	0.021371	-7.25
-7.18308842	0.020865	-5.75
-7.21998638	0.019657	-4.05
-7.23236359	0.019218	-3.65
-7.29080843	0.016813	-2.15
-7.3457419	0.013584	-0.85
-7.37558471	0.01012	0.25
-7.07383652	2.26E-03	2.85
-6.36058562	1.04E-03	3.55
-5.43230418	5.90E-04	3.95
-4.03311807	3.04E-04	4.35
-2.49586205	1.44E-04	4.75
-1.08949436	5.23E-05	5.25
-0.025592522	1.09E-06	7.05
-3.20E-07	1.37E-11	12.25

Table 3. Orsay-Paris Functional: Planar Slab. Mean field, density, and z coordinate values for the Orsay-Paris density functional, corresponding to Figures 1 and 2. The z coordinate has a z-shift of -22.308 Å to align 50 % density to $z = 0$.

Orsay-Paris Functional:		Planar Slab
U (z) (Kelvin)	ρ (z) (Å^{-3})	z (Å)
-7.17963166	0.02156733	-9.18696
-7.18669776	0.021366572	-7.58717
-7.19131269	0.021096816	-6.40587
-7.21032311	0.020556026	-4.97967
-7.24113141	0.019949234	-4.02887
-7.26295432	0.018975642	-3.07807
-7.40964861	0.016509995	-1.6281
-7.59752841	0.014229431	-0.81992
-7.69209377	0.012132262	-0.27321
-7.49805296	0.006827085	0.86775
-6.1839569	0.001904589	2.24641
-4.05740072	0.000300893	3.55376
-2.18909464	3.49E-05	4.76603
-0.99766472	2.71E-06	6.04961
-0.17895406	1.76E-09	9.52003
-0.06127091	1.79E-12	13.08553

Table 4. Orsay-Trento Functional: Planar Slab. Mean field, density, and *z* coordinate values for the Orsay-Trento density functional, corresponding to Figures 1 and 2. The *z* coordinate has a *z*-shift of -20.4909 Å to align 50 % density to $z = 0$.

Orsay-Trento Functional: Planar Slab

U (z) (Kelvin)	ρ (z) (Å^{-3})	z (Å)
-7.16036	0.02169	-11.554
-7.1834	0.02131	-7.349
-7.2679	0.01985	-3.8221
-7.3549	0.017253	-1.7632
-7.9399	0.011188	-0.03282
-7.25274	0.006558	0.778
-6.18337	0.002867	1.6318
-5.12003	0.001013	2.4641
-4.21877	0.000396	3.0993
-3.0669	1.1 E-04	3.86595
-1.5051	9.61E-06	5.15824
-0.94719	2.04E-06	5.92485
-0.12367	2.50E-10	10.4581
-0.0514	4.55E-12	13.7001
-0.03296	5.45E-13	15.7594

The quantum kinetic energy density and free energy densities are calculated for the Orsay-Paris functional to show the alignment of the mean field to the right of the density profile. Figure 7 plots the density profile, kinetic energy density, and free energy density to show the location of the energetic properties with respect to the pattern of density decay. This graph provides a correlation of the location of the mean field shifted to the right of the density profile as seen in a comparison of Figures 5 and 6 in relation to the $z = 0$ position.

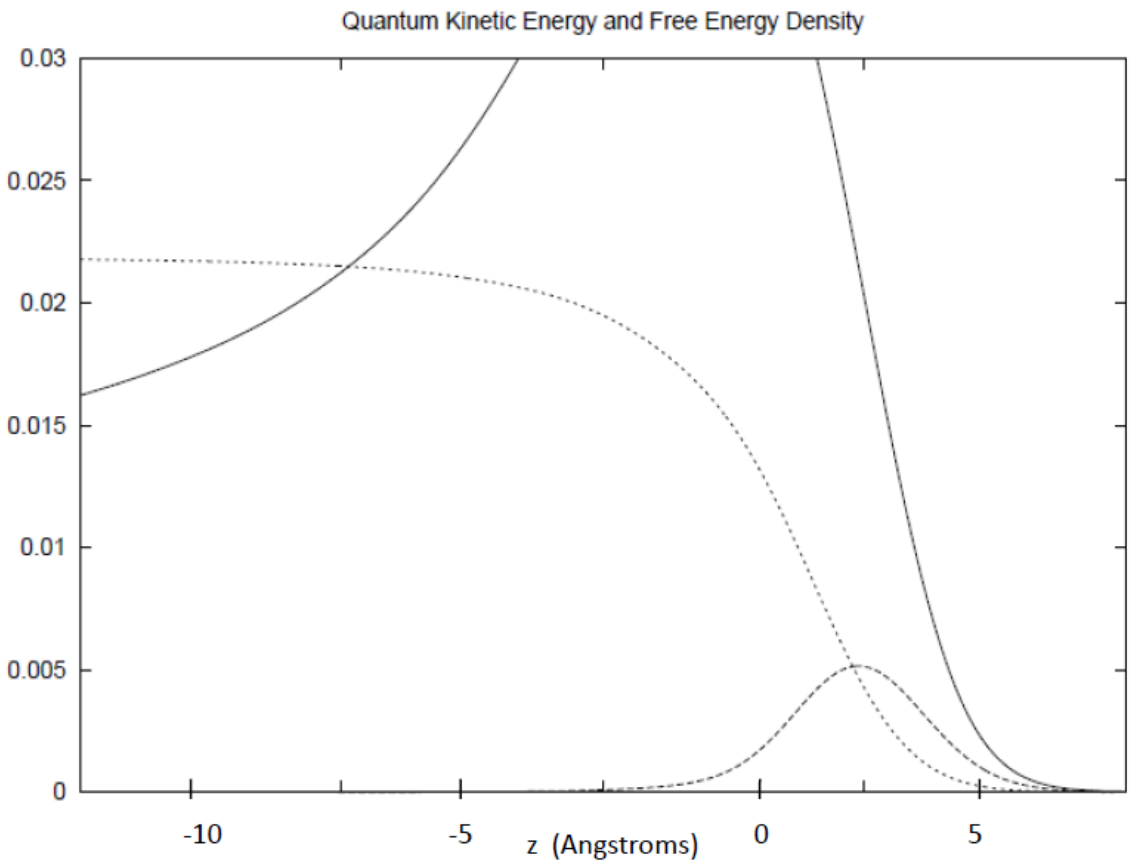

Figure 7. Quantum Kinetic Energy and Free Energy Density. Orsay-Paris functional for a free planar slab of superfluid ^{4}He. Solid line: free energy density (KÅ^{-3}). Long dashed line: quantum kinetic energy density (KÅ^{-3}). Small dashed line: density profile (Å^{-3}). 50 % density aligned with $z = 0$.

From corrections added to the correlation energy and improvements to the energy functional, also seen in the mean field expressions, minute oscillations are observed in the Orsay-Trento calculations. The presence of these fluctuations is also predicted by Monte Carlo studies and is believed to arise from phonon-roton dispersion effects along with the phenomenon of backflow.[15,16]

5.2 Spherical droplets

For the case of spherical droplets, results are shown below. Figure 8 is a comparison, similar to before, of the density profile and mean field of spherical symmetry between density functional methods. Plots are aligned to 50 % density along the r axis. It is interesting and difficult to note that there is a slight deviation in the point at $r = 0$ for calculations of the coarse-grained density in the Orsay-Paris pure droplet systems. This point does not affect doped droplets due to zero density at $r = 0$. The deviant point stems from the inherent error in the trapezoid approximation technique employed for integration. However, the stray point can only be recognized upon acute scrutiny in this region; and it is determined that the slight discrepancy does not infringe upon optimization of the droplet system. Due to time constraints, data for the Orsay-Trento collaboration is not yet complete for spherical droplet systems.

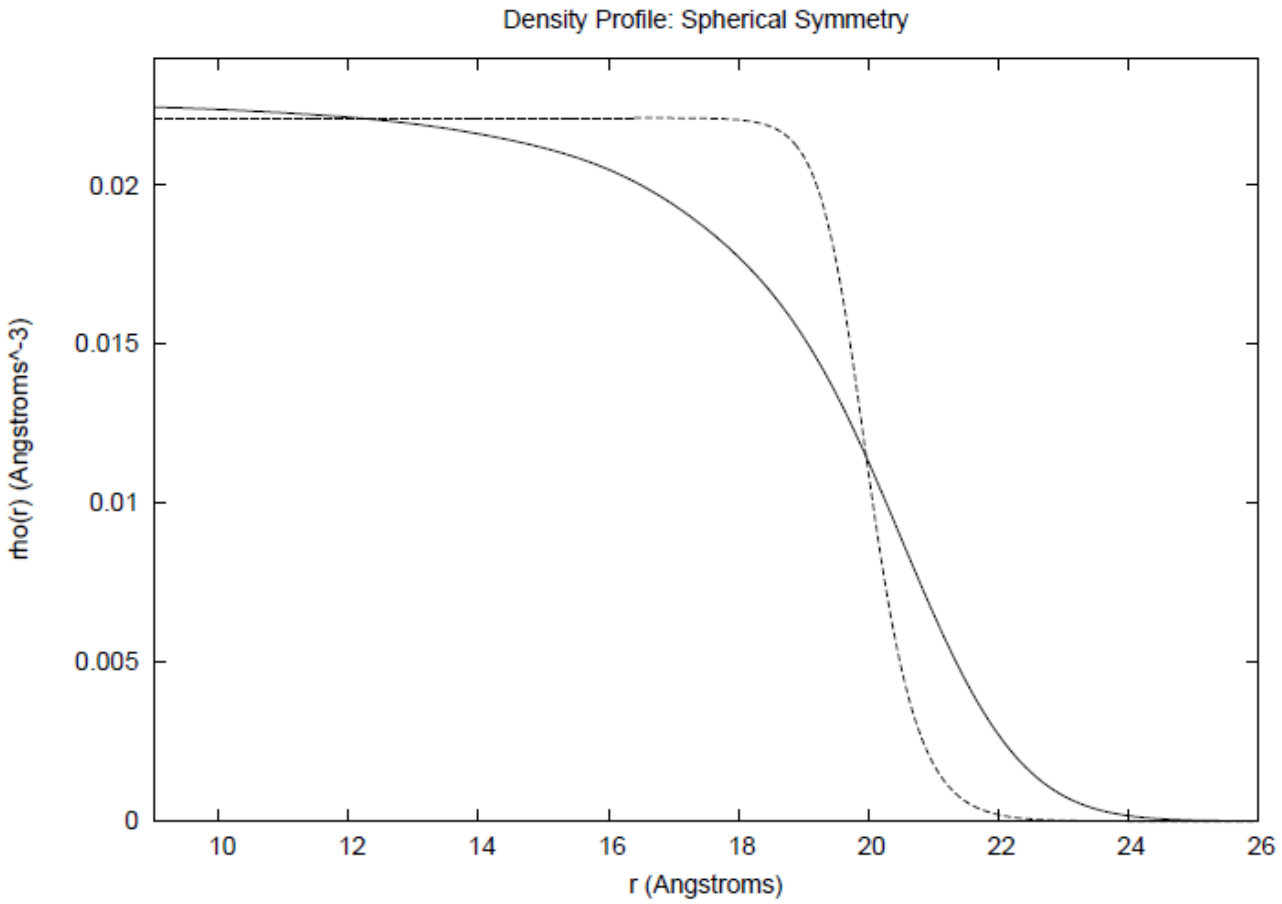

Figure 8. Density Profile: Spherical Symmetry. Comparison between density functional methods with spherical symmetry. Long dash: Stringari and Treiner (-0.4065 *r*-shift). Solid line: Orsay-Paris (-0.51351 *r*-shift). Note: Density profiles are shifted to align 50 % density at $r = 20$.

In Figure 8, the Stringari and Treiner and Orsay-Paris functionals model a droplet of 795 atoms. Chemical potentials are given previously in Table 1. The Stringari and Treiner functional yields a steep decay along the fluid-vacuum interface, along with a diminished depiction of the mean field and chemical potential in comparison to the Orsay-Paris calculation.

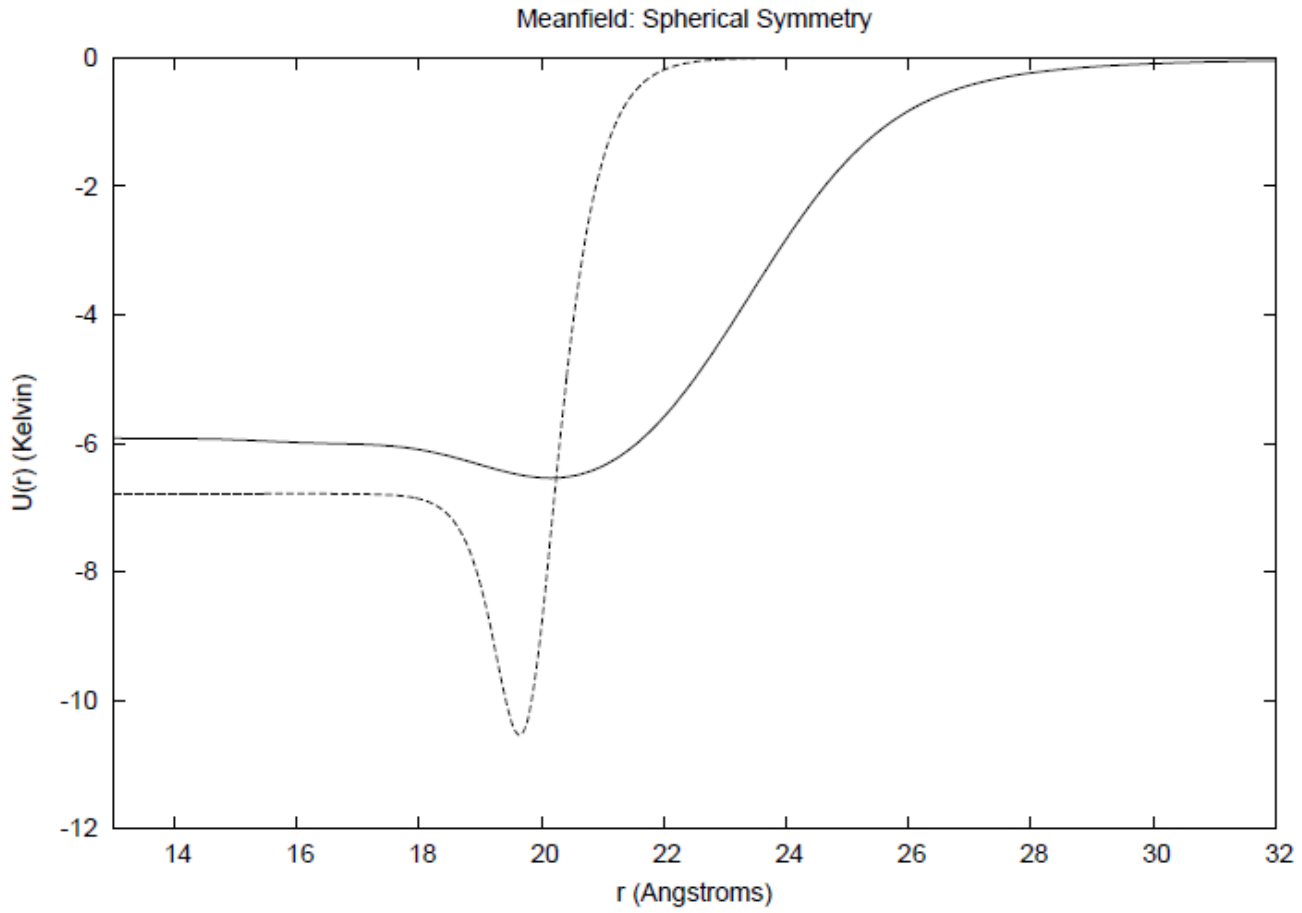

Figure 9. Mean Field: Spherical Symmetry. Comparison of density functional methods with spherical symmetry. Long dash: Stringari and Treiner. Solid line: Orsay-Paris. Note: mean fields correspond to the shifts in Figure 8, aligning 50 % density with $r = 20$.

The following plots compare droplet sizes within the same functional approach for the Orsay-Paris collaboration. Due to the diminished ability of the Stringari and Treiner functional to scrutinize spherical symmetry, an examination with this method is not significant. Figure 10 shows three droplets of different sizes defined by the number of atoms n using the Orsay-Paris collaboration.

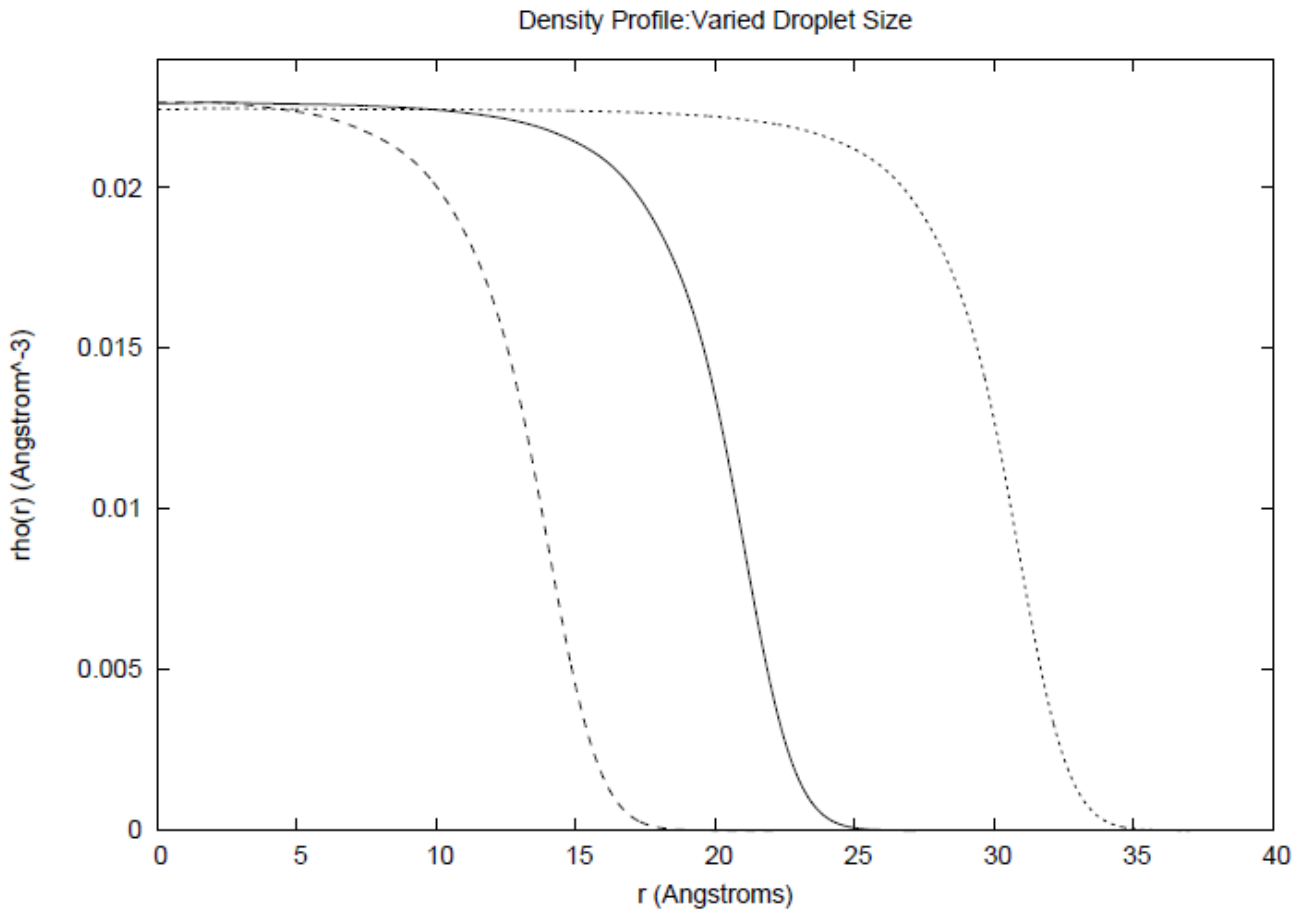

Figure 10. Density Profile: Varied Droplet Size (OP). Long dashed line: n = 232 atoms. Solid line: n = 795 atoms. Short dashed line: n = 2252 atoms.

Figure 11 is the corresponding mean field for density profiles in Figure 10 using the Orsay-Paris collaboration.

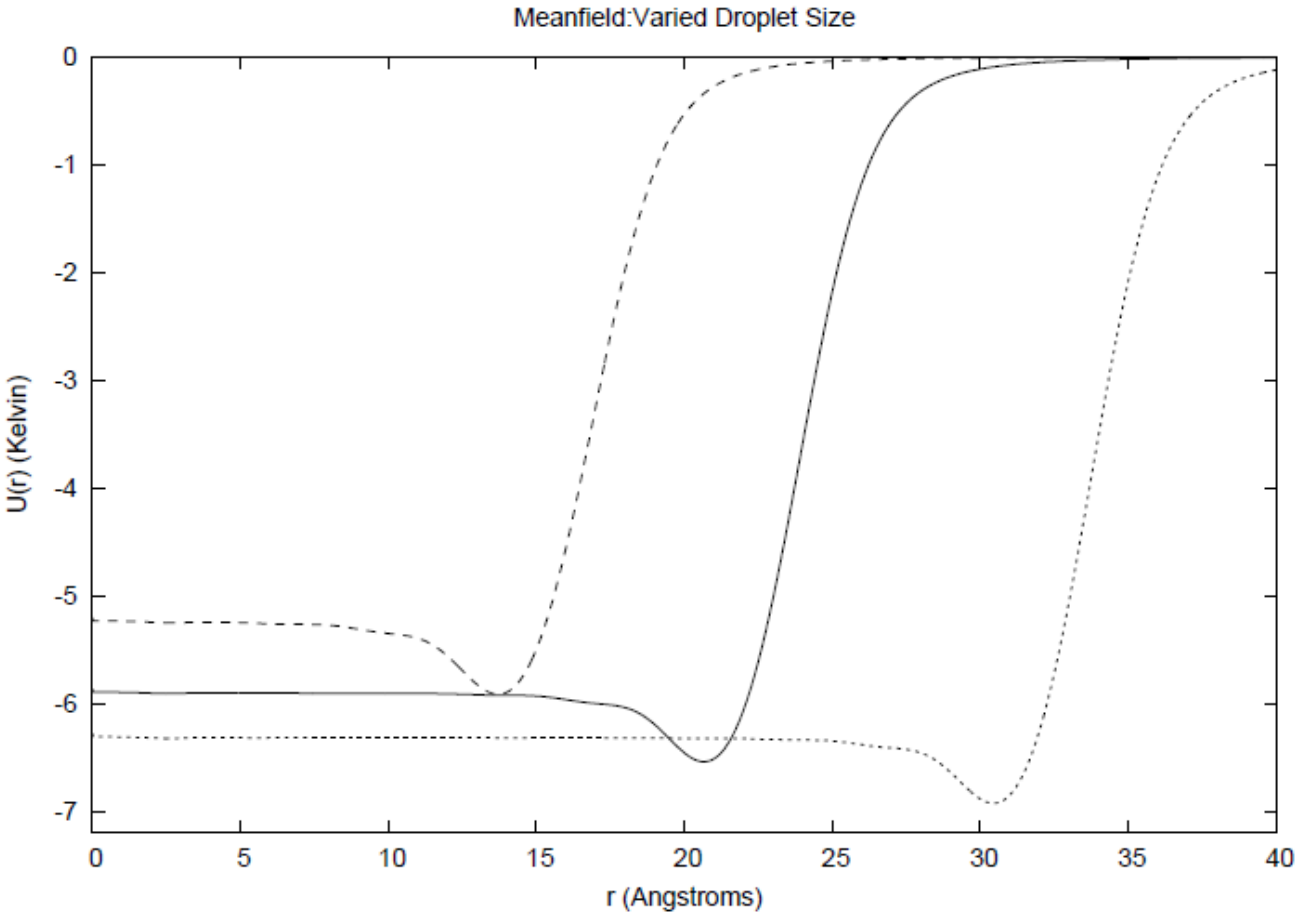

Figure 11. Mean Field: Varied Droplet Size (OP). Long dashed line: n = 232 atoms. Solid line: n = 795 atoms. Short dashed line: n = 2252 atoms. Corresponds to density profiles from Figure 10.

Smaller droplets have less of a contribution to the chemical potential, compare -5.237 *K*, -5.903 *K*, and -6.319 *K* with increasing values of n. The most negative chemical potential of n = 2252 atoms is the most favorable.

From the initial examination of pure helium droplets, helium droplets with the added impurity interaction are calculated. Data is given in the following section.

5.3 Droplets with atomic dopants

The Stringari and Treiner functional failed upon the addition of an atomic dopant and self-consistency was never reached. Therefore, no results are reported here for a doped droplet with the Stringari and Treiner functional. Data for the Orsay-Trento collaboration will be available in a later publication.

Figures 12 – 13 depict doped droplets with varied potentials for the Orsay-Paris collaboration. Plots visualize the interaction with an atomic dopant placed at $r = 0$ through the effective change to the density profile and mean field potential.

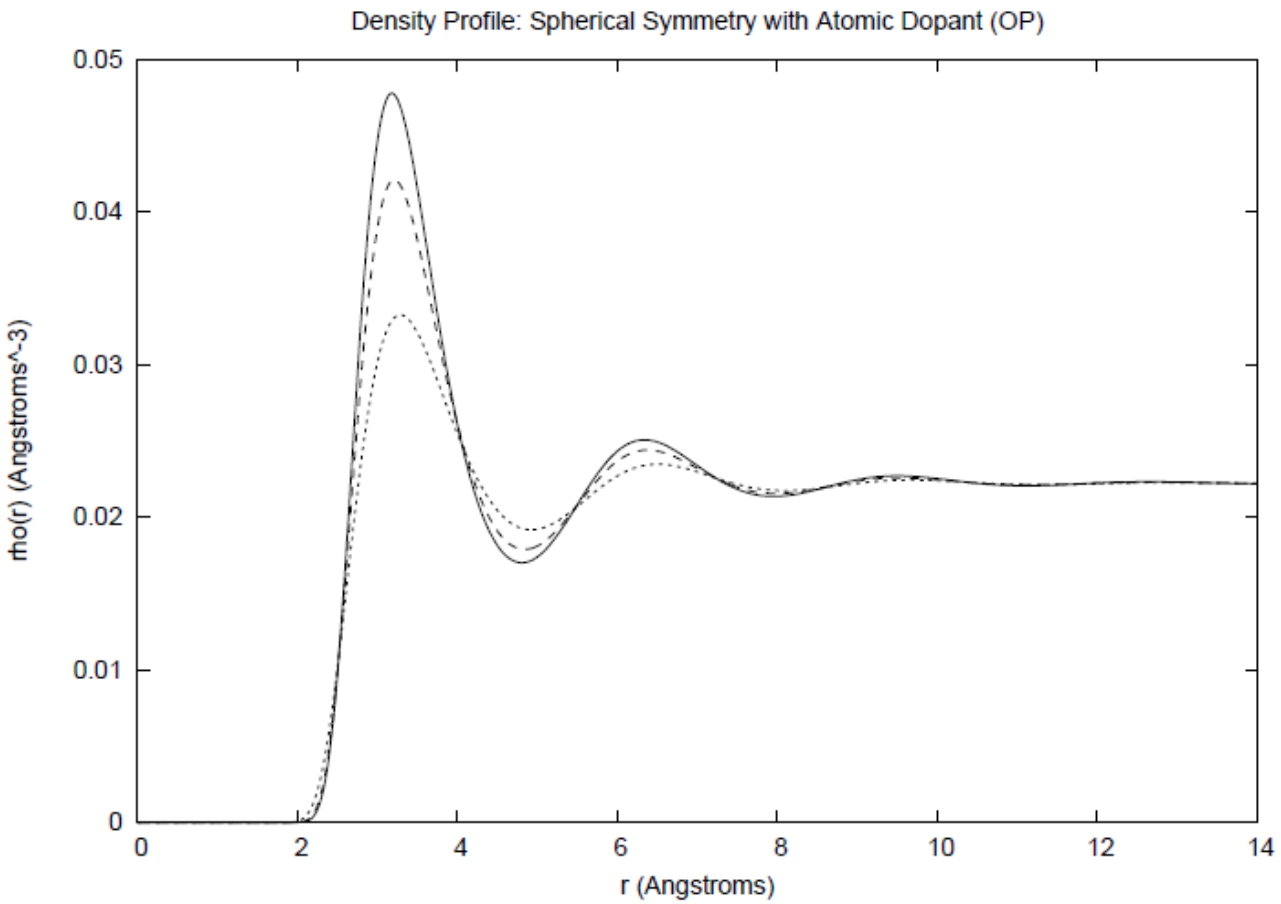

Figure 12. Density Profile: Spherical Symmetry with Atomic Dopant (OP). Density profiles with spherical symmetry and varied dopant-He potentials. Solid line: 2 x Lennard-Jones He-He potential. Long dash: 1.5 x Lennard-Jones He-He potential. Short dash: 0.703898 x Lennard-Jones He-He potential, mimicking the He-Mg interaction potential from Hinde.[15] Droplet size is held constant at 12,165 atoms. Dopant is located at $r = 0$.

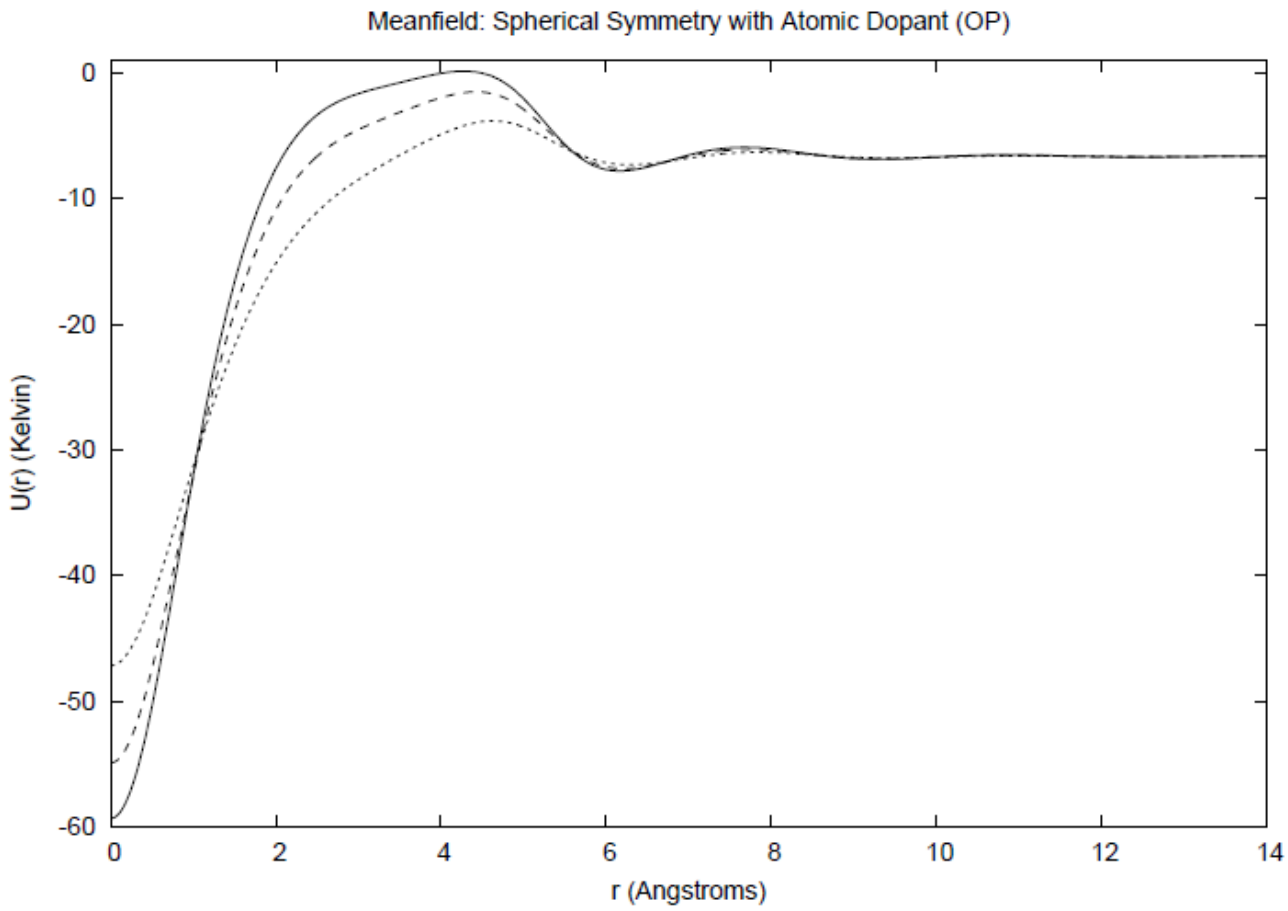

Figure 13. Mean Field: Spherical Symmetry with Atomic Dopant (OP). Mean fields corresponding to density profiles in Figure 12 with spherical symmetry and varied dopant-He potentials. Solid line: 2 x Lennard-Jones He-He potential. Long dash: 1.5 x Lennard-Jones He-He potential. Short dash: 0.703898 x Lennard-Jones He-He potential, mimicking the He-Mg interaction potential from Hinde.[15] Chemical potential μ = -6.671 *K*.

Although the mean field functions vary at distances shorter than 14 Å from $r = 0$, the calculated chemical potential stays consistent while varying the relative strengths of the He-dopant interaction. This is observed because there is little contribution from the

atomic dopant to the remainder of the droplet. The decay character of the meanfield at the liquid to vacuum interface as the density drops to zero also remains steady with a change in He-dopant interaction strength. Upon altering the He-dopant exchange, an adjustment to the chemical potential would be expected for droplets that are significantly smaller in size. The factor of 2 x Lennard-Jones interaction potential explores an upper limit of the attractive nature of the dopant. Densities reached exceed those of solid helium.

Integration of the density profiles (Figure 12) provides an indication of the number of atoms in each solvation shell. From the density profiles with an added dopant, it looks as though there are three obvious solvation shells for each system examined, with the possibility of a minor fourth shell. Solvation shells are detailed in Table 5. Notice the r location of each shell also recorded. Here, the value of r indicates the outer limit or endpoint of the solvation shell.

Table 5. Integration of Solvation Shells. Chart indicates the endpoint *r* value of each shell and the number of atoms in the shell rounded to the nearest whole number. Data is given for the Orsay-Paris at the varied He-dopant potentials.

Integration of Solvation Shells: Mg-He Potential

	r_{OP} (Å)	# of atoms
1st shell	4.92	11
2nd shell	8.106	39
3rd shell	11.267	84
quasi-4th shell	14.428	147

Integration of Solvation Shells: 1.5 x LJ Potential

	r_{OP} (Å)	# of atoms
1st shell	4.894	11
2nd shell	7.986	37
3rd shell	11.124	81
quasi-4th shell	14.262	142

Integration of Solvation Shells: 2 x LJ Potential

	r_{OP} (Å)	# of atoms
1st shell	4.802	11
2nd shell	7.962	38
3rd shell	11.124	81
quasi-4th shell	14.286	144

Upon freezing, helium may develop the hexagonal close-packed lattice formation with each atom surrounded by 12 others.[17] It is interesting to note that the calculations indicate a trend towards 12 atoms in the first solvation shell for both the 1.5 and 2 x LJ dopant potential. Maximum density values, reported in Table 1, in the first solvation shell for the 1.5 and 2 x LJ dopant potential supports the prospect of solid formation. The He-Mg impurity potential lies close to this borderline, also leaning towards the possibility of freezing densities in the first solvation shell.

Upon conclusion of the current work, the reader should have gained some insight of the approach taken to model droplets of helium and doped droplets with a density functional model. This research is intended to contribute to the pursuit of a detailed understanding of quantum systems of superfluid helium and the nature of solvation effects.

Chapter 6: Items for future work

Future work will include the comparison between Orsay-Paris and Orsay-Trento funcionals of droplet systems and droplet systems with impurities. One of the main considerations, which is not thoroughly examined here, is how size dependence alters the calculations of droplets with atomic dopants. Future work should investigate the relationship of droplet size to impurity solvation. This could be done with the same processes outlined in the current research with multiple calculations to model doped droplets under a wide range in the number of atoms. The simulations could also compare data between the Orsay-Paris and Orsay-Trento functionals with calculations of droplets of the exact size.

Prospective research should also improve upon the model used to delineate the He-dopant potential with more descriptive methods. Helium-impurity pair potentials can be found in recent literature studies and an improvement to this area of the current research could be used to augment the technique detailed here.

Further examination of density functional theory of helium droplets will be necessary to determine the importance of three-body interactions at the point where atomic dopants produce solid densities, particularly in the first solvation shell surrounding an impurity. Research of this nature should be approached with a correlation of density functional theory and Monte Carlo simulations. Diffusion Monte Carlo simulations should first be used to model the Bose-Einstein condensate with a pair-wise interaction potential, and then progress with the addition of a three-body potential to examine the contribution of three-body interactions. Due to the simplistic nature of superfluid helium, diffusion Monte Carlo simulations may be in order to evaluate the

delicate contribution of three-body terms. Without dispute, two-body interactions contribute the majority to the interaction potential. However, to increase computational ability, three-body terms cannot be disregarded.

In order to separate two-body from three-body interactions, two different diffusion Monte Carlo methods could be utilized. First, the Monte Carlo simulations would include only a pairwise-additive potential to compare directly with DFT calculations. Then, simulations would be expanded to incorporate the presence of three-body interactions. Two aspects should be examined here—how important is the contribution of three-body interactions in doped ^{4}He droplets that approach densities of solid helium and what are the limitations of DFT methods with such systems as doped ^{4}He droplets.

References

1. Stringari, S., Treiner, J.: J. Chem. Phys. **87**, 5021 (1987).

2. Stringari, S., Treiner, J.: Physical Review B **36** (16), 8369 (1987).

3. Dupont-Roc, J., Himbert, M., Pavloff, N., Treiner, J.: J. Low Temp. Phys. **81**, 31 (1990).

4. Pricaupenko, L., Treiner, J.: J. Low Temp. Phys. **96** (1-2), 19 (1994)

5. Stringari, S.: Z. Phys. D - Atoms, Molecules and Clusters **20**, 219 (1991).

6. Lastri, A., Dalfovo, F., Pitaevskii, L., Stringari, S.: J. of Low Temp. Physics, **98** (3/4), 227 (1995).

7. Montfrooij, W., Svensson, E. C.: Physica B **241-243**, 924 (1998).

8. Matthias, J. R., Inkson, J. C., Sobnack, M. B.: Czech. J. Phys. **46**, 387 (1996).

9. Matthias, J. R., Sobnack, M. B., Inkson, J. C., Fung, J. C. H.: J. of Low Temp. Phys. **121** (5-6), 345 (2000).

10. Dalfovo, F., Fracchetti, A., Lastri, A., Pitaevskii, L., Stringari, S.: Phys. Rev. Letters **75** (13), 2510 (1995).

11. Dalfovo, F., Lastri, A., Pricaupenko, L., Stringari, S., Treiner, J.: Physical Review B **52** (2), 1193 (1995).

12. Toennies, J. P. and Vilesov, A. F.: Angnew. Chem. Int., Ed. **43**, 2622-2648.

(2004).

13. Mella, M., Calderoni, G., Cargnoni, F.: J. of Chemical Physics **123**, 054328 (2005).

14. Hernando, A., Barranco, M., Mayol, R., Pi, M.: Phys. Rev. B **77**, 024513 (2008).

15. Hinde, R.: J. Phys. B: At. Mol. Opt. Phys. **36**, 3119 (2003).

16. Dalfovo, F.: Z. Phys. D **29**, 61 (1994).

17. Ancilotto, F., Barranco, M., Caupin, F., Mayol, R., Pi, M.: Phys. Rev. B **72**, 214522 (2005).

18. Khalos, M., Michael, A., Whitlock, P.: Phys. Rev. B **24** (1), 115 (1981).

19. Keller, C., de Llano, M., Ren, S., Buendia, E., Guardiola, R.: Phys. Rev. B **40**, (16) (1989).

20. Garberoglio, G. and Harvey, A.: J. Rex. Natl. Stan. Technol., **114**, 249 (2009).

21. Garberoglio, G. and Harvey, A.: J. Chem. Phys. **134**, 134106 (2011).

22. Lotrich, V. and Szalewicz, K.: J. Chem. Phys. **112** (1), (2000)

23. Axilrod, B.: J. of Chem. Phys. **19** (6), (1951).

24. Szybisz, L. Eur. Phys. J. B **14**, 733 (2000).

25. McMahon, M., Barnett, R., Whaley, K.: Z. Phys. B **98**, 421 (1995).

26. Jakse, N., Bomont, J., Charpentier, I., Bretonnet, J.: Phys. Rev. E **62** (3), (2000).

27. Eloranta, J., Schwentner, N., Apkarian, V.: J. Chem. Phys. **116** (10), 4039 (2002).

28. Casas, M., Dalfovo, F., Lastri, A., Serra, Ll., Stringari, S.: Z. Phys. D **35**, 67 (1995).

29. Mur-Petit, J., Sarsa, A., Navarro, J., Polls, A.: Physical Review B **72**, 104513 (2005)

30. Dalfovo, F., Stringari, S.: Physical Review B **46** (21), 13 991 (1992)

31. Guirao, A., Centelles, M., Barranco, M., Pi, M., Polls, A., Viñas, X.: J. Phys.: Condens. Matter **4**, 667 (1992)

32. Davies, K. T. R., Flocard, H., Krieger, S., Weiss, M. S.: Nuclear Physics **A342**, 111 (1980)

33. Dalfovo, F., Stringari, S.: J. Low Temp. Phys. **89** (1-2), 325 (1992)

34. Szybisz, L., Urrutia, I.: Physical Review B **68**, 054518 (2003)

35. Giacomazzi, L., Toigo, F., Ancilotto, F.: Physical Review B **67**, 104501 (2003)

36. Balbás, L. C., Mañanes, A., Membrado, M., Pacheco, A. F., Sañudo, J.: J. Chem. Phys. **94** (11), 7335 (1991)

37. Enss, C., Hunklinger, S.: *Low Temperature Physics.* Springer Berlin Heidelberg, 2005.

38. Kinoshita, K., Yamada, T.: Nature **357**, 313 (1992)

39. Wilks, J. : *An Introduction to Liquid Helium.* Oxford, 1970.

Appendices

Appendix A
Fortran Code

Program 1: Stringari and Treiner
Planar Symmetry

```
implicit real*8 (a-h, o-z)
      real*8 mass
      dimension rhoorig(400), hmat(800, 800), tmat(800, 800), p(800)
      dimension z(800), vmat(800, 800), psinew(800), rho(800)
      dimension psi(800), U(400), UU(800), rhogam(400), delsq(400)
      dimension rhonew(800), rhohybrid(800), rhogamma(800), p1(800)
      dimension delsqrho(800), psiold(800), rhoave(400), differ(800)

c      DEFINE  VARIABLES:
c      Hmat = HAMILTONIAN MATRIX
c      Vmat = POTENTIAL ENERGY MATRIX
c      Tmat = KINETIC ENERGY MATRIX
c      rhoorig = DENSITY from original fxn
c      z = COORDINATE VALUE
c      rhogamma and delsqRho are used to calculate U fxn
c      U = original meanfield from rhoorig
c      rho = includes mirror image of rhoorig and is replaced by rhohybrid
c      UU = includes mirror image of U fxn
c      psinew = WAVEFXN imported from subroutine
c      psi = WAVEFXN from density rhohybrid
c      rhonew = calculated from psinew
c      rhohybrid =  99:1 ratio of old:new density fxns


      open (16, file='summary2.out')

      nmax=800
      nmax1=400
      dz=0.10d0
      rho0=0.021836d0

c     Z COORDINATE RANGE FROM -60 to +19.9  (Angstroms)

      z(1)=-60.0d0

      do n=2, nmax
         z(n)=z(n-1)+dz
c         write (6, *) z(n)
      end do

c     CONSTANTS
```

```
c     mass=kg, hbar=kg*m^2*s-1, boltz=kg*m^2*s-2*K-1

      mass=4.002602*1.6605402d-27
      hbar=(1.05457266d-34)*1.0d20
      boltz=(1.380658d-23)*1.0d20
      const=-(hbar**2)/(2*mass*boltz)
c      dtau=(0.05d0*boltz*mass*dz**2)/(2.0d0*hbar**2)
c      write (6, *)  hbar, boltz, const



c     IMPORT MEANFIELD (Kelvin)

      open (9, file='meaneqn26.out')
      do n=1, nmax1
         read (9, *) rhoorig(n), U(n)
      end do

      close (9)

      do n=1, nmax1
         UU(n+400)=U(n)
         UU(401-n)=U(n)
         rho(n+400)=rhoorig(n)
         rho(401-n)=rhoorig(n)
       end do

c     trapezoidal rule integration of original density rho(n)

      summ=0.0d0
      a1=z(1)
      b1=z(800)


      do n=1, nmax

         if (n.eq.1.or.n.eq.nmax) then
         k=1
         summ=summ+k*rho(n)
         else if (n.gt.1.and.n.lt.nmax) then
         k=2
         summ=summ+k*rho(n)
         end if

      end do
         fxn1=((b1-a1)/(2*nmax))*summ


c     Tmat and Vmat INITIATE WITH ZEROES

      do n=1, nmax
      do o=1, nmax
         tmat(n, o)=0.0d0
```

```
         vmat(n, o)=0.0d0
       end do
       end do

c    ITERATION LOOP

c      goto 400

       do iteration=1, 50000


c      Tmat and Vmat INITIATE VALUES

       do n=1, nmax
       do o=1, nmax
          if (n.eq.o) then
             vmat(n, o)=UU(n)
             tmat(n, o)=(hbar**2/(mass*boltz*dz**2))
          else if (o.eq.(n+1).or.o.eq.(n-1)) then
             tmat(n, o)=-(hbar**2/(2*mass*boltz*dz**2))
          end if
       end do
       end do

       do n=1, nmax
       do o=1, nmax
          hmat(n, o)=vmat(n, o) + tmat(n, o)
       end do
       end do


       call calcpsi(hmat, psinew, eval)

c      NORMALIZE PSINEW(N)

       sum2=0.0d0
       do n=1, nmax
          sum2=sum2+psinew(n)
       end do

       do n=1, nmax
          psinew(n)=psinew(n)/sum2
c          write (6, *)  psinew(n), z(n)
       end do

c      CALCULATE RHONEW(N)

       do n=1, nmax
          rhonew(n)=((psinew(n))**2)
       end do

c      makes density symmetrical by taking average of two values
       do n=1, nmax1
          rhoave(n)=(rhonew(n)+rhonew(801-n))/2
```

```
c          write (6, *) rhoave(n), z(n)
      end do

      do n=1, nmax1
         rhonew(n)=rhoave(n)
         rhonew(801-n)=rhoave(n)
      end do

c     initiate summ to zero
c     trapezoidal rule integration of rhonew to rescale density
ccccccccccccc

      summ=0.0d0

      a2=z(1)
      b2=z(800)

      do n=1, nmax
         if (n.eq.1.or.n.eq.nmax) then
         k=1
         summ=summ+k*rhonew(n)
         else if (n.gt.1.and.n.lt.nmax) then
         k=2
         summ=summ+k*rhonew(n)
         end if

      end do
         fxn2=((b2-a2)/(2*nmax))*summ


      do n=1, nmax
         rhonew(n)=rhonew(n)/fxn2
      end do

      do n=1, nmax
         rhonew(n)=fxn1*rhonew(n)
      end do
ccccccccccccc


c     scale density to equal integration of original density
c     rescale


c     OUTPUT new dens=rhonew,
c       hybrid dens=rhohybrid
c       bigdiff to see difference of densities btw iterations

      bigdiff=0.0d0

      do n=1, nmax
         rhohybrid(n)=(0.995d0*rho(n))+(0.005d0*rhonew(n))
         differ(n)=abs(rhohybrid(n)-rhonew(n))
         if (differ(n).gt.bigdiff) then
```

```
            bigdiff=differ(n)
         else
            bigdiff=bigdiff
         end if
c         write (6, *) rhohybrid(n), rho(n), rhonew(n), z(n)
      end do

      write (6, *) bigdiff, eval

      write (16, *) bigdiff, eval, fxn1, fxn2

      call flush(16)

c      calculates second derivative of rhohybrid(n)
      do n=1, nmax
         if (n.eq.1.or.n.eq.nmax) then
         delsqrho(n)=0
         else
         delsqrho(n)=(1/dz**2)*(rhohybrid(n+1)-2*rhohybrid(n)+
     .   rhohybrid(n-1))
         end if
      end do


      b=-8.88810d2
      c=1.04554d7
      gamm=2.8d0
      coeff=(2.0d0+gamm)/2.0d0
      d=2.383d3

c      open a file for the output of only this iteration

      open (18, file='output2.txt')

c      meanfield output U(n)
      do n=1, nmax
         rhogamma(n)=rhohybrid(n)**(1+gamm)
         UU(n)=b*rhohybrid(n)+coeff*c*rhogamma(n)-(2.0d0*d*delsqrho(n))
      write (6, *) UU(n), rho(n), rhohybrid(n), z(n)
      write (18, *) UU(n), rho(n), rhohybrid(n), z(n)
      end do

      close (18)

c      WAVEFXN FROM SQRT(rhohybrid(N))
      do n=1, nmax
         psi(n)=sqrt(rhohybrid(n))
c         write (6, *) psi(n), z(n)
      end do

c     define rhohybrid as rho for the next loop. continues cycle
      do n=1, nmax
         rho(n)=rhohybrid(n)
c         write (6, *) rho(n), z(n)
```

```
      end do


c      END ITERATION LOOP
      end do

400   continue


      stop
      end
```

Program 2: Stringari and Treiner
Spherical Droplets

```
  implicit real*8 (a-h, o-z)
      real*8 mass
      dimension rho(1861), hmat(1861, 1861), tmat(1861, 1861)
      dimension r(1861), vmat(1861, 1861), psinew(1861)
      dimension U(1861), delsqrho(1861), differ(1861)
      dimension rhonew(1861), rhohybrid(1861), rhogamma(1861)


c      Hmat = HAMILTONIAN MATRIX
c      Vmat = POTENTIAL ENERGY MATRIX
c      Tmat = KINETIC ENERGY MATRIX
c      rho = DENSITY
c      r = COORDINATE VALUE
c      rhogamma and delsqRho are used to calculate U fxn
c      U = original meanfield from rho
c      psinew = WAVEFXN imported from subroutine
c      psi = WAVEFXN from density rhohybrid
c      rhonew = calculated from psinew
c      rhohybrid =  99.5:0.5 ratio of old:new density fxns


      open (16, file='summary.out')



c     CONSTANTS
c     mass=kg, hbar=kg*m^2*s-1, boltz=kg*m^2*s-2*K-1

      pi=3.1415926535d0
      mass=4.002602*1.6605402d-27
      hbar=(1.05457266d-34)*1.0d20
      boltz=(1.380658d-23)*1.0d20
      const=-(hbar**2)/(2*mass*boltz)

c      write (6, *)  hbar, boltz, const

      b=-8.88810d2
      c=1.04554d7
      gamm=2.8d0
      coeff=(2.0d0+gamm)/2.0d0
      d=2.383d3

      nmax=1861
      dr=0.02377d0
      r(1)=0.0d0
      h0=2.377d0

      rho0=0.021836d0
```

```
c     R COORDINATE RANGE FROM 0 to 44.2122 (Angstroms)

      do n=2, nmax
         r(n)=r(n-1)+dr
c         write (6, *) r(n)
      end do


c     initial guess of denisty profile using Treiner eqn 26


      open (17, file='densitytest.out')
      do n=1, nmax

         read (17, *) rho(n)

      end do

      close (17)

c     trapezoidal rule integration of original density rho(n)   = fxn1

      sum1=0.0d0
      a1=r(1)
      b1=r(1861)


      do n=1, nmax

         if (n.eq.1.or.n.eq.nmax) then
         k=1
         sum1=sum1+(k*4.0d0*rho(n)*pi*r(n)**2)
         else if (n.gt.1.and.n.lt.nmax) then
         k=2
         sum1=sum1+(k*4.0d0*rho(n)*pi*r(n)**2)
         end if

      end do
         fxn1=((b1-a1)/(2*nmax))*sum1


c     Tmat and Vmat INITIATE WITH ZEROES

      do n=1, nmax
      do o=1, nmax
         tmat(n, o)=0.0d0
         vmat(n, o)=0.0d0
      end do
      end do

c    BEGIN  ITERATION LOOP


      do iteration=1, 50000
```

```
c    calculates second derivative of rho(n). assumes density is constant at r=0 and
r=44.2122 A

      do n=1, nmax
         if (n.eq.1) then
         delsqrho(n)=(1.0d0/dr**2)*(2.0d0*rho(n+1)-2.0d0*rho(n))
         else if (n.eq.nmax) then
         delsqrho(n)=(1.0d0/dr**2)*(2.0d0*rho(n-1)-2.0d0*rho(n))
         else
         delsqrho(n)=((1.0d0/dr**2)*(rho(n+1)-2*rho(n)+rho(n-1)))*
     .   ((1.0d0/(r(n)*dr))*(rho(n+1)-rho(n-1)))
         end if
      end do


c      meanfield U(n)
      do n=1, nmax
         rhogamma(n)=rho(n)**(1.0d0+gamm)
         U(n)=b*rho(n)+coeff*c*rhogamma(n)-(2.0d0*d*delsqrho(n))
c      write (6, *) U(n), rho(n), r(n)

      end do


c     Tmat and Vmat INITIATE VALUES
c     special case of r=0 use x, y, z for kinetic energy operator

      do n=1, 1
      do o=1, 2
         if (o.eq.1) then
            vmat(n, o)=U(n)
            tmat(n, o)=((3.0d0*hbar**2)/(boltz*mass*dr**2))
         else if (o.eq.2) then
            tmat(n, o)=-((3.0d0*hbar**2)/(boltz*mass*dr**2))
         end if
      end do
      end do

c     kinetic energy operator in all other cases

      do n=2, nmax
      do o=1, nmax
         if (n.eq.o) then
            vmat(n, o)=U(n)
            tmat(n, o)=(hbar**2/(mass*boltz*dr**2))
         else if (o.eq.(n+1)) then
            tmat(n, o)=-(hbar**2/(2.0d0*mass*boltz*dr**2))-(hbar**2/(
     .mass*boltz*2.0d0*dr*r(n)))
         else if (o.eq.(n-1)) then
            tmat(n, o)=-(hbar**2/(2.0d0*mass*boltz*dr**2))+(hbar**2/(
     .mass*boltz*2.0d0*dr*r(n)))
         end if
```

```
      end do
      end do

      do n=1, nmax
      do o=1, nmax
         hmat(n, o)=vmat(n, o) + tmat(n, o)

c        if (n.lt.5.and.o.lt.5) then

c        write (6, *) n, o, tmat(n, o), vmat(n, o), hmat(n, o)

c        end if

      end do
      end do
ccccccccccccccccccccccccccccccccccccccccccccccccccccccccccccccccccccccccccccccccc

      call calcpsi(hmat, psinew, eval)

      sum5=0.0d0
      do n=1, nmax
         sum5=sum5+(psinew(n)*4.0d0*pi*r(n)**2)
      end do

      do n=1, nmax
         psinew(n)=psinew(n)/sum5
      end do

      do n=1, nmax
         rhonew(n)=psinew(n)**2
c         write (6, *)  psinew(n), r(n), rhonew(n)
      end do


c     trapezoidal rule integration of rhonew to rescale density
c     fxn 8

      sum8=0.0d0
      a8=r(1)
      b8=r(nmax)
      tmax8=nmax-1

      do n=1, nmax
         if (n.eq.1.or.n.eq.nmax) then
         k=1
         sum8=sum8+(k*4.0d0*pi*rhonew(n)*r(n)**2)
         else if (n.gt.1.and.n.lt.nmax) then
         k=2
         sum8=sum8+(k*4.0d0*pi*rhonew(n)*r(n)**2)
         end if
      end do
         fxn8=((b8-a8)/(2.0d0*tmax8))*sum8
c         write (6, *) fxn8
```

```
      do n=1, nmax
         rhonew(n)=fxn1*(rhonew(n)/fxn8)
      end do

ccccccccccccccccccccccccccccccccccccccccccccccccccccc
c     OUTPUT original density=rho, new density=rhonew,
c       hybrid density=rhohybrid
c       bigdiff to see difference of densities btw iterations

      bigdiff=0.0d0

      do n=1, nmax
         rhohybrid(n)=(0.9975d0*rho(n))+(0.0025d0*rhonew(n))
         differ(n)=abs(rhohybrid(n)-rhonew(n))
         if (differ(n).gt.bigdiff) then
             bigdiff=differ(n)
         else
             bigdiff=bigdiff
         end if
c         write (6, *) rhohybrid(n), rho(n), U(n), r(n)
      end do

      write (6, *) bigdiff, eval

      write (16, *) bigdiff, eval, fxn1, fxn8

      call flush(16)

c      open a file for the output of only this iteration

      open (18, file='output.txt')

c ccccccccc     meanfield output U(n)    ccccccccccccc

      do n=1, nmax

         write (6, *) U(n), rho(n), rhohybrid(n), psinew(n), r(n)
         write (18, *) U(n), rho(n), rhohybrid(n), psinew(n), r(n)

      end do

      close (18)

cccccc     define rho as rhohybrid for the next loop. continues cycle ccccccccc
      do n=1, nmax
         rho(n)=rhohybrid(n)
c         write (6, *) rho(n), r(n)
      end do

ccc   end iteration loop
      end do

      stop
      end
```

Program 3: Orsay-Paris Collaboration
Planar Symmetry

```
implicit real*8 (a-h, o-z)
      real*8 mass

      dimension rho(4001), z(4001), U(4001), fxnI(4001), fxnF(4001)
      dimension rhobar(4001), hmat(4001, 4001)
      dimension vmat(4001, 4001), differ(4001), psinew(4001), fxnH(4001)
      dimension rhonew(4001), rhb(4001), tmat(4001, 4001)
      dimension rhohybrid(4001), drho(4001), fxnG(4001)
      dimension UtermG(4001), UtermE(4001), UtermD(4001), UtermA(4001)
      dimension UtermB(4001), UtermF1(4001), UtermF2(4001)
      dimension UtermC(4001), fxnA(4001)
      dimension fxnB(4001), fxnC(4001), fxnE(4001)
      dimension rhobg(4001), Utemp(4001)


c     initial parameters

      nmax=4001
      dz=0.02377d0
      rho0=0.021836d0

c     z coordinate system

      z(1)=-47.54d0

      do n=2, nmax
         z(n)=z(n-1)+dz
      end do

c    IMPORT initial density profile

      open (22, file='temp.txt')
      do n=1, nmax

         read (22, *) Utemp(n), rho(n)

      end do

      close (22)


c    fxn1 is the normalization of the droplet size

      sum1=0.0d0
      a1=z(1)
      b1=z(nmax)
      tmax1=nmax-1

      do n=1, nmax
```

```
         if (n.eq.1.or.n.eq.nmax) then
         k=1
         sum1=sum1+k*rho(n)
         else if (n.gt.1.and.n.lt.nmax) then
         k=2
         sum1=sum1+k*rho(n)
         end if

      end do

         fxn1=((b1-a1)/(2.0d0*tmax1))*sum1
c         write (6, *) fxn1


c     CONSTANTS

      h=2.377d0
      pi=3.1415926535d0
      epsilom=10.22d0
      alpha=2.556d0
      alph0=2.556d0/2.377d0
      gamm=2.8d0
      c=1.04554d7

      mass=4.002602*1.6605402d-27
      hbar=(1.05457266d-34)*1.0d20
      boltz=(1.380658d-23)*1.0d20

c     COEFFICIENTs

      coeffrhb=(3.0d0/(4.0d0*h))

      coeffA=4.0d0*pi*epsilom*alpha**2
      coeffB=4.0d0*pi*epsilom*alpha**2
      coeffC=4.0d0*pi*epsilom*alpha**2

      coeffD=c/2.0d0
      coeffE=((3.0d0*c)/(8.0d0*h))*(gamm+1.0d0)


ccccccccccccc     Tmat and Vmat INITIATE WITH ZEROES ccccccccccccc

      do n=1, nmax
      do o=1, nmax
         tmat(n, o)=0.0d0
         vmat(n, o)=0.0d0
      end do
      end do


c     open file for bigdiff

      open (26, file='summary.out')
```

```
c     BEGIN ITERATION LOOP

      do iteration=1, 50000


c    rhobar   coarse-grained density


      do n=1, 101

        rhobar(n)=0.0d0
        rhobg(n)=0.0d0

c        write (6, *) rhobar(n), z(n)

      end do

      do n=102, 3901

        i=n-100
        j=n+100
        nmaxrhb=200
        sumrhb=0.0d0
        arhb=z(i)
        brhb=z(j)


        do n1=i, j

        rhb(n1)=(1.0d0-((z(n)-z(n1))/h)**2)*rho(n1)

        if (n1.eq.i.or.n1.eq.j) then
         k=1
         sumrhb=sumrhb+k*rhb(n1)
        else if (n1.gt.i.and.n1.lt.j) then
         k=2
         sumrhb=sumrhb+k*rhb(n1)
        else
         sumrhb=0.0d0
      end if
      end do
       rhobar(n)=coeffrhb*((brhb-arhb)/(2.0d0*nmaxrhb))*sumrhb
       rhobg(n)=exp(2.8d0*dlog(rhobar(n)))
c        write (6, *) rhobar(n), z(n)

      end do


      do n=3902, 4001

        rhobar(n)=0.0d0
        rhobg(n)=0.0d0
```

```
c        write (6, *) rhobar(n), z(n)

       end do


c      remainder of Uterms and calculation of U(n)


       do n=1, 100

         U(n)=0.0d0

c        write (6, *) U(n), rho(n), z(n)

       end do


       do n=101, 3900

       i=n-100
       j=n+100

       sumA=0.0d0
       nmaxA=i
       aA=z(1)
       bA=z(i)


c        limits -inf to z-h

          do n1=1, i

          fxnA(n1)=rho(n1)*((alpha/(z(n)-z(n1)))**4)*((0.2d0*
     .    ((alpha/(z(n)-z(n1)))**6))-0.5d0)

         if (n1.eq.1.or.n1.eq.i) then
          k=1
          sumA=sumA+k*fxnA(n1)
         else if (n1.gt.1.and.n1.lt.i) then
          k=2
          sumA=sumA+k*fxnA(n1)
         else
          sumA=0.0d0
         end if
         end do

          UtermA(n)=coeffA*((bA-aA)/(2.0d0*nmaxA))*sumA


c        limits z-h to z+h

         sumC=0.0d0
         nmaxC=200
```

```
      aC=z(i)
      bC=z(j)

      sumE=0.0d0
      nmaxE=200
      aE=z(i)
      bE=z(j)

       do n1=i, j

       fxnC(n1)=(rho(n1)*(alph0**4))*((((8.0d0/15.0d0)*(alph0**6))-
     .   (5.0d0/6.0d0))-(1.0d0/3.0d0)*(((z(n)-z(n1))/h)**6)*
     .   ((alph0**6)-1.0d0))

       fxnE(n1)=(rho(n1)*rhobg(n1))*(1.0d0-(((z(n)-z(n1))/h)**2))

      if (n1.eq.i.or.n1.eq.j) then
       k=1
       sumC=sumC+k*fxnC(n1)
       sumE=sumE+k*fxnE(n1)
      else if (n1.gt.i.and.n1.lt.j) then
       k=2
       sumC=sumC+k*fxnC(n1)
       sumE=sumE+k*fxnE(n1)
      else
       sumC=0.0d0
       sumE=0.0d0
      end if
      end do


       UtermC(n)=coeffC*((bC-aC)/(2.0d0*nmaxC))*sumC

       UtermE(n)=coeffE*((bE-aE)/(2.0d0*nmaxE))*sumE


c     limits z+h to +inf

       sumB=0.0d0
       nmaxB=nmax-j
       aB=z(j)
       bB=z(nmax)

       do n1=j, nmax

       fxnB(n1)=rho(n1)*((alpha/(z(n)-z(n1)))**4)*((0.2d0*
     .   ((alpha/(z(n)-z(n1)))**6))-0.5d0)

      if (n1.eq.j.or.n1.eq.nmax) then
       k=1
       sumB=sumB+k*fxnB(n1)
      else if (n1.gt.j.and.n1.lt.nmax) then
       k=2
       sumB=sumB+k*fxnB(n1)
```

```
        else
         sumB=0.0d0
        end if
        end do

        UtermB(n)=coeffB*((bB-aB)/(2.0d0*nmaxB))*sumB

        UtermD(n)=coeffD*(rhobar(n)**(gamm+1.0d0))

        U(n)=UtermA(n)+UtermB(n)+UtermC(n)+UtermD(n)+UtermE(n)

c      write (6, *) UtermA(n), UtermB(n), UtermC(n), z(n)
c      write (6, *) UtermE(n), UtermD(n), z(n)

c       write (6, *) U(n), rho(n), z(n)

      end do


      do n=3901 , nmax

        U(n)=0.0d0
c        write (6, *) U(n), rho(n), z(n)

      end do

c      goto 4004
ccccccccccccccc     Tmat and Vmat INITIATE VALUES   ccccccccccccccccccc

      do n=1, nmax
      do o=1, nmax
         if (n.eq.o) then
            vmat(n, o)=U(n)
            tmat(n, o)=(hbar**2/(mass*boltz*dz**2))
         else if (o.eq.(n+1).or.o.eq.(n-1)) then
            tmat(n, o)=-(hbar**2/(2.0d0*mass*boltz*dz**2))
         end if
      end do
      end do

      do n=1, nmax
      do o=1, nmax
         hmat(n, o)=vmat(n, o) + tmat(n, o)
      end do
      end do



      call calcpsi(hmat, psinew, eval)

      sumpsi=0.0d0

      do n=1, nmax
         sumpsi=sumpsi+psinew(n)
```

```
      end do

      do n=1, nmax
         psinew(n)=psinew(n)/sumpsi
      end do

      do n=1, nmax
         rhonew(n)=psinew(n)**2
c         write (6, *)  psinew(n), z(n), rhonew(n)
      end do



ccccccccccccccc     trapezoidal rule integration of rhonew to rescale density
ccccccccccccc


      sum8=0.0d0
      a8=z(1)
      b8=z(nmax)
      tmax8=nmax-1

      do n=1, nmax
         if (n.eq.1.or.n.eq.nmax) then
         k=1
         sum8=sum8+(k*rhonew(n))
         else if (n.gt.1.and.n.lt.nmax) then
         k=2
         sum8=sum8+(k*rhonew(n))
         end if
      end do
         fxn8=((b8-a8)/(2.0d0*tmax8))*sum8
c         write (6, *) fxn8

      do n=1, nmax
         rhonew(n)=fxn1*(rhonew(n)/fxn8)
      end do




c     OUTPUT original density=rhomirror, new dens=rhonew,
c       hybrid dens=rhohybrid
c       bigdiff to see difference of densities btw iterations

      bigdiff=0.0d0

      do n=1, nmax
         rhohybrid(n)=(0.9985d0*rho(n))+(0.0015d0*rhonew(n))
         differ(n)=abs(rhohybrid(n)-rhonew(n))
         if (differ(n).gt.bigdiff) then
             bigdiff=differ(n)
         else
```

```
               bigdiff=bigdiff
            end if
c            write (6, *) rhohybrid(n), rho(n), U(n), z(n)
      end do

      write (6, *) bigdiff, eval

      write (26, *) bigdiff, eval, fxn1, fxn8

      call flush(26)


      open (25, file='output.txt')

c ccccccccc     meanfield output U(n)    ccccccccccccc

      do n=1, nmax

         write (6, *) U(n), rho(n), rhohybrid(n), psinew(n), z(n)
         write (25, *) U(n), rho(n), rhohybrid(n), psinew(n), z(n)

      end do

      close (25)

cccccc     define rhohybrid as rhomir for the next loop. continues cycle ccccccccc
      do n=1, nmax
         rho(n)=rhohybrid(n)
c         write (6, *) rho(n), z(n)
      end do

4004   continue

c     END ITERATION LOOP

      end do

      stop
      end
```

Program 4: Orsay-Paris Collaboration
Spherical Droplets with Atomic Dopant

```
implicit real*8 (a-h, o-z)
      real*8 mass
      dimension rho(3162), r(3162), rhobar(3162), rhobg(3162)
      dimension rhbtermA(3162), rhbtermAa(3162), rhbtermB(3162)
      dimension rhbtermBb(3162), rhbtermC(3162), rhbtermCc(3162)
      dimension termA1(3162), termAa(3162), termB1(3162), termC1(3162)
      dimension termC2(3162), termA2(3162), termB2(3162), termD1(3162)
      dimension psi(3162), U(3162), termD2(3162), termCc(3162)
      dimension termE1(3162), termE2(3162), termF1(3162), termF2(3162)
      dimension termF3(3162), termF4(3162), termG1(3162), termG2(3162)
      dimension termFf(3162), psinew(3162), tmat(3162, 3162)
      dimension hmat(3162, 3162), vmat(3162, 3162), rhohybrid(3162)
      dimension differ(3162), rhoave(3162), rhonew(3162)
      dimension dopant(3162), Utmp(3162)

ccccccccccccc    initial parameters of coordinate array

      nmax=3162
      dr=0.02377d0
      r(1)=0.0d0
      h0=2.377d0

      rho0=0.021836d0

ccccccccccccc    r coordinate range (Angstroms)

      do n=2, nmax
         r(n)=r(n-1)+dr
c         write (6, *) r(n)
      end do


ccccccccccccc     initial guess of denisty profile using Treiner eqn 26
ccccccccccccc     density = rho(n)
ccccccccccc        imported from density of r coordinate system


      open (91, file='tempinput.txt')
      do n=1, nmax

         read (91, *) Utmp(n), rho(n)

      end do

      close (91)

ccccccccccccc     Tmat and Vmat INITIATE WITH ZEROES ccccccccccccc

      do n=1, nmax
```

```
      do o=1, nmax
         tmat(n, o)=0.0d0
         vmat(n, o)=0.0d0
      end do
      end do

ccccccccccccccc     constants

c     mass=kg, hbar=kg*m^2*s-1, boltz=kg*m^2*s-2*K-1

      mass=4.002602*1.6605402d-27
      hbar=(1.05457266d-34)*1.0d20
      boltz=(1.380658d-23)*1.0d20
      const=-(hbar**2)/(2*mass*boltz)

c      dtau=(0.05d0*boltz*mass*dz**2)/(2.0d0*hbar**2)
c      write (6, *)  hbar, boltz, const

c      coefficients for terms in meanfield function

c     define constants

      epsilom=10.22d0
      pi=3.1415926535d0
      alpha=2.556d0
      alph0=alpha/h0
      c=1.04554d7


c     define dopant potential as a Lennard Jones function
c     using a value of 2 times epsilom to indicate an attractive impurity centered
at the middle c     of the droplet



      dopant(1)=5.8d30

      do n=2, nmax

      dopant(n)=(4.0d0*epsilom*2.0d0)*((alpha/r(n))**12-(alpha/r(n))**6)

      end do

c      do n=1, nmax
c        write (6, *) dopant(n), r(n)

c      end do

c     define coefficients

      coeffA1=((8.0d0*pi*epsilom)/(h0**4))*((alph0**12)-
     .(alph0**6))
      coeffA2=(3.0d0/h0**3)*((c*3.8d0)/2.0d0)
```

```
       coeffB1=((4.0d0*pi*epsilom)/(3.0d0*h0**4))*((alph0**12)-
      .(alph0**6))
       coeffB2=(3.0d0*3.8d0*c)/(8.0d0*h0**3)

       coeffC1=(4.0d0*pi*epsilom*alpha**12)/5.0d0
       coeffC2=-(2.0d0*pi*epsilom*alpha**6)


       coeffD1=(8.0d0*pi*epsilom*alpha**12)
       coeffD2=-(8.0d0*pi*epsilom*alpha**6)

       coeffE1=(4.0d0*pi*epsilom*alpha**12)/5.0d0
       coeffE2=(-2.0d0*pi*epsilom*alpha**6)

       coeffF1=(3.0d0*c*3.8d0)/(8.0d0*h0**3)
       coeffF2=((4.0d0*pi*epsilom)/(3.0d0*h0**4))*(alph0**12-alph0**6)
       coeffF3=(4.0d0*pi*epsilom*alpha**12)/5.0d0
       coeffF4=(-2.0d0*pi*epsilom*alpha**6)

       coeffG1=(4.0d0*pi*epsilom*alpha**12)/5.0d0
       coeffG2=(-2.0d0*pi*epsilom*alpha**6)

ccccccccccccc    trapezoidal rule integration of original density rho(n)
ccccccccccccc     used to normalize density
c       Main Explanation of Term Notation
c   numbers are used to indicate the order that trapezoid rule functions appear in
the code
c   letters beginning with A1, A2, B1, F4,... are used to indicate intermediate
functions used in order that they appear in the code. double letters Aa are further
encased intermediates.
c   represent coefficients used within the function to simplify the expression.

c   sum1 becomes additive function during subsequent trapezoid integrations
c   a1 first r-coordinate in trapezoid integration
c   b1 is endpoint r-coordinate in trapezoid integration
c   tmax1 is the number of sections that the function is divided into for trap.
integration

c    fxn1 is the normalization of the droplet size

       sum1=0.0d0
       a1=r(1)
       b1=r(nmax)
       tmax1=nmax-1

       do n=1, nmax

          if (n.eq.1.or.n.eq.nmax) then
          k=1
          sum1=sum1+(k*4.0d0*pi*rho(n)*r(n)**2)
          else if (n.gt.1.and.n.lt.nmax) then
          k=2
          sum1=sum1+(k*4.0d0*pi*rho(n)*r(n)**2)
          end if
```

```
      end do

         fxn1=((b1-a1)/(2.0d0*tmax1))*sum1
c         write (6, *) fxn1

ccccccccccccccccccccc     rho bar^gamma=rhobg(n)    rho bar=rhobar(n)
ccccccccccccccccc

c    trapezoid integration of rhobar(n) for r-values where r < h
c    ii  is the ending n1 value for the trapezoid integration
c    here variables with 2 indicate inside the sphere from 0 to h-r limits
c    a is the starting r-coordinate for the trap int
c    b is the endpoint r-coordinate for the trap int
c    tmax is the number of sections over which the trap int is done
c    sum becomes the integration function added to with each subsequent loop
c    variables with 3 indicate inside the sphere from h-r to r+h limits

      open (70, file='dopedsummary.out')
ccccccccccccccccccc     ITERATION LOOP        ccccccccccccccccccc


      do iteration=1, 50000


c      define parameters  rhobar and rhobargamma for    r<h

      do n=1, 101

         ii=102-n
         i=n-100
         j=n+100

         a2=r(1)
         b2=r(ii)
         tmax2=ii-1

         tmax3=j-ii
         a3=r(ii)
         b3=r(j)

         sum2=0.0d0
         sum3=0.0d0

         do n1=1, ii
            rhbtermAa(n1)=(r(n1)**2)*rho(n1)
            if (n1.eq.1.or.n1.eq.ii) then
               k=1
               sum2=sum2+k*rhbtermAa(n1)
            else if (n1.gt.1.and.n1.lt.ii) then
               k=2
               sum2=sum2+k*rhbtermAa(n1)
            else
               sum2=0.0d0
```

```
            end if
         end do

            if (tmax2.eq.0) then
             rhbtermA(n)=0.0d0
            else
             rhbtermA(n)=(3.0d0/h0**3)*((b2-a2)/dble(2*tmax2))*sum2
            end if


         do n1=ii, j
            rhbtermBb(n1)=((rho(n1)*r(n1))/(2*r(n)))*
     .((2.0d0*r(n1)*r(n))-(-(h0**2)+r(n1)**2+r(n)**2))
            if (n1.eq.ii.or.n1.eq.j) then
               k=1
               sum3=sum3+k*rhbtermBb(n1)
            else if (n1.gt.ii.or.n1.lt.j) then
               k=2
               sum3=sum3+k*rhbtermBb(n1)
            else
               sum3=0.0d0
            end if
         end do

            if (n.eq.1) then
            rhbtermB(n)=0.0d0
            else
            rhbtermB(n)=(3.0d0/(2.0d0*h0**3))*((b3-a3)/dble(2*tmax3))
     .*sum3
            end if

            rhobar(n)=rhbtermA(n)+rhbtermB(n)
            rhobg(n)=exp(2.8d0*dlog(rhobar(n)))

c         write (6, *) rhobar(n), r(n), rho(n), rhbtermA(n), rhbtermB(n)
      end do


c     rhobar(n) for values r > h


c     tmax4 accounts for the 200 points within the coarse grain density sphere.
r(n1) limits are  between  r-h and r+h
c     a4 is the first r(n) coordinate at r-h
c     b4 is the endpoint r(n) coordinate at r+h
c     sum4 is the value of the function during the trap int.
c     termZ(n1) defines the function. termZz(n1) is the intermediate to the
expression of termZ(n1)

c     define parameters


      do n=102, 3061
```

```
          sum4=0.0d0
          a4=r(i)
          b4=r(j)
          tmax4=200

          ii=102-n
          i=n-100
          j=n+100

          do n1=i, j

          rhbtermCc(n1)=(rho(n1)*r(n1)**2)

          rhbtermC(n1)=(1.0d0-((-h0**2+r(n1)**2+r(n)**2)/(2*r(n1)*r(n))))
     .*rhbtermCc(n1)

          if (n1.eq.i.or.n1.eq.j) then
           k=1
           sum4=sum4+k*rhbtermC(n1)
          else if (n1.gt.i.and.n1.lt.j) then
           k=2
           sum4=sum4+k*rhbtermC(n1)
          else
           sum4=0.0d0
          end if

          end do

          rhobar(n)=(3.0d0/(2.0d0*h0**3))*((b4-a4)/dble(2*tmax4))*sum4

          rhobg(n)=exp(2.8d0*dlog(rhobar(n)))

c          write (6, *)  rhobar(n), r(n), rho(n)
       end do

c     once the density has decayed to zero, rhobar and rhobar^gamma do as well.
here
each is defined as zero for the last 100 points.

       do n=3062, nmax
          rhobar(n)=0.0d0
          rhobg(n)=0.0d0
c          write (6, *)  rhobar(n), r(n), rho(n)
       end do


ccccccccccccccccc      U(n) output    defining the mean-field function

c    meanfield function for values r < h

       do n=1, 101


c    inside the inner sphere
```

```
          sumA1=0.0d0
          sumA2=0.0d0

c     define parameters
          ii=102-n
          i=n-100
          j=n+100

          aA=r(1)
          bA=r(ii)
          tmaxA=ii-1


          do n1=1, ii

         if (n.eq.1) then
         termA1(n1)=2.0d0*rho(n1)*r(n1)**6
         else
         termA1(n1)=((r(n1)*rho(n1))/(6.0d0*r(n)))*(-((r(n1)**2)+
     .r(n)**2-(2.0d0*r(n1)*r(n)))**3+((r(n1)**2)+r(n)**2+(2.0d0*
     .r(n1)*r(n)))**3)
          end if

          termA2(n1)=(r(n1)**2)*rho(n1)*rhobg(n1)

           if (n1.eq.1.or.n1.eq.ii) then
            k=1
            sumA1=sumA1+k*termA1(n1)
            sumA2=sumA2+k*termA2(n1)
           else if (n1.gt.1.and.n1.lt.ii) then
            k=2
            sumA1=sumA1+k*termA1(n1)
            sumA2=sumA2+k*termA2(n1)
           else
            sumA1=0.0d0
            sumA2=0.0d0
           end if

c      write (6, *) r(n), r(n1), rho(n), rho(n1)
c       write (6, *) r(n), termAa(n1), termA1(n1)

        end do

          if (tmaxA.gt.0) then
          fxnA1=((bA-aA)/(2.0d0*tmaxA))*sumA1
          fxnA2=((bA-aA)/(2.0d0*tmaxA))*sumA2
          else
          fxnA1=0.0d0
          fxnA2=0.0d0
          end if

c    UtermA defines the meanfield function from boundaries 0 to h-r for r<h
```

```
      UtermA1=fxnA1*coeffA1
      UtermA2=fxnA2*coeffA2
      UtermA3=(c/2.0d0)*(rhobar(n)*rhobg(n))

c      write (6, *) UtermA1, UtermA2, UtermA3, r(n)


c    inside the outer portion of the sphere defined by sum6 btw h-r and h+r
c    outside the sphere but within the h-r and h+r boundaries defined by sum7

         ii=102-n
         j=n+100

      sumB1=0.0d0
      sumB2=0.0d0
      sumC1=0.0d0
      sumC2=0.0d0

      aBC=r(ii)
      bBC=r(j)
      tmaxBC=j-ii

         do n1=ii, j
         termB1(n1)=((r(n1)*rho(n1))/r(n))*(-((r(n1)**2)+(r(n)**2)
     .-(2.0d0*r(n1)*r(n)))**3+h0**6)

         termB2(n1)=((rho(n1)*r(n1)*rhobg(n1))/(r(n)))
     .*((2.0d0*r(n1)*r(n))-(-h0**2+r(n1)**2+r(n)**2))

         termCc(n1)=(-(h0**2)+(r(n1)**2)+(r(n)**2))

         termC1(n1)=((rho(n1)*r(n1))/r(n))*((((r(n1)**2)+(r(n)**2)-
     .termCc(n1))**-5)-(((r(n1)**2)+(r(n)**2)+(2.0d0*r(n1)*r(n)))**-5))

         termC2(n1)=((rho(n1)*r(n1))/r(n))*((((r(n1)**2)+(r(n)**2)-
     .termCc(n1))**-2)-(((r(n1)**2)+(r(n)**2)+(2.0d0*r(n1)*r(n)))**-2))

          if (n1.eq.ii.or.n1.eq.j) then
            k=1
            sumB1=sumB1+k*termB1(n1)
            sumB2=sumB2+k*termB2(n1)
            sumC1=sumC1+k*termC1(n1)
            sumC2=sumC2+k*termC2(n1)
          else if (n1.gt.ii.and.n1.lt.j) then
            k=2
            sumB1=sumB1+k*termB1(n1)
            sumB2=sumB2+k*termB2(n1)
            sumC1=sumC1+k*termC1(n1)
            sumC2=sumC2+k*termC2(n1)
          else
            sumB1=0.0d0
            sumB2=0.0d0
            sumC1=0.0d0
            sumC2=0.0d0
```

```
          end if
        end do

          if (tmaxBC.gt.0) then
           fxnB1=((bBC-aBC)/(2.0d0*tmaxBC))*sumB1
           fxnB2=((bBC-aBC)/(2.0d0*tmaxBC))*sumB2
           fxnC1=((bBC-aBC)/(2.0d0*tmaxBC))*sumC1
           fxnC2=((bBC-aBC)/(2.0d0*tmaxBC))*sumC2
          else if (n.eq.1) then
           fxnB1=0.0d0
           fxnB2=0.0d0
           fxnC1=0.0d0
           fxnC2=0.0d0
          else
           fxnB1=0.0d0
           fxnB2=0.0d0
           fxnC1=0.0d0
           fxnC2=0.0d0
          end if


c     UtermB defines the meanfield between region  h-r and r+h for r<h

      UtermB1=fxnB1*coeffB1
      UtermB2=fxnB2*coeffB2
      UtermC1=fxnC1*coeffC1
      UtermC2=fxnC2*coeffC2

c      region from r+h to infinity for r<h outside sphere

          j=n+100

          sumD1=0.0d0
          sumD2=0.0d0

          aD=r(j)
          bD=r(nmax)
          tmaxD=nmax-j

       do n1=j, nmax

       if (n.eq.1) then
        termD1(n1)=(2.0d0*rho(n1))/(r(n1)**10)

        termD2(n1)=(2.0d0*rho(n1))/(r(n1)**4)
       else
        termD1(n1)=((rho(n1)*r(n1))/(10.0d0*r(n)))*(((r(n1)**2+
     .r(n)**2-2.0d0*r(n1)*r(n))**-5)-((r(n1)**2+r(n)**2+2.0d0*
     .r(n1)*r(n))**-5))

        termD2(n1)=((rho(n1)*r(n1))/(4.0d0*r(n)))*(((r(n1)**2+r(n)**2-
     .2.0d0*r(n1)*r(n))**-2)-((r(n1)**2+r(n)**2+2.0d0*r(n1)*r(n))**-2))
       end if
```

```
          if (n1.eq.j.or.n1.eq.nmax) then
           k=1
           sumD1=sumD1+k*termD1(n1)
           sumD2=sumD2+k*termD2(n1)
          else if (n1.gt.j.and.n1.lt.nmax) then
           k=2
           sumD1=sumD1+k*termD1(n1)
           sumD2=sumD2+k*termD2(n1)
          else
           sumD1=0.0d0
           sumD2=0.0d0
          end if
         end do

          if (tmaxD.gt.0) then
            fxnD1=((bD-aD)/(2.0d0*tmaxD))*sumD1
            fxnD2=((bD-aD)/(2.0d0*tmaxD))*sumD2
          else
            fxnD1=0.0d0
            fxnD2=0.0d0
          end if

        UtermD1=fxnD1*coeffD1
        UtermD2=fxnD2*coeffD2

        U(n)=UtermA1+UtermB1+UtermC1+UtermC2+UtermA3+
       .UtermA2+UtermB2+UtermD1+UtermD2

c        write (6, *) U(n), r(n)
c        write (6, *) UtermA1+UtermB1+UtermC1+UtermC2+
c       .UtermA3+UtermA2+UtermB2+UtermD1+UtermD2, r(n)
c        write (6, *) UtermA1+UtermB1, r(n)
c        write (6, *) UtermA2+UtermB2, r(n)
c        write (6, *) UtermC1+UtermC2, r(n)
c        write (6, *) UtermD2+UtermD1, r(n)
c        write (6, *) UtermA3, r(n)
c        write (6, *) UtermA1, r(n)
        end do


        do n=102, 3062

        i=n-100

        tmaxE=i
        aE=r(1)
        bE=r(i)

        sumE1=0.0d0
        sumE2=0.0d0


          do n1=1, i
```

```
      termE1(n1)=((rho(n1)*r(n1))/r(n))*(((r(n1)**2+r(n)**2-2.0d0*
.r(n1)*r(n))**-5)-((r(n1)**2+r(n)**2+2.0d0*r(n1)*r(n))**-5))

      termE2(n1)=((rho(n1)*r(n1))/r(n))*(((r(n1)**2+r(n)**2-2.0d0*
.r(n1)*r(n))**-2)-((r(n1)**2+r(n)**2+2.0d0*r(n1)*r(n))**-2))



   if (n1.eq.1.or.n1.eq.i) then
      k=1
      sumE1=sumE1+k*termE1(n1)
      sumE2=sumE2+k*termE2(n1)
   else if (n1.gt.1.and.n1.lt.i) then
      k=2
      sumE1=sumE1+k*termE1(n1)
      sumE2=sumE2+k*termE2(n1)
   else
      sumE1=0.0d0
      sumE2=0.0d0
   end if
   end do


    if (tmaxE.gt.0) then
    fxnE1=((bE-aE)/(2.0d0*tmaxE))*sumE1
    fxnE2=((bE-aE)/(2.0d0*tmaxE))*sumE2
    else
    fxnE1=0.0d0
    fxnE2=0.0d0
    end if

 UtermE1=fxnE1*coeffE1

 UtermE2=fxnE2*coeffE2

 UtermA3=(c*rhobg(n)*rhobar(n))/2.0d0

 i=n-100
 j=n+100

 tmaxF=200
 aF=r(i)
 bF=r(j)

 sumF1=0.0d0
 sumF2=0.0d0
 sumF3=0.0d0
 sumF4=0.0d0

   do n1=i, j
     termF1(n1)=((r(n1)*rho(n1)*rhobg(n1))/r(n))*(2.0d0*r(n)*
.r(n1)-(-h0**2+r(n1)**2+r(n)**2))

     termF2(n1)=((rho(n1)*r(n1))/r(n))*(h0**6-(r(n1)**2+
```

```
.r(n)**2-2.0d0*r(n1)*r(n))**3)

     termFf(n1)=(-(h0**2)+(r(n1)**2)+(r(n)**2))

     termF3(n1)=((rho(n1)*r(n1))/r(n))*((((r(n1)**2)+(r(n)**2)-
.termFf(n1))**-5)-(((r(n1)**2)+(r(n)**2)+(2.0d0*r(n1)*r(n)))**-5))

     termF4(n1)=((rho(n1)*r(n1))/r(n))*((((r(n1)**2)+(r(n)**2)-
.termFf(n1))**-2)-(((r(n1)**2)+(r(n)**2)+(2.0d0*r(n1)*r(n)))**-2))


  if (n1.eq.i.or.n1.eq.j) then
     k=1
     sumF1=sumF1+k*termF1(n1)
     sumF2=sumF2+k*termF2(n1)
     sumF3=sumF3+k*termF3(n1)
     sumF4=sumF4+k*termF4(n1)
  else if (n1.gt.i.and.n1.lt.j) then
     k=2
     sumF1=sumF1+k*termF1(n1)
     sumF2=sumF2+k*termF2(n1)
     sumF3=sumF3+k*termF3(n1)
     sumF4=sumF4+k*termF4(n1)
  else
     sumF1=0.0d0
     sumF2=0.0d0
     sumF3=0.0d0
     sumF4=0.0d0
  end if
  end do

    if (tmaxF.gt.0) then
    fxnF1=((bF-aF)/(2.0d0*tmaxF))*sumF1
    fxnF2=((bF-aF)/(2.0d0*tmaxF))*sumF2
    fxnF3=((bF-aF)/(2.0d0*tmaxF))*sumF3
    fxnF4=((bF-aF)/(2.0d0*tmaxF))*sumF4
    else
    fxnF1=0.0d0
    fxnF2=0.0d0
    fxnF3=0.0d0
    fxnF4=0.0d0
    end if

 UtermF1=fxnF1*coeffF1

 UtermF2=fxnF2*coeffF2

 UtermF3=fxnF3*coeffF3

 UtermF4=fxnF4*coeffF4


    i=n-100
    j=n+100
```

```
          aG=r(j)
          bG=r(nmax)
          tmaxG=nmax-j

          sumG1=0.0d0
          sumG2=0.0d0

          do n1=j, nmax

            termG1(n1)=((rho(n1)*r(n1))/r(n))*(((r(n1)**2+r(n)**2-2.0d0*
     .r(n1)*r(n))**-5)-((r(n1)**2+r(n)**2+2.0d0*r(n1)*r(n))**-5))

            termG2(n1)=((rho(n1)*r(n1))/r(n))*(((r(n1)**2+r(n)**2-2.0d0*
     .r(n1)*r(n))**-2)-((r(n1)**2+r(n)**2+2.0d0*r(n1)*r(n))**-2))


         if (n1.eq.j.or.n1.eq.nmax) then
            k=1
            sumG1=sumG1+k*termG1(n1)
            sumG2=sumG2+k*termG2(n1)
         else if (n1.gt.j.and.n1.lt.nmax) then
            k=2
            sumG1=sumG1+k*termG1(n1)
            sumG2=sumG2+k*termG2(n1)
         else
            sumG1=0.0d0
            sumG2=0.0d0
         end if
         end do


          if (tmaxG.gt.0) then
          fxnG1=((bG-aG)/(2.0d0*tmaxG))*sumG1
          fxnG2=((bG-aG)/(2.0d0*tmaxG))*sumG2
          else
          fxnG1=0.0d0
          fxnG2=0.0d0
          end if

       UtermG1=fxnG1*coeffG1

       UtermG2=fxnG2*coeffG2


       U(n)=UtermE1+UtermE2+UtermF1+UtermF2+UtermF3+UtermF4+UtermG1+
     .UtermG2+UtermA3

c       write (6, *) UtermF1, r(n)
c       write (6, *) UtermF3+UtermF4, r(n)
c       write (6, *) UtermF2, r(n)
c       write (6, *) UtermE1+UtermE2, r(n)
c       write (6, *) UtermG1+UtermG2, r(n)
c       write (6, *) UtermA3, r(n)
```

```
c      write (6, *) U(n), r(n)
       end do

       do n=3063, nmax

          U(n)=0.0d0

c      write (6, *) U(n), r(n)
       end do

ccccccccccccccc     Tmat and Vmat INITIATE VALUES   ccccccccccccccccccc

cc special case of r=0 use x, y, z for kinetic energy operator

       do n=1, 1
       do o=1, 2
          if (o.eq.1) then
             vmat(n, o)=U(n)+dopant(n)
             tmat(n, o)=((3.0d0*hbar**2)/(boltz*mass*dr**2))
          else if (o.eq.2) then
             tmat(n, o)=-((3.0d0*hbar**2)/(boltz*mass*dr**2))
          end if
       end do
       end do

cc      kinetic energy operator in all other cases

       do n=2, nmax
       do o=1, nmax
          if (n.eq.o) then
             vmat(n, o)=U(n)+dopant(n)
             tmat(n, o)=(hbar**2/(mass*boltz*dr**2))
          else if (o.eq.(n+1)) then
             tmat(n, o)=-(hbar**2/(2.0d0*mass*boltz*dr**2))-(hbar**2/(
     .mass*boltz*2.0d0*dr*r(n)))
          else if (o.eq.(n-1)) then
             tmat(n, o)=-(hbar**2/(2.0d0*mass*boltz*dr**2))+(hbar**2/(
     .mass*boltz*2.0d0*dr*r(n)))
          end if
       end do
       end do

       do n=1, nmax
       do o=1, nmax
          hmat(n, o)=vmat(n, o) + tmat(n, o)

c         if (n.lt.5.and.o.lt.5) then

c         write (6, *) n, o, tmat(n, o), vmat(n, o), hmat(n, o)

c         end if

       end do
       end do
```

```
ccccccccccccccccccccccccccccccccccccccccccccccccccccccccccccccccccccccccccccccccccccccccccccccccc

cc       sum5 to normalize psinew

      call calcpsi(hmat, psinew, eval)

      sum5=0.0d0
      do n=1, nmax
         sum5=sum5+(psinew(n)*4.0d0*pi*r(n)**2)
      end do

      do n=1, nmax
         psinew(n)=psinew(n)/sum5
      end do

      do n=1, nmax
         rhonew(n)=psinew(n)**2
c         write (6, *)  psinew(n), r(n), rhonew(n)
      end do


c     initiate summ to zero
ccccccccccccccc     trapezoidal rule integration of rhonew to rescale density
ccccccccccccc


      sum8=0.0d0
      a8=r(1)
      b8=r(nmax)
      tmax8=nmax-1

      do n=1, nmax
         if (n.eq.1.or.n.eq.nmax) then
         k=1
         sum8=sum8+(k*4.0d0*pi*rhonew(n)*r(n)**2)
         else if (n.gt.1.and.n.lt.nmax) then
         k=2
         sum8=sum8+(k*4.0d0*pi*rhonew(n)*r(n)**2)
         end if
      end do
         fxn8=((b8-a8)/(2.0d0*tmax8))*sum8
c         write (6, *) fxn8

      do n=1, nmax
         rhonew(n)=fxn1*(rhonew(n)/fxn8)
      end do


ccccccccccccccccccccccccccccccccccccccccccccccccccccccccc
c     OUTPUT original density=rho, new density=rhonew,
c       hybrid density=rhohybrid
c       bigdiff to see difference of densities btw iterations
```

```
      bigdiff=0.0d0

      do n=1, nmax
         rhohybrid(n)=(0.999d0*rho(n))+(0.001d0*rhonew(n))
         differ(n)=abs(rhohybrid(n)-rhonew(n))
         if (differ(n).gt.bigdiff) then
             bigdiff=differ(n)
         else
             bigdiff=bigdiff
         end if
c         write (6, *) rhohybrid(n), rho(n), U(n), r(n)
      end do

      write (6, *) bigdiff, eval

      write (70, *) bigdiff, eval, fxn1, fxn8

      call flush(70)


      open (76, file='dopedoutput.txt')

c ccccccccc     meanfield output U(n)    ccccccccccccc

      do n=1, nmax

         write (6, *) U(n), rho(n), rhohybrid(n), psinew(n), r(n)
         write (76, *) U(n), rho(n), rhohybrid(n), psinew(n), r(n)

      end do

      close (76)

cccccc     define rhohybrid as rhomir for the next loop. continues cycle ccccccccc
      do n=1, nmax
         rho(n)=rhohybrid(n)
c         write (6, *) rho(n), r(n)
      end do

ccc   end iteration loop
      end do



      stop
      end
```

Program 5: Orsay-Trento Collaboration
Planar Symmetry

```
implicit real*8 (a-h, o-z)
      real*8 mass

      dimension rho(4001), z(4001), U(4001), fxnI(4001), fxnF(4001)
      dimension rhobar(4001), rhowtave(4001), hmat(4001, 4001)
      dimension vmat(4001, 4001), differ(4001), psinew(4001), fxnH(4001)
      dimension rhonew(4001), rhb(4001), rhowta(4001), tmat(4001, 4001)
      dimension rhohybrid(4001), fxnIi(4001), drho(4001), fxnG(4001)
      dimension UtermG(4001), UtermE(4001), UtermD(4001), UtermA(4001)
      dimension UtermH(4001), UtermB(4001), UtermF1(4001), UtermF2(4001)
      dimension UtermC(4001), fxnF1(4001), fxnF2(4001), fxnA(4001)
      dimension fxnB(4001), fxnC(4001), fxnD(4001), fxnE(4001)
      dimension dfxnI(4001), dfxnH(4001), Utemp(4001)


c     initial parameters

      nmax=4001
      dz=0.02190323d0
      rho0=0.02184d0

c     z coordinate system

      z(1)=-43.806d0

      do n=2, nmax
         z(n)=z(n-1)+dz
      end do

c    IMPORT initial density profile

      open (22, file='temp.txt')
      do n=1, nmax

         read (22, *) Utemp(n), rho(n)

      end do

      close (22)


c    fxn1 is the normalization of the system size

      sum1=0.0d0
      a1=z(1)
      b1=z(nmax)
```

```
      tmax1=nmax-1

      do n=1, nmax

         if (n.eq.1.or.n.eq.nmax) then
         k=1
         sum1=sum1+k*rho(n)
         else if (n.gt.1.and.n.lt.nmax) then
         k=2
         sum1=sum1+k*rho(n)
         end if

      end do

         fxn1=((b1-a1)/(2.0d0*tmax1))*sum1
c         write (6, *) fxn1

cccc here alpha corresponds to the Lennard-Jones parameter sigma given in
cccccccc representative equations and alphas corresponds to alpha0s


c     CONSTANTS

      h=2.190323d0
      pi=3.1415926535d0
      epsilom=10.22d0
      alpha=2.556d0
      alphs=54.31d0
      c1=-2.411857d4
      c11=1.858496d6
      rho0s=0.04d0

      mass=4.002602*1.6605402d-27
      hbar=(1.05457266d-34)*1.0d20
      boltz=(1.380658d-23)*1.0d20

c     COEFFICIENTs


      coeffA=4.0d0*pi*epsilom*alpha**2
      coeffB=4.0d0*pi*epsilom*alpha**2
      coeffC=4.0d0*pi*epsilom*alpha**2

      coeffD=c1/2.0d0
      coeffE=c11/3.0d0

      coeffF1=(3.0d0/(4.0d0*h))*c1
      coeffF2=(3.0d0/(4.0d0*h))*c11

      coeffG=(alphs*hbar**2)/(2.0d0*mass*boltz*rho0s)

      coeffH=(alphs*hbar**2)/(2.0d0*mass*boltz)

ccccccccccccc     Tmat and Vmat INITIATE WITH ZEROES ccccccccccccc
```

```
      do n=1, nmax
      do o=1, nmax
         tmat(n, o)=0.0d0
         vmat(n, o)=0.0d0
      end do
      end do


c     open file for bigdiff

      open (16, file='summary.out')


c     BEGIN ITERATION LOOP

      do iteration=1, 50000



c    rhowtave  =  weighted average density. close to actual density value, however,
intended to be c    important at denisties near the liquid-solid interface
c    fxnF = Gaussian 1D weight function

      do n=1, nmax

        sumrhwta=0.0d0
        nmaxrhwta=nmax-1
        arhwta=z(1)
        brhwta=z(nmax)

        do n1=1, nmax

        fxnF(n1)=(1.0d0/sqrt(pi))*(exp(-(z(n)-z(n1))**2))

        rhowta(n1)=fxnF(n1)*rho(n1)

        if (n1.eq.1.or.n1.eq.nmax) then
         k=1
         sumrhwta=sumrhwta+k*rhowta(n1)
        else if (n1.gt.1.and.n1.lt.nmax) then
         k=2
         sumrhwta=sumrhwta+k*rhowta(n1)
        else
         sumrhwta=0.0d0
        end if
        end do
        rhowtave(n)=((brhwta-arhwta)/dble(2*nmaxrhwta))*sumrhwta

c      write (6, *) rhowtave(n), z(n), rho(n)

      end do

c    rhobar   coarse-grained density
```

```
      do n=1, 101

        rhobar(n)=0.0d0

c        write (6, *) rhobar(n), z(n)

      end do

      do n=102, 3901

        i=n-100
        j=n+100
        nmaxrhb=200
        sumrhb=0.0d0
        arhb=z(i)
        brhb=z(j)


        do n1=i, j

        rhb(n1)=(1.0d0-((z(n)-z(n1))/h)**2)*rho(n1)

        if (n1.eq.i.or.n1.eq.j) then
         k=1
         sumrhb=sumrhb+k*rhb(n1)
        else if (n1.gt.i.and.n1.lt.j) then
         k=2
         sumrhb=sumrhb+k*rhb(n1)
        else
         sumrhb=0.0d0
      end if
      end do
       rhobar(n)=(3.0d0/(4.0d0*h))*((brhb-arhb)/(2.0d0*nmaxrhb))*sumrhb

c        write (6, *) rhobar(n), z(n)

      end do


      do n=3902, 4001

        rhobar(n)=0.0d0

c        write (6, *) rhobar(n), z(n)

      end do


c    first derivative fxn of rho

      do n=1, nmax
```

```
          if (n.eq.1.or.n.eq.nmax) then
          drho(n)=0.0d0
          else
          drho(n)=(rho(n+1)-rho(n-1))/(2.0d0*dz)
          end if

       end do

c      fxnI


       do n=1, nmax

          sumfxnI=0.0d0
          nmaxfxnI=nmax-1
          afxnI=z(1)
          bfxnI=z(nmax)

          do n1=1, nmax

          fxnF(n1)=(1.0d0/sqrt(pi))*(exp(-(z(n)-z(n1))**2))

          fxnIi(n1)=(1.0d0-(rhowtave(n1)/rho0s))*fxnF(n1)*drho(n1)

         if (n1.eq.1.or.n1.eq.nmax) then
          k=1
          sumfxnI=sumfxnI+k*fxnIi(n1)
         else if (n1.gt.1.and.n1.lt.nmax) then
          k=2
          sumfxnI=sumfxnI+k*fxnIi(n1)
         else
          sumfxnI=0.0d0
         end if
         end do
         fxnI(n)=((bfxnI-afxnI)/(2.0d0*nmaxfxnI))*sumfxnI

c       write (6, *) fxnI(n), z(n)

       end do


c       UtermG   meanfield term 7 with limits of  -inf to +inf

       do n=1, nmax

       nmaxG=nmax-1
       sumG=0.0d0
       aG=z(1)
       bG=z(nmax)

          do n1=1, nmax

          fxnF(n1)=(1.0d0/sqrt(pi))*(exp(-(z(n)-z(n1))**2))
```

```
         fxnG(n1)=fxnF(n1)*fxnI(n1)*drho(n1)

        if (n1.eq.1.or.n1.eq.nmax) then
         k=1
         sumG=sumG+k*fxnG(n1)
        else if (n1.gt.1.and.n1.lt.nmax) then
         k=2
         sumG=sumG+k*fxnG(n1)
        else
         sumG=0.0d0
        end if
        end do

        UtermG(n)=coeffG*((bG-aG)/(2.0d0*nmaxG))*sumG

        UtermD(n)=coeffD*(rhobar(n)**2)
        UtermE(n)=coeffE*(rhobar(n)**3)

c       write (6, *) UtermG(n), UtermE(n), UtermD(n), rho(n), z(n)

      end do


c      UtermH

      do n=1, nmax

         fxnH(n)=(fxnI(n)*rhowtave(n))/rho0s

c        write (6, *) fxnH(n), z(n)

      end do

      do n=1, nmax

         if (n.eq.1.or.n.eq.nmax) then
          dfxnI(n)=0.0d0
          dfxnH(n)=0.0d0
         else
          dfxnI(n)=(fxnI(n+1)-fxnI(n-1))/(2.0d0*dz)
          dfxnH(n)=(fxnH(n+1)-fxnH(n-1))/(2.0d0*dz)
         end if

        UtermH(n)=coeffH*(dfxnI(n)-dfxnH(n))

c        write (6, *) UtermH(n), z(n)

      end do

c     remainder of Uterms and calculation of U(n)


      do n=1, 100
```

```
        U(n)=UtermD(n)+UtermE(n)+UtermG(n)+UtermH(n)

c        write (6, *) U(n), rho(n), z(n)

      end do


      do n=101, 3900

      i=n-100
      j=n+100

      sumA=0.0d0
      nmaxA=i
      aA=z(1)
      bA=z(i)


c       limits -inf to z-h

         do n1=1, i

         fxnA(n1)=rho(n1)*((alpha/(z(n)-z(n1)))**4)*((0.2d0*
     .   ((alpha/(z(n)-z(n1)))**6))-0.5d0)

        if (n1.eq.1.or.n1.eq.i) then
         k=1
         sumA=sumA+k*fxnA(n1)
        else if (n1.gt.1.and.n1.lt.i) then
         k=2
         sumA=sumA+k*fxnA(n1)
        else
         sumA=0.0d0
        end if
        end do

         UtermA(n)=coeffA*((bA-aA)/(2.0d0*nmaxA))*sumA


c       limits z-h to z+h

        sumC=0.0d0
        nmaxC=200
        aC=z(i)
        bC=z(j)

        sumF1=0.0d0
        sumF2=0.0d0
        nmaxF=200
        aF=z(i)
        bF=z(j)

         do n1=i, j
```

```
      fxnC(n1)=(rho(n1)*((alpha/h)**4))*(0.2d0*((alpha/h)**6)-0.5d0)

      fxnF1(n1)=(rho(n1)*rhobar(n1))*
     .  (1.0d0-(((z(n)-z(n1))/h)**2))

      fxnF2(n1)=(rho(n1)*(rhobar(n1)**2))*
     .  (1.0d0-(((z(n)-z(n1))/h)**2))

     if (n1.eq.i.or.n1.eq.j) then
      k=1
      sumC=sumC+k*fxnC(n1)
      sumF1=sumF1+k*fxnF1(n1)
      sumF2=sumF2+k*fxnF2(n1)
     else if (n1.gt.i.and.n1.lt.j) then
      k=2
      sumC=sumC+k*fxnC(n1)
      sumF1=sumF1+k*fxnF1(n1)
      sumF2=sumF2+k*fxnF2(n1)
     else
      sumC=0.0d0
      sumF1=0.0d0
      sumF2=0.0d0
     end if
     end do


      UtermC(n)=coeffC*((bC-aC)/(2.0d0*nmaxC))*sumC

      UtermF1(n)=coeffF1*((bF-aF)/(2.0d0*nmaxF))*sumF1

      UtermF2(n)=coeffF2*((bF-aF)/(2.0d0*nmaxF))*sumF2


c     limits z+h to +inf

      sumB=0.0d0
      nmaxB=nmax-j
      aB=z(j)
      bB=z(nmax)

      do n1=j, nmax

      fxnB(n1)=rho(n1)*((alpha/(z(n)-z(n1)))**4)*((0.2d0*
     .  ((alpha/(z(n)-z(n1)))**6))-0.5d0)

     if (n1.eq.j.or.n1.eq.nmax) then
      k=1
      sumB=sumB+k*fxnB(n1)
     else if (n1.gt.j.and.n1.lt.nmax) then
      k=2
      sumB=sumB+k*fxnB(n1)
     else
      sumB=0.0d0
     end if
```

```
        end do

        UtermB(n)=coeffB*((bB-aB)/(2.0d0*nmaxB))*sumB


        U(n)=UtermA(n)+UtermB(n)+UtermC(n)+UtermE(n)+UtermF1(n)+
     .  UtermF2(n)+UtermG(n)+UtermH(n)+UtermD(n)

c       write (6, *) UtermH(n), UtermA(n), UtermB(n), UtermC(n), z(n)
c       write (6, *) UtermG(n), UtermE(n), UtermF1(n), UtermF2(n), z(n)

c       write (6, *) U(n), rho(n), z(n)

      end do


      do n=3901 , nmax

        U(n)=UtermD(n)+UtermE(n)+UtermG(n)+UtermH(n)

c        write (6, *) U(n), rho(n), z(n)

      end do


ccccccccccccccc     Tmat and Vmat INITIATE VALUES   ccccccccccccccccccc

      do n=1, nmax
      do o=1, nmax
         if (n.eq.o) then
            vmat(n, o)=U(n)
            tmat(n, o)=(hbar**2/(mass*boltz*dz**2))
         else if (o.eq.(n+1).or.o.eq.(n-1)) then
            tmat(n, o)=-(hbar**2/(2.0d0*mass*boltz*dz**2))
         end if
      end do
      end do

      do n=1, nmax
      do o=1, nmax
         hmat(n, o)=vmat(n, o) + tmat(n, o)
      end do
      end do



      call calcpsi(hmat, psinew, eval)

      sumpsi=0.0d0

      do n=1, nmax
         sumpsi=sumpsi+psinew(n)
      end do
```

```
      do n=1, nmax
         psinew(n)=psinew(n)/sumpsi
      end do

      do n=1, nmax
         rhonew(n)=psinew(n)**2
c         write (6, *)  psinew(n), z(n), rhonew(n)
      end do



ccccccccccccccc     trapezoidal rule integration of rhonew to rescale density
ccccccccccccc


      sum8=0.0d0
      a8=z(1)
      b8=z(nmax)
      tmax8=nmax-1

      do n=1, nmax
         if (n.eq.1.or.n.eq.nmax) then
         k=1
         sum8=sum8+(k*rhonew(n))
         else if (n.gt.1.and.n.lt.nmax) then
         k=2
         sum8=sum8+(k*rhonew(n))
         end if
      end do
         fxn8=((b8-a8)/(2.0d0*tmax8))*sum8
c         write (6, *) fxn8

      do n=1, nmax
         rhonew(n)=fxn1*(rhonew(n)/fxn8)
      end do



c     OUTPUT original density=rhomirror, new dens=rhonew,
c       hybrid dens=rhohybrid
c       bigdiff to see difference of densities btw iterations

      bigdiff=0.0d0

      do n=1, nmax
         rhohybrid(n)=(0.9985d0*rho(n))+(0.0015d0*rhonew(n))
         differ(n)=abs(rhohybrid(n)-rhonew(n))
         if (differ(n).gt.bigdiff) then
             bigdiff=differ(n)
         else
             bigdiff=bigdiff
         end if
```

```
c          write (6, *) rhohybrid(n), rho(n), U(n), z(n)
      end do

      write (6, *) bigdiff, eval

      write (16, *) bigdiff, eval, fxn1, fxn8

      call flush(16)


      open (18, file='output.txt')

c ccccccccc     meanfield output U(n)    ccccccccccccc

      do n=1, nmax

         write (6, *) U(n), rho(n), rhohybrid(n), psinew(n), z(n)
         write (18, *) U(n), rho(n), rhohybrid(n), psinew(n), z(n)

      end do

      close (18)

cccccc     define rhohybrid as rhomir for the next loop. continues cycle ccccccccc
      do n=1, nmax
         rho(n)=rhohybrid(n)
c         write (6, *) rho(n), z(n)
      end do



c     END ITERATION LOOP

      end do

      stop
      end
```

Appendix B
Orsay-Trento Mean Field Equations for Spherical Symmetry

For $r = 0$, the coarse-grained density is defined by equation (B1) and the mean field by equation (B2).

(B1)

$$\bar{\rho}_r = \frac{3}{h^3}\int_0^h dr'\,(r')^2\rho(r')$$

(B2)

$$U(r) = 16\pi\varepsilon\int_h^\infty dr'\;\rho(r')\left\{\left[\frac{\sigma^{12}}{(r')^{10}}\right]-\left[\frac{\sigma^6}{(r')^4}\right]\right\}+\frac{c_2}{2}(\bar{\rho}_r)^2+\frac{3c_2}{h^3}\int_0^h dr'\;(r')^2\rho(r')\,\bar{\rho}_{r'}+\frac{c_3}{3}(\bar{\rho}_r)^3$$

$$+\frac{3c_3}{h^3}\int_0^h dr'\;(r')^2\rho(r')(\bar{\rho}_{r'})^2+\frac{\hbar^2}{m\sqrt{\pi}}\,\alpha_s\left[1-\frac{\rho(r)}{\rho_{0s}}\right]\int_0^\infty dr'\;\frac{d\rho(r')}{dr'}\left[1-\frac{\rho(r')}{\rho_{0s}}\right]$$

$$\times\left\{\frac{1}{2}\left(\frac{-e^{-(r+r')^2}-2\,r\,r'e^{-(r+r')^2}-2\,r^2(r')^2e^{-(r+r')^2}+e^{-(r-r')^2}-2\,r\,r'e^{-(r-r')^2}+2\,r^2(r')^2e^{-(r-r')^2}}{r^3}\right)\right.$$

$$\left.-2\left(\frac{e^{\left(-(r')^2-r^2-r\,r'\right)}+r\,r'e^{\left(-(r')^2-r^2-r\,r'\right)}-e^{\left(-(r')^2-r^2+r\,r'\right)}+r\,r'e^{\left(-(r')^2-r^2+r\,r'\right)}}{r}\right)\right\}$$

For limits of r less than or equal to the value of h, the coarse-grained density becomes equation (B3).

(B3)

$$\bar{\rho}_r = \frac{3}{h^3}\int_0^{h-r} dr'\,(r')^2\rho(r') + \frac{3}{2h^3}\int_{h-r}^{r+h} dr'\,(r')^2\rho(r')\left(1-\frac{-h^2+r^2+(r')^2}{2\,r\,r'}\right)$$

The mean field in the region of $r \le h$ is given by equation (B4).

(B4)

$$U(r) = 8\pi\varepsilon\int_{r+h}^{\infty} dr'\,\frac{r'\rho(r')}{r}\left\{\frac{\sigma^{12}}{10}\left(\frac{1}{(r^2+(r')^2-2\,r\,r')^5}-\frac{1}{(r^2+(r')^2+2\,r\,r')^5}\right)\right.$$
$$\left.-\frac{\sigma^6}{4}\left(\frac{1}{(r^2+(r')^2-2\,r\,r')^2}-\frac{1}{(r^2+(r')^2+2\,r\,r')^2}\right)\right\}$$

$$+8\pi\varepsilon\int_{h-r}^{r+h} dr'\,\frac{r'\rho(r')}{r}\left\{\frac{\sigma^{12}}{10}\left(\frac{1}{h^{10}}-\frac{1}{(r^2+(r')^2+2\,r\,r')^5}\right)-\frac{\sigma^6}{4}\left(\frac{1}{h^4}-\frac{1}{(r^2+(r')^2+2\,r\,r')^2}\right)\right\}$$
$$+\frac{c_2}{2}(\bar{\rho}_r)^2+\frac{3c_2}{h^3}\int_0^{h-r} dr'\,(r')^2\rho(r')\bar{\rho}_{r'}+\frac{3c_2}{2h^3}\int_{h-r}^{r+h} dr'\,(r')^2\rho(r')\bar{\rho}_{r'}\left(1-\frac{-h^2+r^2+(r')^2}{2\,r\,r'}\right)$$
$$+\frac{c_3}{3}(\bar{\rho}_r)^3+\frac{3c_3}{h^3}\int_0^{h-r} dr'\,(r')^2\rho(r')(\bar{\rho}_{r'})^2+\frac{3c_3}{2h^3}\int_{h-r}^{r+h} dr'\,(r')^2\rho(r')(\bar{\rho}_{r'})^2\left(1-\frac{-h^2+r^2+(r')^2}{2\,r\,r'}\right)$$
$$+\frac{\hbar^2}{m\sqrt{\pi}}\,\alpha_s\left[1-\frac{\rho(r)}{\rho_{0s}}\right]\int_0^{\infty} dr'\,\frac{d\rho(r')}{dr'}\left[1-\frac{\rho(r')}{\rho_{0s}}\right]$$

$$\times\left\{\frac{1}{2}\left(\frac{-e^{-(r+r')^2}-2\,r\,r'\,e^{-(r+r')^2}-2\,r^2(r')^2e^{-(r+r')^2}+e^{-(r-r')^2}-2\,r\,r'\,e^{-(r-r')^2}+2\,r^2(r')^2e^{-(r-r')^2}}{r^3}\right)\right.$$

$$\left.-2\left(\frac{e^{\left(-(r')^2-r^2-r\,r'\right)}+r\,r'\,e^{\left(-(r')^2-r^2-r\,r'\right)}-e^{\left(-(r')^2-r^2+r\,r'\right)}+r\,r'\,e^{\left(-(r')^2-r^2+r\,r'\right)}}{r}\right)\right\}$$

For values of r greater than h, the coarse-grained density and mean field are defined by equation (B5) and (B6), respectively.

(B5)

$$\bar{\rho}_r=\frac{3}{2h^3}\int_{r-h}^{r+h}dr'\,(r')^2\rho(r')\left(1-\frac{-h^2+r^2+(r')^2}{2\,r\,r'}\right)$$

(B6)

$$U(r)=8\pi\varepsilon\int_0^{r-h}dr'\;\frac{r'\rho(r')}{r}\left\{\frac{\sigma^{12}}{10}\left(\frac{1}{(r^2+(r')^2-2\,r\,r')^5}-\frac{1}{(r^2+(r')^2+2\,r\,r')^5}\right)\right.$$

$$\left.-\frac{\sigma^6}{4}\left(\frac{1}{(r^2+(r')^2-2\,r\,r')^2}-\frac{1}{(r^2+(r')^2+2\,r\,r')^2}\right)\right\}$$

$$+8\pi\varepsilon\int_{r+h}^{\infty}dr'\;\frac{r'\rho(r')}{r}\left\{\frac{\sigma^{12}}{10}\left(\frac{1}{(r^2+(r')^2-2\,r\,r')^5}-\frac{1}{(r^2+(r')^2+2\,r\,r')^5}\right)\right.$$

$$\left.-\frac{\sigma^6}{4}\left(\frac{1}{(r^2+(r')^2-2\,r\,r')^2}-\frac{1}{(r^2+(r')^2+2\,r\,r')^2}\right)\right\}$$

$$+8\pi\varepsilon\int_{r-h}^{r+h}dr'\frac{r'\rho(r')}{r}\left\{\frac{\sigma^{12}}{10}\left(\frac{1}{h^{10}}-\frac{1}{(r^2+(r')^2+2\,r\,r')^5}\right)-\frac{\sigma^6}{4}\left(\frac{1}{h^4}-\frac{1}{(r^2+(r')^2+2\,r\,r')^2}\right)\right\}$$

$$+\frac{c_2}{2}(\bar{\rho}_r)^2+\frac{3c_2}{2h^3}\int_{r-h}^{r+h}dr'(r')^2\rho(r')\,\bar{\rho}_{r'}\left(1-\frac{-h^2+r^2+(r')^2}{2\,r\,r'}\right)$$

$$+\frac{c_3}{3}(\bar{\rho}_r)^3+\frac{3c_3}{2h^3}\int_{r-h}^{r+h}dr'(r')^2\rho(r')\,(\bar{\rho}_{r'})^2\left(1-\frac{-h^2+r^2+(r')^2}{2\,r\,r'}\right)$$

$$+\frac{\hbar^2}{m\sqrt{\pi}}\,\alpha_s\left[1-\frac{\rho(r)}{\rho_{0s}}\right]\int_0^{\infty}dr'\,\frac{d\rho(r')}{dr'}\left[1-\frac{\rho(r')}{\rho_{0s}}\right]$$

$$\times\left\{\frac{1}{2}\left(\frac{-e^{-(r+r')^2}-2\,r\,r'e^{-(r+r')^2}-2\,r^2(r')^2e^{-(r+r')^2}+e^{-(r-r')^2}-2\,r\,r'e^{-(r-r')^2}+2\,r^2(r')^2e^{-(r-r')^2}}{r^3}\right)\right.$$

$$\left.-2\left(\frac{e^{\left(-(r')^2-r^2-r\,r'\right)}+r\,r'e^{\left(-(r')^2-r^2-r\,r'\right)}-e^{\left(-(r')^2-r^2+r\,r'\right)}+r\,r'e^{\left(-(r')^2-r^2+r\,r'\right)}}{r}\right)\right\}$$

Vita

Ellen Cofer Brown was born to loving parents in 1985. She studied at the University of North Carolina at Asheville, receiving a B.S. in Biochemistry in 2007. She has lived in many places throughout the United States and will continue to travel throughout her life, while pursuing her interests in teaching.